

**The Assessment of Cephalometric Measurements at Various Degrees of Skull
Orientation in the Sagittal Axis**

BY

KAN TSUNODA

B.S., Brigham Young University, Provo, Utah, 2003

D.C., Palmer College of Chiropractic, Iowa, 2008

D.M.D., Midwestern University College of Dental Medicine, Illinois 2016

THESIS

Submitted as partial fulfillment of the requirements
for the degree of Master of Science in Oral Sciences
in the Graduate College of the
University of Illinois at Chicago, 2019
Chicago, Illinois

Defense Committee:

Jennifer Caplin, Chair and Advisor
Budi Kusnoto
Grace Viana
Mohammed Elnagar
Ales Obrez, Restorative Dentistry

I dedicate this thesis to my wife, Tsukasa Tsunoda, whose encouragement, endless support and unconditional love allows me to achieve new heights and reach new goals. To my children who cheered on through endless hugs and kisses.

ACKNOWLEDGEMENTS

Sincere thanks to Dr. Jennifer Caplin, Department of Orthodontics, University of Illinois-Chicago, for her knowledge and co-operation as primary advisor, to Dr. Muhammed Elnagar for input on Dolphin 3D® software, CBCT analysis and protocol preparation, to Grace Viana for computation and statistical analyses of data, to Dr. Budi Kusnoto for his knowledge in Dolphin® cephalometric analysis and support, to Dr. Ales Obrez for suggestions and support for the research.

KT

TABLE OF CONTENTS

<u>CHAPTER</u>	<u>PAGE</u>
I. INTRODUCTION.....	1
1.1 Background.....	1
1.2 Specific Aims.....	1
1.3 Significance of the Current Study.....	1
1.4 Null Hypothesis	2
II. REVIEW OF LITERATURE.....	3
2.1 Lateral Cephalometric Radiographs	3
2.2 Cephalometric Analysis	4
2.3 General Principles of Cephalometric Radiography	5
2.4 Magnification & Distortion.....	6
2.5 Errors in Lateral Cephalometrics	7
2.5.1 Errors Due to Landmark Identification.....	8
2.5.2 Errors Due to Head Position	9
III. MATERIALS AND METHODS.....	12
3.1 Approval	12
3.2 Design and Sample	12
3.3 Inclusion and Exclusion Criteria.....	13
3.3.1 Inclusion Criteria	13
3.3.2 Exclusion Criteria	13
3.4 Radiographic Technique	14
3.4.1 Creation of Lateral Cephalometric Radiographs from CBCT Image	14
3.5 Cephalometric Landmark and Tracing	18
3.6 Dolphin 3D® Custom Cephalometric Analysis	20
3.7 Reliability Testing.....	21
3.8 Data Analysis	22
IV. RESULTS.....	23
4.1 Reliability.....	23
4.2 Rotated Skull Cephalograms vs Ideal 0° Cephalogram.....	23
4.3 Output Results.....	31
V. DISCUSSION	36
5.1 Relation to Other Studies	36
5.1.1 Landmarking.....	36
5.1.2 Linear Measurements.....	38
5.1.3 Angular Measurements.....	39
5.1.4 General Trend Observed in Cephalometric Measurement Errors.....	42
5.1.6 Clinical Relevance and Application.....	43
5.2 Limitations of the Current Study	46

CITED LITERATURE	50
APPENDICES	55
APPENDIX A.....	55
APPENDIX B.....	56
APPENDIX C.....	80
VITA	102

LIST OF TABLES

<u>TABLE</u>		<u>PAGE</u>
I.	LINEAR AND ANGULAR MEASUREMENTS	21
II.	TEST RESULTS FOR ANGULAR MEASUREMENTS	24
III.	TEST RESULTS FOR LINEAR MEASUREMENTS	25
IV.	DISTANCE (+/-) FROM 0° WITH AVERAGE STATISTICALLY SIGNIFICANT MEAN DIFFERENCES	28
V.	95% CONFIDENCE INTERVAL OF THE DIFFERENCE	29
VI.	CONSIDERING ± 0.5 (°) DISTANCE OF CLINICAL SIGNIFICANCE	30

LIST OF FIGURES

<u>FIGURE</u>	<u>PAGE</u>
1. Cephalometric Machine.....	6
2. Diagram of rotational axis.	13
3. Frontal view of 3D CBCT.....	15
4. Lateral Right view of 3D CBCT with Frankfort Horizontal Parallel to the Floor.....	16
5. Generated Cephalometric Radiograph in Ideal Position (0°).	17
6. Skull 1: Cephalometric radiographs taken under 0° (A), 3° (B), 6° (C), 9° (D), 12° (E), 15° (F), -3° (G), -6° (H), -9° (I), -12° (J), -15° (K)	18
7. Cephalometric Radiograph Tracing.....	20
8. Graph/Bar by group distances-mm	26
9. Graph/Bar by group distances-degrees	27
10. A: Ideal Skull Position, B: Skull at -15° Rotation	37
11. A: Condyles in Ideal Skull Position. B: Condyles in +15° Skull Position.	42
12. Examples of head rotations when viewed from the front 0° (A), 3° (B), 6° (C), 9° (D), 12° (E), 15° (F), -15° (G), -12° (H), -9° (I), -6° (J), -3° (K), 0° (L).....	45
13. Skull 2. Cephalometric radiographs taken under 0° (A), 3° (B), 6° (C), 9° (D), 12° (E), 15° (F), -3° (G), -6° (H), -9° (I), -12° (J), -15° (K)	57
14. Skull 3. Cephalometric radiographs taken under 0° (A), 3° (B), 6° (C), 9° (D), 12° (E), 15° (F), -3° (G), -6° (H), -9° (I), -12° (J), -15° (K)	58
15. Skull 4. Cephalometric radiographs taken under 0° (A), 3° (B), 6° (C), 9° (D), 12° (E), 15° (F), -3° (G), -6° (H), -9° (I), -12° (J), -15° (K)	59
16. Skull 5. Cephalometric radiographs taken under 0° (A), 3° (B), 6° (C), 9° (D), 12° (E), 15° (F), -3° (G), -6° (H), -9° (I), -12° (J), -15° (K)	60
17. Skull 6. Cephalometric radiographs taken under 0° (A), 3° (B), 6° (C), 9° (D), 12° (E), 15° (F), -3° (G), -6° (H), -9° (I), -12° (J), -15° (K)	61
18. Skull 7. Cephalometric radiographs taken under 0° (A), 3° (B), 6° (C), 9° (D), 12° (E), 15° (F), -3° (G), -6° (H), -9° (I), -12° (J), -15° (K)	62

LIST OF FIGURES (continued)

19. Skull 8. Cephalometric radiographs taken under 0° (A), 3° (B), 6° (C), 9° (D), 12° (E), 15° (F), -3° (G), -6° (H), -9° (I), -12° (J), -15° (K)	63
20. Skull 9. Cephalometric radiographs taken under 0° (A), 3° (B), 6° (C), 9° (D), 12° (E), 15° (F), -3° (G), -6° (H), -9° (I), -12° (J), -15° (K)	64
21. Skull 10. Cephalometric radiographs taken under 0° (A), 3° (B), 6° (C), 9° (D), 12° (E), 15° (F), -3° (G), -6° (H), -9° (I), -12° (J), -15° (K)	65
22. Skull 11. Cephalometric radiographs taken under 0° (A), 3° (B), 6° (C), 9° (D), 12° (E), 15° (F), -3° (G), -6° (H), -9° (I), -12° (J), -15° (K)	66
23. Skull 12. Cephalometric radiographs taken under 0° (A), 3° (B), 6° (C), 9° (D), 12° (E), 15° (F), -3° (G), -6° (H), -9° (I), -12° (J), -15° (K)	67
24. Skull 13. Cephalometric radiographs taken under 0° (A), 3° (B), 6° (C), 9° (D), 12° (E), 15° (F), -3° (G), -6° (H), -9° (I), -12° (J), -15° (K)	68
25. Skull 14. Cephalometric radiographs taken under 0° (A), 3° (B), 6° (C), 9° (D), 12° (E), 15° (F), -3° (G), -6° (H), -9° (I), -12° (J), -15° (K)	69
26. Skull 15. Cephalometric radiographs taken under 0° (A), 3° (B), 6° (C), 9° (D), 12° (E), 15° (F), -3° (G), -6° (H), -9° (I), -12° (J), -15° (K)	70
27. Skull 16. Cephalometric radiographs taken under 0° (A), 3° (B), 6° (C), 9° (D), 12° (E), 15° (F), -3° (G), -6° (H), -9° (I), -12° (J), -15° (K)	71
28. Skull 17. Cephalometric radiographs taken under 0° (A), 3° (B), 6° (C), 9° (D), 12° (E), 15° (F), -3° (G), -6° (H), -9° (I), -12° (J), -15° (K)	72
29. Skull 18. Cephalometric radiographs taken under 0° (A), 3° (B), 6° (C), 9° (D), 12° (E), 15° (F), -3° (G), -6° (H), -9° (I), -12° (J), -15° (K)	73
30. Skull 19. Cephalometric radiographs taken under 0° (A), 3° (B), 6° (C), 9° (D), 12° (E), 15° (F), -3° (G), -6° (H), -9° (I), -12° (J), -15° (K)	74
31. Skull 20. Cephalometric radiographs taken under 0° (A), 3° (B), 6° (C), 9° (D), 12° (E), 15° (F), -3° (G), -6° (H), -9° (I), -12° (J), -15° (K)	75
32. Skull 21. Cephalometric radiographs taken under 0° (A), 3° (B), 6° (C), 9° (D), 12° (E), 15° (F), -3° (G), -6° (H), -9° (I), -12° (J), -15° (K)	76
33. Skull 22. Cephalometric radiographs taken under 0° (A), 3° (B), 6° (C), 9° (D), 12° (E), 15° (F), -3° (G), -6° (H), -9° (I), -12° (J), -15° (K)	77
34. Skull 23. Cephalometric radiographs taken under 0° (A), 3° (B), 6° (C), 9° (D), 12° (E), 15° (F), -3° (G), -6° (H), -9° (I), -12° (J), -15° (K)	78

LIST OF FIGURES (continued)

35. Skull 24. Cephalometric radiographs taken under 0° (A), 3° (B), 6° (C), 9° (D), 12° (E), 15° (F), -3° (G), -6° (H), -9° (I), -12° (J), -15° (K) 79

LIST OF ABBREVIATIONS

3-D	Three-Dimensional
ALARA	As Low As Reasonably Achievable
ANB	A Point-Nasion-B Point Angle
ANOVA	Analysis of Variance
ANS	Anterior Nasal Spine
ANS-PNS	Anterior Nasal Spine-Posterior Nasal Spine (Maxillary Length)
Ar	Articulare
Ar-Go-Me	Articulare-Gonion-Menton (Gonial Angle)
CBCT	Cone Beam Computer Tomography
Co	Condylion
FH	Frankfort Horizontal
FMA	Frankfort Horizontal-Mandibular Plane Angle
Gn	Gnathion
Go	Gonion
Go-Me	Gonion-Menton (Mandibular Length)
L1-MP	Lower Incisal to Mandibular Plane
Me	Menton
MP-SN	Sella-Nasion Line to Mandibular Plane Angle
N	Nasion
N-Me	Nasion-Menton Length (Anterior Facial Height)
NA-APo	Nasion-A Point to A-Point-Pogonion
Or	Orbitale
P-A	Posterior-Anterior

LIST OF ABBREVIATIONS (continued)

Po	Porion
Pog	Pogonion
PP-U1	Palatal Plane to Maxillary Central Incisor Angle
PNS	Posterior Nasal Spine
S	Sella
S-Go	Sella-Gonion (Posterior Facial Height)
SGn-FH	Sella-Gnathion to Frankfort Horizontal
SMV	Submentovertex
S-N	Sella-Nasion Length - Anterior Cranial Base
SN-U1	Sella-Nasion Line to Maxillary Central Incisor Angle
SNA	Sella-Nasion Line to A point Angle
SNB	Sella-Nasion to B point Angle
U1-PP	Upper Central Incisor to Palatal Plane Angle
U1-SN	Upper Central Incisor to Sella-Nasion Angle

SUMMARY

Lateral cephalometric radiographs are taken as a standard record in orthodontic treatment. The lateral cephalometric radiograph is analyzed based on bony and soft tissue landmarks which are then used to diagnose, guide proper treatment planning, study treatment progress, and assess final treatment outcome. During cephalometric radiograph exposure, the patient's head can be unintentionally rotated within the head positioning device, resulting in error when collecting cephalometric linear and angular measurements. The focus of this research is to identify potential measurement errors on lateral cephalometric radiographs due to head rotation along the sagittal axis during exposure.

Existing iCAT™ 3D Cone Beam Computed Tomography (CBCT) images of 24 de-identified dry human skulls were used in this study. Lateral cephalometric radiographs were taken under 11 different head positions. The ideal head position (0 degrees) was taken with the head in natural head position with Frankfort Horizontal parallel to the floor. Synthetic lateral cephalograms generated from the CBCT images were then rotated along the sagittal axis at -15, -12, -9, -6, -3, +3, +6, +9, +12, +15 degrees. Measurements were extracted from the lateral cephalograms and analyzed to look for variability between the different angles of rotations.

The study found that head tilt had a significant effect on both linear and angular cephalometric measurements, especially when skull rotations, either towards the film or away from the film about the sagittal axis, were greater than 6 degrees.

I. INTRODUCTION

1.1 **Background**

Cephalometric radiographs can be taken during the initial orthodontic exam to aid in diagnosis, during orthodontic care to monitor progress, and after treatment to evaluate treatment results. Many studies evaluating the reliability of lateral, posterioranterior (P-A) and submentovertex (SMV) cephalometric radiographs have concluded that inadvertent head rotations along the vertical or transverse axis can introduce errors in cephalometric measurements (Ahlqvist, Eliasson, and Welander 1986; Baumrind and Frantz 1971; Bergersen 1980; Forsberg, Burstone, and Hanley 1984; Ghafari, Cater, and Shofer 1995; Hsiao, Chang, and Liu 1997). The operator must be attentive when taking cephalometric radiographs and carefully assess the head position. Particular attention must be paid during cephalometric analysis and landmark identification or the analysis will be of limited value (Yoon 2001). In order to have lateral cephalometric radiography recognized as a valid technique and regarded as the gold standard of cephalometrics analysis, there is a need for standardized, reproducible head positioning and exact landmark identification to improve quantitative studies of craniofacial growth, evaluation of treatment effects, and classification of cases.

1.2 **Specific Aims**

This study will evaluate the effect of rotating the head around the sagittal axis during exposure on the accuracy of cephalometric radiograph measurements.

1.3 **Significance of the Current Study**

Being critical when positioning the patient in the lateral cephalometric machine will help reduce potential sources of measurement errors during cephalometric analysis. Previous studies have assessed head rotations along the transverse axis and vertical axis. To our knowledge, no previous study evaluated the effects of head rotation in the sagittal axis with the axis of rotation near the center of the skull. This study will help clinicians understand the adverse effects of improper head posture around the sagittal axis on linear and angular cephalometric measurements. The significance of this study is to allow operators to evaluate whether or not a cephalometric radiograph taken while the head was rotated in the sagittal axis is reliable, or if re-exposure of the patient to radiation for a re-take is necessary.

1.4 **Null Hypothesis**

There is no significant difference in cephalometric measurements when the skull is rotated at different degrees around the sagittal axis vs when the skull is oriented ideally at 0°.

II. REVIEW OF LITERATURE

2.1 Lateral Cephalometric Radiographs

Lateral cephalometric radiographs have been valuable and widely used in orthodontics in the analysis and diagnosis of skeletal and dental abnormalities. They are also important as a clinical method to assess growth, study treatment effects, and classify cases (McWilliam and Welander 1978). However, they do not contain information on the quality of growth and development (Salzmann 1964). The cephalometric radiograph of the head is taken with the central x-ray beam perpendicular to the film and patient's sagittal plane. The patient's head is in the natural head position, eyes forward with Frankfort Horizontal (FH) parallel to the floor. The patient's head is positioned and centered by the head holding device and ear rods, which are then adjusted until the ear rods are approximately at the height of the otic canals. The nasal positioner, with built-in millimeter scale, is placed at the bridge of the patient's nose. Together, the ear rods and nasal positioner help to obtain stable images that are standardized and reproducible, minimizing the errors that can be introduced by head rotation.

The lateral cephalometric radiograph is a useful tool for the development of an orthodontic treatment plan because it shows the width of the symphysis region, which houses the lower incisor roots, and its relationship to the buccal cortex. It is also useful in evaluating vertical dimension, maxillary and mandibular skeletal relationship, soft tissue profile, and relative positions of the anterior teeth to the skull.

2.2 Cephalometric Analysis

Cephalometry is the proportional measurement and study of the human face and skull where cephalometric analysis is the clinical application of said cephalometry, although it is not an exact science (McNamara 1984). After a lateral cephalometric radiograph is obtained, certain skeletal and soft tissue landmarks or points are identified and traced on the radiograph to allow the clinician to analyze the skeletal and dental relationships of the skull, compare the patient to normal values, and identify deviations from the average. This method of analysis is often used by orthodontists and oral surgeons as a treatment planning tool and to predict growth and development related changes.

There are many different types of cephalometric analyses such as Down's analysis, Steiner analysis, Tweed analysis, Wits analysis, and McNamara analysis. Down's analysis is one of the more frequently used and it consists of a total of ten parameters, of which five are skeletal and five are dental. The ten parameters include the following: facial angle, angle of convexity, A-B plane angle, mandibular plane angle, Y-axis, cant of occlusal plane, interincisal angle, interocclusal plane angle, incisor mandibular plane angle, upper incisor to A-Pog line (Downs 1948, 1952). Steiners analysis parameters include: Sella-Nasion Line to A point Angle (SNA), Sella-Nasion Line to B point Angle (SNB), A point to Nasion to B point (ANB), mandibular plane angle, occlusal plane angle, upper incisor to N-A angle, N-A linear, lower incisor to N-B angle, N-B linear, and S-line for soft tissue analysis (esthetic plane of Steiner) (Steiner 1953, 1960). Tweed analysis utilizes 3 planes, Frankfort Horizontal plane, Mandibular plane, and long axis of lower incisors. This analysis is based on the lower mandibular incisor inclination to the basal bone and the vertical relation of the mandible to the cranium (C. H. Tweed 1946; Charles H. Tweed 1953).

Wits analysis measures the relationship between the maxilla and the mandible against each other and to the sagittal plane. This analysis is often useful when the ANB is not reliable. Perpendicular lines are drawn from A point and B point to the functional occlusal plane forming A point to functional occlusal plane (AO) and B point to functional occlusal plane (BO). Wits appraisal is the measured distance between points AO and BO whereby the severity or degree of antero-posterior jaw dysplasia is measured (Jacobson 1975, 1976). A modern analysis known as McNamara analysis is helpful in orthodontics and orthognathic surgery patients because this method not only analyzes the position of teeth in bone but also considers the relationship between the jaw and the cranial base. This analysis divides the craniofacial complex into 5 major sections: cranial base to maxilla, maxilla to mandible, mandible to cranial base, dentition, and airway (McNamara 1984).

2.3 **General Principles of Cephalometric Radiography**

The lateral cephalogram is a 2-D radiograph of the side of the head. The equipment necessary to obtain the image consists of an X-ray source, cephalostat, ear rods, film, intensifying screens, chassis (Rino Neto et al. 2013), nose support (with mm ruler), and base (Figure 1).



Figure 1. Cephalometric Machine.

All of the components are attached to each other as a unit. The patient is positioned 15 cm in front of the film and approximately 5 ft from the X-ray source. The X-ray source is oriented perpendicular to the patient's head (Bergersen 1980). The technician positions the patient in natural head posture, in maximum intercuspation, with lips at rest. Exposure takes approximately 10 seconds.

2.4 **Magnification & Distortion**

One of the disadvantages of cephalometric radiographs include superimposition of bilateral structures, which creates double images. They are also poor tools for assessing the quality of bone (Midtgård, Björk, and Linder-Aronson 1974). Distortion and enlargement can be problematic in cephalometric radiographs. Distortion specifically refers to inaccurate duplication and enlargement refers to proportional magnification of a structure (Bergersen 1980). Distortion can

result from this radiographic technique because of its sensitivity to operator technique. Lateral cephalometric radiographs also utilize intensifying screens where resolution and sharpness are reduced (Resnik and Misch 2015). According to Bergensen, the cephalometric devices magnify lateral cephalometric radiographs by 4.6% to 7.2% (Bergensen 1980) whereas periapical radiographs are typically magnified by less than 5% (Larheim and Eggen 1979).

When the head rotates around the sagittal axis the X-ray beams are no longer perpendicular to the midsagittal plane of the patient, thereby distorting the image. This causes duplication and overlapping of anatomical structures, which introduces inaccuracies in the cephalometric analysis performed. While the patient may be positioned perpendicular to the X-ray source, the source itself has a diverging pattern that creates a variation of magnification of the object in the radiograph. The closer the object is to the X-ray source the more divergent the rays, and more magnification occurs. The operator should always consider increasing the distance between the object and source utilizing the flatter central beam (Rino Neto et al. 2013). As the object to source distance increases, the object to film distance decreases, reducing the magnification. Therefore, anatomical structures located near the film will have less magnification compared to structures closer to the X-ray source (Savage, Showfety, and Yancey 1987). Magnification of craniofacial structures can vary up to 24% depending on how close the head is to the film, where structures closer to the film will have less magnification in comparison to structures that are midsagittal (Weems and Jacobson 1995). Therefore, to minimize distortion and magnification, the operator should strive to keep a constant distance between the film and patient to obtain consistent measurements.

2.5 Errors in Lateral Cephalometrics

2.5.1 **Errors Due to Landmark Identification**

Lateral cephalometrics is valuable and has led to the development of cephalometric analyses, which compare a patient to the population standards. This is done via landmark identification, followed by analyzing the relationship between those landmarks. Landmarks are recognizable points of hard and soft tissue anatomical structures on cephalometric radiographs. Several limitations do exist in cephalometric analysis which may include, but are not limited to, difficulty identifying specific landmarks either due to distortion or superimposition of structures, poor operator technique, and the difficulty found in reproducing the head posture consistently (Ahlqvist, Eliasson, and Welander 1986; Baumrind and Frantz 1971). These can inadvertently introduce errors in the linear and angular measurements of cephalometrics.

The inherent errors found in positioning the head could be due to the ear rods and nasal positioner contacting movable soft tissue areas of the ear canal or bridge of nose causing distortion (Major et al. 1996). Although the ear rods are intended to prevent head rotations, the actual size and location of the bilateral otic canals can vary widely among individuals. When the ear rods are placed, they can produce unwanted head tilts and rotations because of the potential asymmetric locations of the otic canals and thus introduce skull orientation errors. These various head positions can cause errors in the analysis of cephalometrics.

Landmark errors play a significant role in the variability of cephalometric measurements (Macri and Wenzel 1993; Stabrun and Danielsen 1982). Many authors have stated that the major source of error in cephalometric measurements are directly related to the location of landmarks (Baumrind and Frantz 1971; Midtgård, Björk, and Linder-Aronson 1974). Therefore, precise landmark identification and cephalometric tracing is key to minimizing measurement errors.

Identification and reproducibility of the traced image can entirely depend on the specific structure, but clinicians' experience or the quality of the radiograph itself was not associated (Savage, Showfety, and Yancey 1987). Cephalometric radiographs were also influenced by individual bony variation (Salzmann 1964) and some landmarks are simply ambiguous and not very precise (Baumrind and Frantz 1971).

Thus landmark precision, complexity of superimposed structures, and radiographic quality are all contributing factors to landmark errors (Hatton and Grainger 1958; McWilliam and Welander 1978). Other authors have added that even small errors may change the analysis of craniofacial growth in cephalometric radiographs (Yoon 2001). Landmark identification becomes even more difficult when asymmetry in subjects result in multiple locations of anatomic structures in addition to the distortion and magnification of cephalometric radiographs. It should also be noted that each landmark is marked at a different distance from the rotational axis, where landmarks closer to the rotational axis move smaller distances on the resultant image than landmarks further away from the rotational axis, ultimately changing landmark relationships on the cephalogram (Major et al. 1996). Bilateral structures are situated on opposite sides of the rotational axis hence landmarks will move in opposite directions when the skull is rotated. In this particular instance, the resultant image can either increased in superimposition and obscuring the landmark or decrease in superimposition and increasing clarity and the ease of identifying landmarks.

2.5.2 **Errors Due to Head Position**

The goal of cephalometric analysis is to evaluate the relationship of the skull in both the horizontal and vertical dimensions of the face. This includes the following structures:

cranium/cranial base, skeletal maxillae and mandible, maxillary dentition and alveolar process, mandibular dentition, and alveolar processes. The cephalometric analysis outputs data as either a linear measurement (mm or % proportion) or as an angle measurement (degrees). Linear measurements are often affected by radiographic projection; since radiographic projection is proportional, it seldom affects angular measures (Dibbets and Nolte 2002).

When taking a lateral cephalometric radiograph, slight rotation of the head within the head holding device can occur in the sagittal, vertical, or transverse axes. Gaddam et al. identified potential projection errors by rotating 10 human dry skulls along a sagittal axis located near the mid chest. The skulls were rotated toward the X-ray film from 0° to -20° at 5° intervals, where the (-) implied rotation of the head towards the film (Gaddam et al. 2015). The authors found that horizontal linear measurements decreased as the skull rotated towards the film and that horizontal linear measurements had more errors than vertical linear measurements (Gaddam et al. 2015). They also found that angular measurements had fewer errors compared to linear measurements, especially when the angular measurements had multiple landmarks along the midsagittal plane (Gaddam et al. 2015). It was concluded that angular measurements are more valuable than linear measurements when analyzing lateral cephalometric radiographs in an effort to minimize projection errors associated with rotations of the head in the sagittal axis (Gaddam et al. 2015).

The other study to measure the effect of head rotation on lateral cephalometric radiographs used 17 human dry skulls (Yoon 2001). The head was rotated in the vertical axis from 0° to $\pm 15^{\circ}$ at 1° intervals. Codes (+) and (-) were used to indicate skull rotation towards the X-ray source and rotation towards the film respectively. Yoon et al found that cephalometric angular measurements were more advantageous and useful than linear measurements in minimizing errors associated with

head rotation in the vertical axis (Yoon 2001). A decrease in linear measurement was seen when the skull was rotated towards the film, whereas length increased, then decreased, when rotated towards the source. They concluded that head rotation away from the film increases magnification, and that the large degree of rotation itself causes shortening of the images (Yoon 2001). Although many studies report measurement errors due to various head positions, none of the studies to our knowledge investigate the effects of head positions on the sagittal axis rotating at the center of the skull on cephalometric linear and angular measurements.

III. MATERIALS AND METHODS

3.1 **Approval**

The institutional review board (Protocol # 2018-0914) of University of Illinois at Chicago (UIC) approved the analysis and data collection of existing iCAT™ CBCT images of 24 human dry skulls.

3.2 **Design and Sample**

An existing sample of iCAT™ CBCT images (iCAT, Images Sciences International LLC, Hatfield, PA) of twenty-four de-identified dry human skull were used in the current study. CBCT images were converted into lateral cephalometric radiographs under 11 different skull positions with the head rotated (-15° , -12° , -9° , -6° , -3° , 0° , $+3^{\circ}$, $+6^{\circ}$, $+9^{\circ}$, $+12^{\circ}$, $+15^{\circ}$) around the sagittal axis (Figure 2). The (+) indicates the head rotation away from the X-ray film and the (-) indicates head rotation towards the X-ray film. Cephalometric landmarks were placed on the resulting cephalometric radiographs. Cephalometric linear and angular measurements were extracted from the landmarks and analyzed to look for variability between the different angles of rotations.

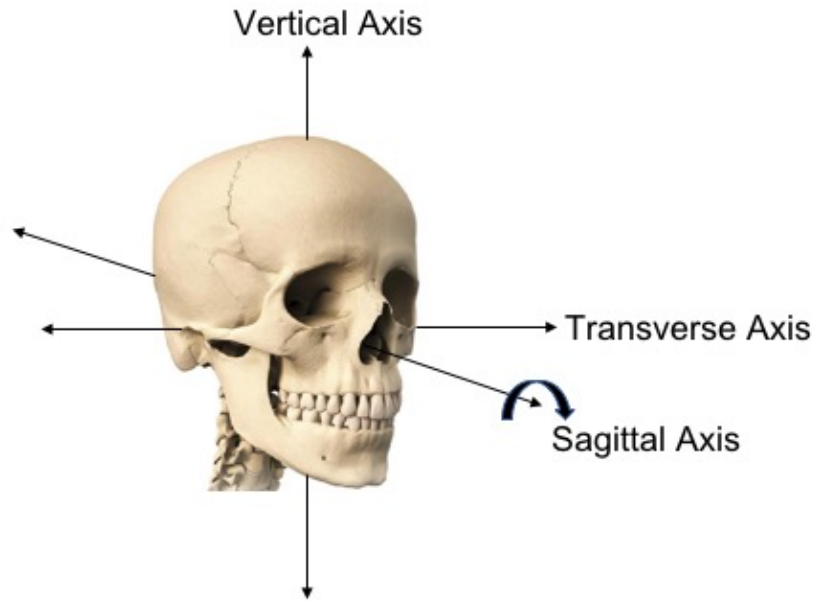


Figure 2. Diagram of rotational axis.

3.3 Inclusion and Exclusion Criteria

3.3.1 Inclusion Criteria

- Adolescent and adult skulls with a complete or near complete permanent dentition.
- Intact and well-preserved skull and mandible.
- Good quality CBCT radiographs.

3.3.2 Exclusion Criteria

- Most teeth are broken or missing.
- Gross asymmetry or significant bone damage.
- Lateral cephalometric radiographs where reference points were not clearly visible.

3.4 **Radiographic Technique**

3.4.1 **Creation of Lateral Cephalometric Radiographs from CBCT Image**

iCAT™ CBCT 3D DICOM multi-files were loaded into Dolphin 3D® software (Dolphin Imaging Systems, Chatsworth, California, Version 11.9 Premium). The magnification factor was set at 9.7%, taking into account the same magnification seen in conventional digital cephalometrics (Hatton and Grainger 1958; Park et al. 2012). The skull images were ideally oriented (0°) and calibrated relative to the default coordinate system, where the orbits were aligned parallel to the axial plane when viewed from the front (Figure 3). In the sagittal view, the skull was rotated along the transverse axis so that FH was parallel to the floor (Figure 4). Once proper orientation of all 3D CBCT skulls was established, each 3D CBCT image was rotated along the sagittal axis (located near the center of the skull) in 11 different skull positions (-15°, -12°, -9°, -6°, -3°, 0°, +3°, +6°, +9°, +12°, +15°). Two projection types, orthogonal and perspective were available in Dolphin 3D® software. Orthogonal type creates a non-distorted X-ray where perspective type creates an X-ray with distortion, magnification and warping effects of a traditional X-ray. 2D lateral cephalometric radiograph images were created by constructing X-rays from the 3D volume data with “Right Lateral” X-ray type and “Perspective” projection type for each of the skull positions and loaded into Dolphin 3D® software for a total of 264 JPEG cephalograms. According to Kumar et al., reproduction of conventional cephalograms via CBCT in perspective are accurate when compared to actual skull measurements (V. Kumar et al. 2007; Vandana Kumar et al. 2008). It has been established that an image compressed into JPEG format does not affect the diagnostic quality (Goldberg et al. 1994; MacMahon et al. 1991).

Examples of a generated cephalometric radiograph at ideal skull position of 0° (Figure 5) and rotated head positions (Figure 6) are shown below.

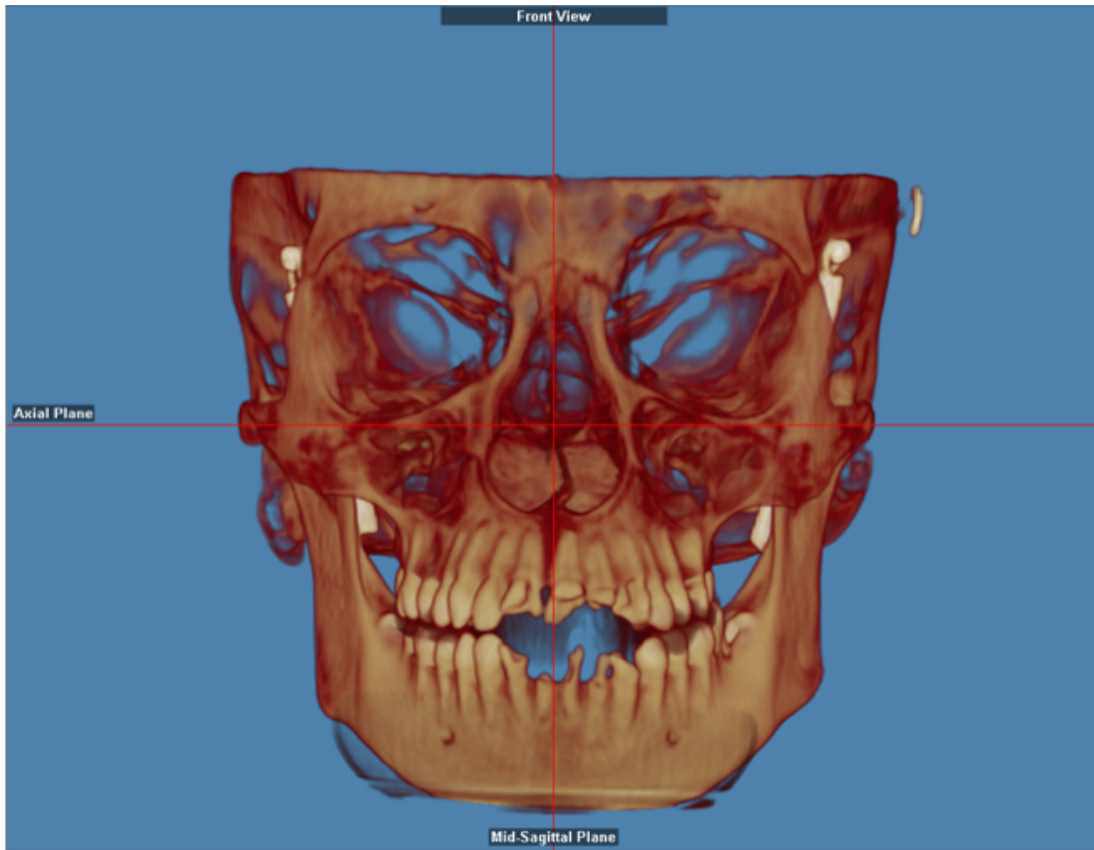


Figure 3. Frontal view of 3D CBCT.

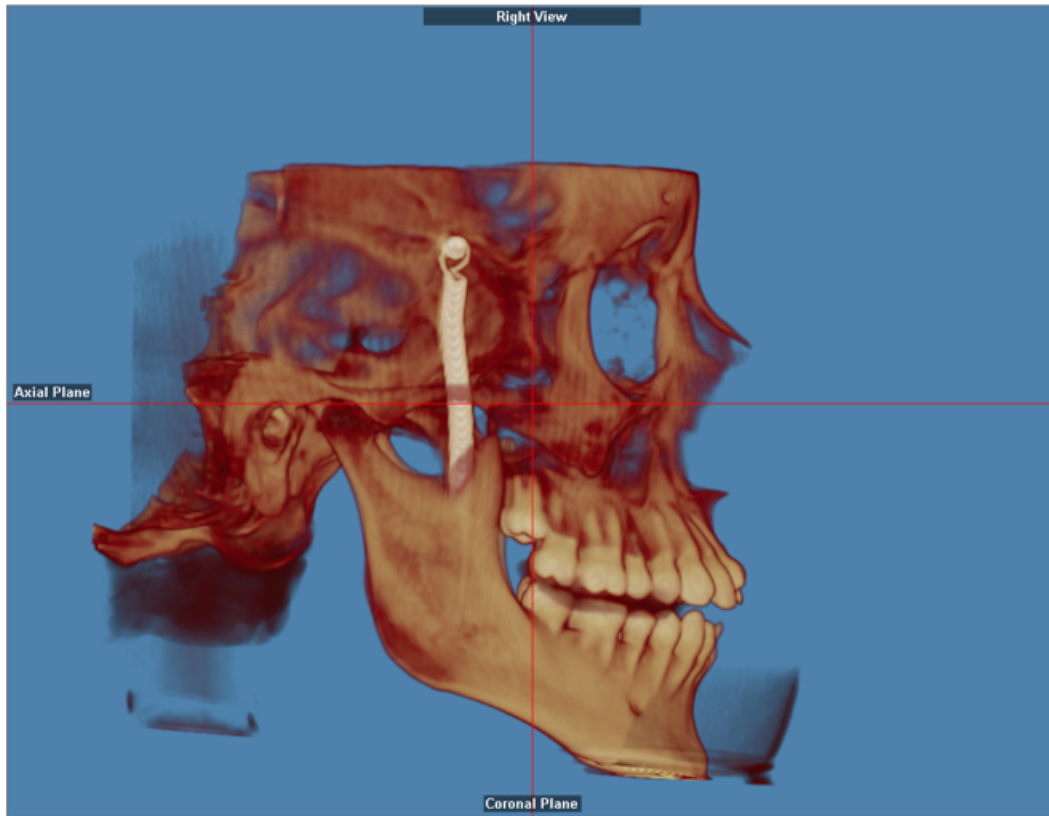


Figure 4. Lateral Right view of 3D CBCT with Frankfort Horizontal Parallel to the Floor.

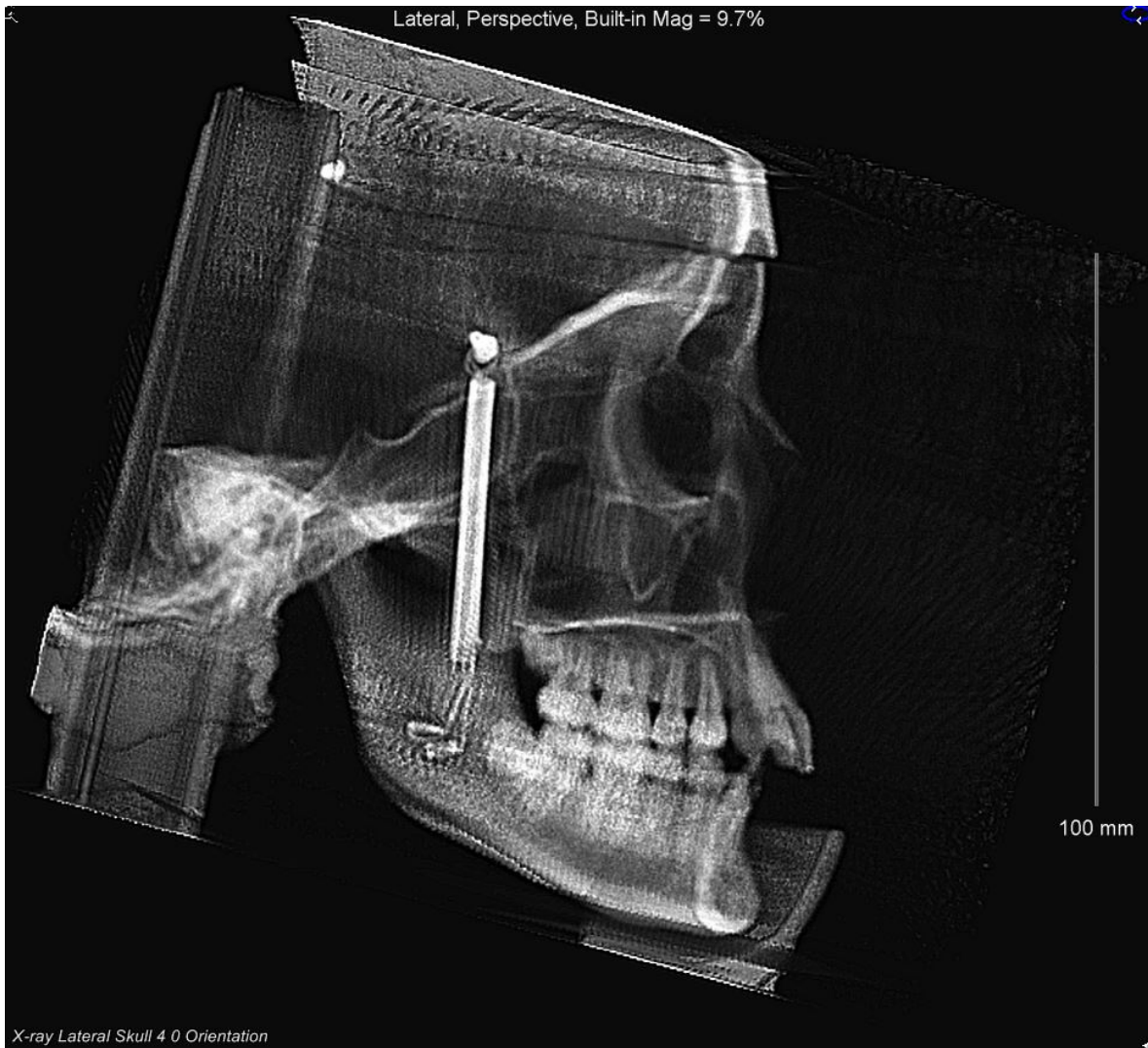


Figure 5. Generated Cephalometric Radiograph in Ideal Position (0°).

Skull 1

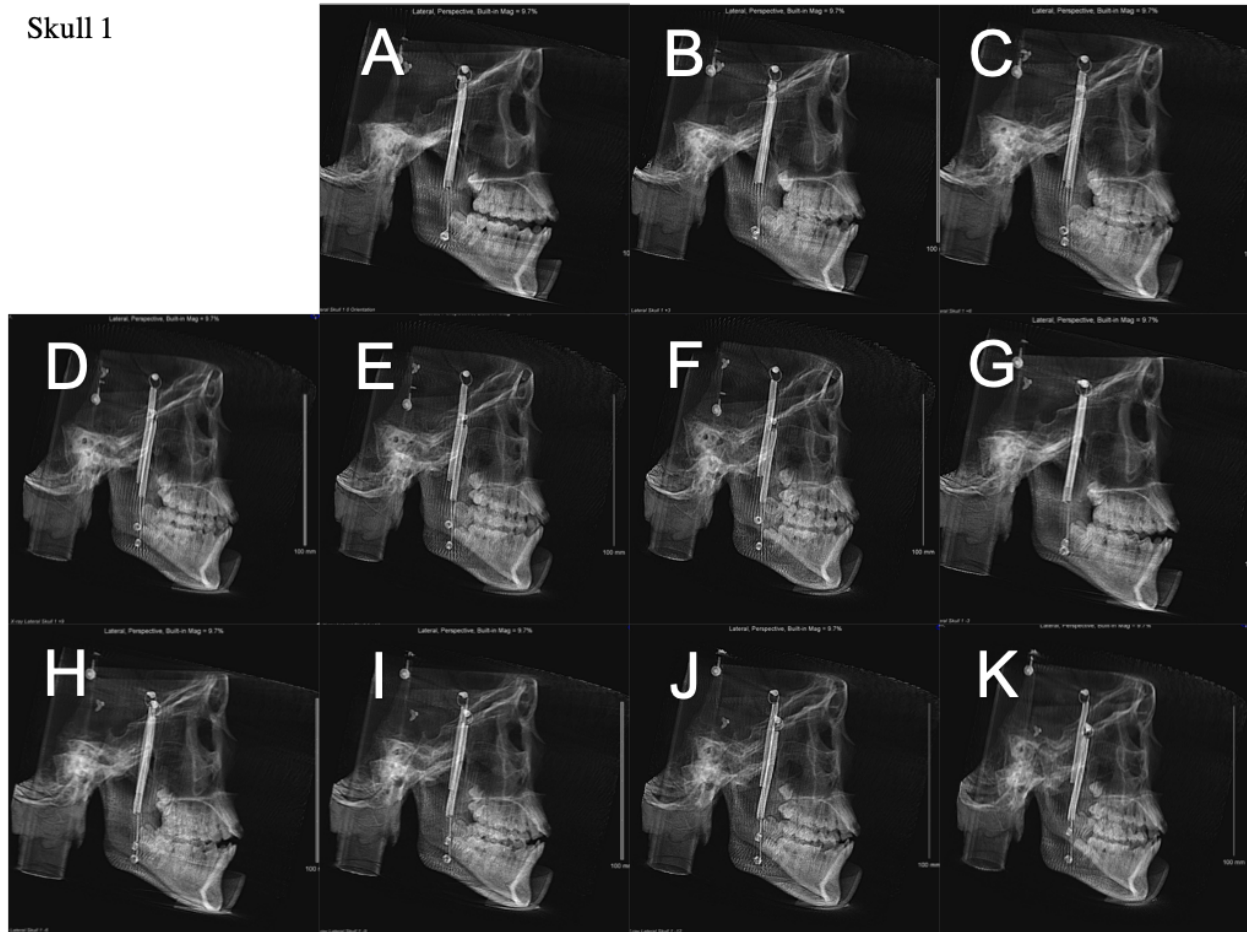


Figure 6. Skull 1: Cephalometric radiographs taken under 0° (A), 3° (B), 6° (C), 9° (D), 12° (E), 15° (F), -3° (G), -6° (H), -9° (I), -12° (J), -15° (K)

3.5 Cephalometric Landmark and Tracing

Each generated JPEG cephalometric radiograph image was landmarked in Dolphin 3D® with the following points:

- Porion
- Orbitale
- Key Ridge
- Temporale
- Sella
- Clinoidale

- Roof of orbit
- Supraorbitale
- Nasion
- Basion
- B point
- Pogonion
- Anatomical Gnathion
- Menton
- Gonion
- Ramus Point
- Mid Ramus
- Sigmoid Notch
- Articulare
- Condylion
- A point
- Anterior nasal spine
- Posterior nasal spine
- L1 Tip
- L1 Root
- Internal Symphysis Superior
- Internal Symphysis Inferior
- U1 Tip
- U1 Root

When difficulty was found with certain landmarks, the operator adjusted the brightness, gamma, contrast, emboss, and/or invert settings to improve visualization of structures.

The 3D CBCT generated lateral cephalograms were loaded into Dolphin 3D® and each cephalogram was traced by a single operator (Figure 7). When bilateral structures appeared as dual images, the operator bisected the difference and selected the midpoint between the two structures.



Figure 7. Cephalometric Radiograph Tracing.

3.6 **Dolphin 3D® Custom Cephalometric Analysis**

A custom analysis was created in Dolphin 3D® for the following linear and angular measurements (Table I):

TABLE I
LINEAR AND ANGULAR MEASUREMENTS

LINEAR MEASUREMENTS	Horizontal Measurements	<ul style="list-style-type: none"> • S-N • Go-Me • ANS-PNS
	Vertical Measurements	<ul style="list-style-type: none"> • N-Me (Anterior Facial Height) • S-Go (Posterior Facial Height)
ANGULAR MEASUREMENTS	<ul style="list-style-type: none"> • SNA • SNB • ANB • FMA • U1-SN • Angle of Convexity (NA-Apo) • Y-axis (SGn-FH) • Gonial Angle (Ar-Go-Me) • L1-MP • Mandibular Plane Angle (MP-SN) • U1-PP 	

Measurements were extracted from Dolphin 3D® and were recorded in Excel® (Microsoft Excel for Mac, Version 16.16.1). A Dell monitor was used for all cephalometric measurements.

3.7 **Reliability Testing**

Intra-examiner and inter-examiner reliability testing were performed for cephalometric radiograph measuring techniques. To assess intra-examiner reliability, the operator landmarked and traced 10 ideally positioned lateral cephalometric radiographs (0°) on two separate occasions one week apart.

To assess inter-operator reliability, another researcher working independently landmarked and traced 10 ideally positioned (0°) lateral cephalometric radiographs.

3.8 **Data Analysis**

Cephalometric radiographs of different orientations were compared to the ideal (0°) cephalometric radiograph. Measurement data recorded in an Excel® spreadsheet were used to obtain a delta (Δ) by subtracting the cephalometric measurements obtained from the ideal (0°) cephalometric radiograph from the cephalometric measurements obtained at various degrees of skull orientation. The average delta value was obtained and plotted in Figure 8, 9. Shapiro-Wilks normality test showed that the majority of the study variables have a normal distribution. Student *t* tests were performed. Statistical significance was set at 0.05.

T-Test/One sample statistic was used to compare the mean differences of linear and angular measurements between the 0° cephalogram and each of the following degrees: -15°, -12°, -9°, -6°, -3°, 0°, +3°, +6°, +9°, +12°, +15°. Statistical significance was set at 0.05. Statistical analysis was performed using IBM SPSS Statistics® for Windows (Version 22.0, IBM Corp., Armonk NY).

IV. RESULTS

4.1 **Reliability**

The inter reliability of the measurement results using the intra-class correlation coefficient (ICC) was good (>0.90). The intraclass correlation coefficients for all study variables range from 0.952 to 0.998 (95% CI; 0.805 – 0.999), p-values <0.05 for all the study variables: S-N, Go-Me, ANS-PNS, N-Me, S-Go, SNA, SNB, ANB, FMA, U1-SN, NA-APo, SGn-FH, Ar-Go-Me, L1-MP, MP-SN, U1-PP.

4.2 **Rotated Skull Cephalograms vs Ideal 0° Cephalogram**

The T-test indicated that angular variables NA-Apo, L1-MP, and U1-PP did not demonstrate statistically significant mean differences in any of the distances from zero (0), p-values >0.05 . Test results for all skull rotations about the sagittal axis are presented in Tables II, III, and IV, V and in Figure 8.

TABLE II

TEST RESULTS FOR ANGULAR MEASUREMENTS

Degrees Angular	3			6			9			12			15			
	N	Mean	Std. Deviation	Sig. (2-tailed)												
SNA	24	0.1292	0.60540	0.307	0.3333	0.81862	0.058	0.7125	0.90377	0.000	0.9833	0.87609	0.000	1.7958	1.64356	0.000
SNB	24	0.2875	0.55350	0.018	0.3042	0.64030	0.029	0.6583	0.65070	0.000	0.8625	0.72521	0.000	1.5792	1.42858	0.000
ANB	24	-0.1417	0.47632	0.159	0.0625	0.45855	0.511	0.0542	0.62134	0.288	0.1250	0.56280	0.288	0.2583	0.56792	0.036
FMA	24	-0.1292	1.38265	0.651	-0.0125	1.86205	0.974	0.0458	2.05807	0.493	-0.3708	2.60826	0.493	-1.7750	2.86148	0.006
U1-SN	24	-0.3542	1.14890	0.145	0.3167	1.74123	0.382	-0.0167	2.20112	0.956	-0.0250	2.20498	0.956	1.3333	2.95144	0.037
NA-Apo	24	-0.3292	0.97868	0.113	0.0708	0.99235	0.730	-0.0042	1.27227	0.626	0.1292	1.28045	0.626	0.1250	1.16218	0.603
SGn-FH	24	0.1083	1.35387	0.699	-0.1000	2.00326	0.809	-0.3000	1.90833	0.145	-0.7667	2.48817	0.145	-2.0000	2.84758	0.002
Ar-Go-Me	24	-0.1042	1.50751	0.738	0.6250	1.82977	0.108	0.7750	1.56573	0.010	1.4417	2.50198	0.010	1.6708	2.74376	0.007
L1-MP	24	0.1500	1.71414	0.672	-0.1083	2.07551	0.800	-0.2167	2.46094	0.750	-0.1708	2.59187	0.750	-0.5208	3.08178	0.416
SN-MP	24	-0.1583	0.81823	0.353	0.0875	1.11016	0.703	0.0125	0.99796	0.018	-0.7042	1.34955	0.018	-1.6250	1.66505	0.000
U1-PP	24	-0.3500	1.36031	0.220	0.4667	1.65967	0.182	0.4667	1.65967	0.747	0.1583	2.37137	0.747	1.1375	3.30689	0.105

Degrees Angular	-3			-6			-9			-12			-15			
	N	Mean	Std. Deviation	Sig. (2-tailed)												
SNA	24	-0.2958	0.59453	0.023	-0.1500	0.97043	0.457	-0.4208	1.15833	0.088	-0.1042	1.22172	0.680	0.2750	1.46740	0.368
SNB	24	-0.2333	0.41668	0.012	-0.2417	0.53966	0.039	-0.4000	0.78906	0.021	-0.1875	0.91286	0.325	0.1875	1.12687	0.423
ANB	24	-0.0583	0.44907	0.531	0.1000	0.70772	0.496	-0.0167	0.66898	0.904	0.0750	0.58551	0.536	0.0792	0.66003	0.563
FMA	24	-0.8500	2.31817	0.086	-0.9333	2.12494	0.042	-0.9583	2.18392	0.042	-1.9167	2.00752	0.000	-1.9958	2.63017	0.001
U1-SN	24	-0.4292	1.32287	0.126	-0.6875	1.57129	0.043	-0.7833	1.75367	0.039	-0.5375	2.02029	0.205	0.2250	2.36335	0.645
NA-Apo	24	-0.3000	1.03083	0.167	0.1042	1.47986	0.733	-0.1708	1.42141	0.562	0.1042	1.19800	0.674	-0.0042	1.47338	0.989
SGn-FH	24	-0.2917	1.73904	0.420	-0.7958	2.09564	0.076	-0.6958	1.81910	0.074	-1.3750	2.17080	0.005	-1.3375	2.83607	0.030
Ar-Go-Me	24	0.5208	1.62828	0.131	0.3583	1.57891	0.278	0.6375	1.75098	0.088	0.4333	2.19697	0.344	0.5250	2.54272	0.322
L1-MP	24	-0.6583	1.75299	0.079	-0.8208	2.16152	0.076	-0.2875	2.95448	0.638	-0.2375	2.69409	0.670	-0.1125	4.20355	0.897
SN-MP	24	0.2250	0.85935	0.212	-0.1500	0.99957	0.470	-0.3500	1.13903	0.146	-1.3958	1.50607	0.000	-2.2583	1.72120	0.000
U1-PP	24	0.1708	1.61796	0.610	-0.5417	1.81848	0.158	-0.1500	1.49376	0.627	0.2667	2.34700	0.583	0.1250	2.46458	0.806

TABLE III

TEST RESULTS FOR LINEAR MEASUREMENTS

Linear	3				6			9			12			15		
	N	Mean	Std. Deviation	Sig. (2-tailed)												
S-N	24	-0.0458	0.45776	0.628	-0.0958	0.47866	0.337	-0.1250	0.56434	0.289	-0.2042	0.55127	0.083	-0.2583	1.24897	0.321
Go-Me	24	0.1333	1.75020	0.712	-0.4958	1.94232	0.224	0.5208	1.81179	0.172	-0.6917	2.29421	0.153	-1.2917	3.06011	0.050
ANS-PNS	24	-0.0167	1.15105	0.944	-0.2042	1.28316	0.444	-0.4875	1.54309	0.135	-0.3292	1.79237	0.378	-0.5958	2.71060	0.293
N-Me	24	-0.0667	0.96173	0.737	-0.4042	0.96300	0.051	-1.1542	0.95461	0.000	-2.4917	1.25071	0.000	-3.8958	1.84213	0.000
S-Go	24	0.1042	1.09484	0.646	-0.1583	1.39873	0.585	-1.1292	1.38045	0.001	-0.7625	1.97260	0.071	-0.9208	1.93053	0.029

Linear	-3				-6			-9			-12			-15		
	N	Mean	Std. Deviation	Sig. (2-tailed)												
S-N	24	0.1208	0.52002	0.267	0.2375	0.58741	0.060	0.3958	0.66364	0.008	0.4917	0.51408	0.000	0.3667	0.96173	0.075
Go-Me	24	-0.2000	1.68342	0.566	-0.4708	2.27758	0.322	-0.7208	2.62082	0.191	-1.5500	1.87036	0.000	-2.1750	3.28279	0.004
ANS-PNS	24	-0.1292	1.40449	0.657	-0.3125	1.28919	0.247	-0.3125	1.74089	0.388	-0.6833	2.12023	0.128	-1.2208	1.78690	0.003
N-Me	24	-0.1167	0.97252	0.562	-0.9542	1.08907	0.000	-1.7125	1.15432	0.000	-3.1042	1.10197	0.000	-4.8958	1.99553	0.000
S-Go	24	-0.2250	1.26706	0.393	-0.4833	1.43335	0.112	-0.9208	1.15381	0.001	-0.8292	2.00748	0.055	-1.4708	2.19178	0.003

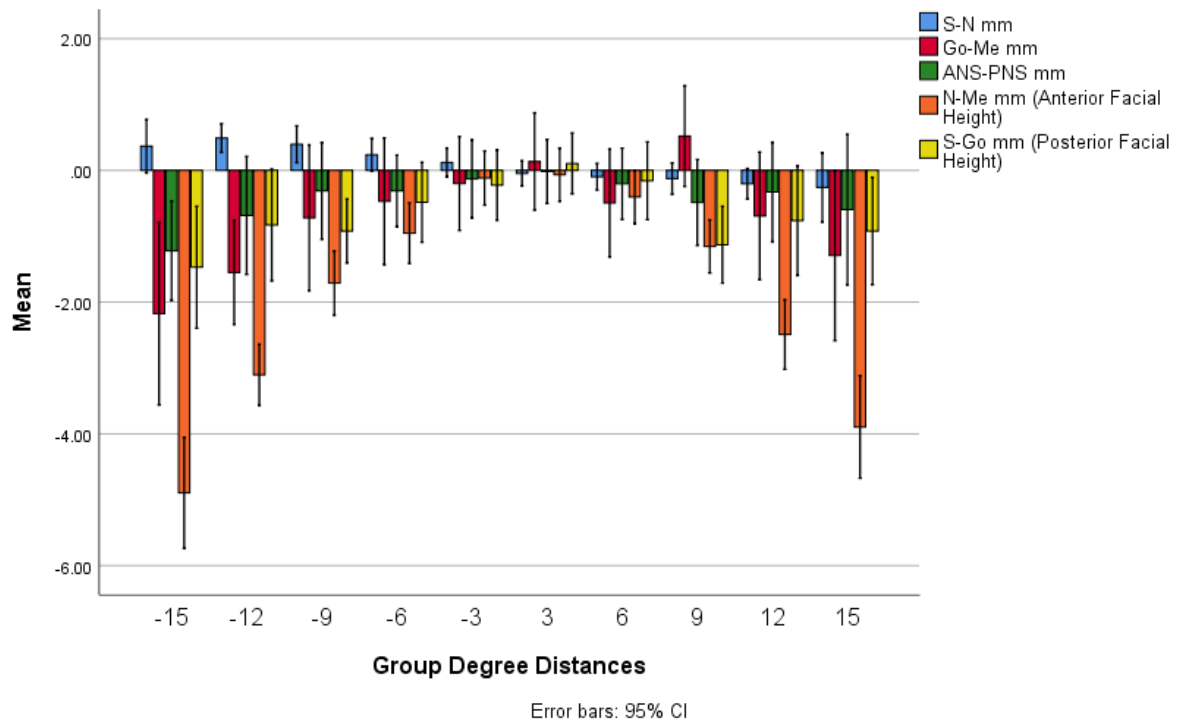


Figure 8. Graph/Bar by group distances-mm.

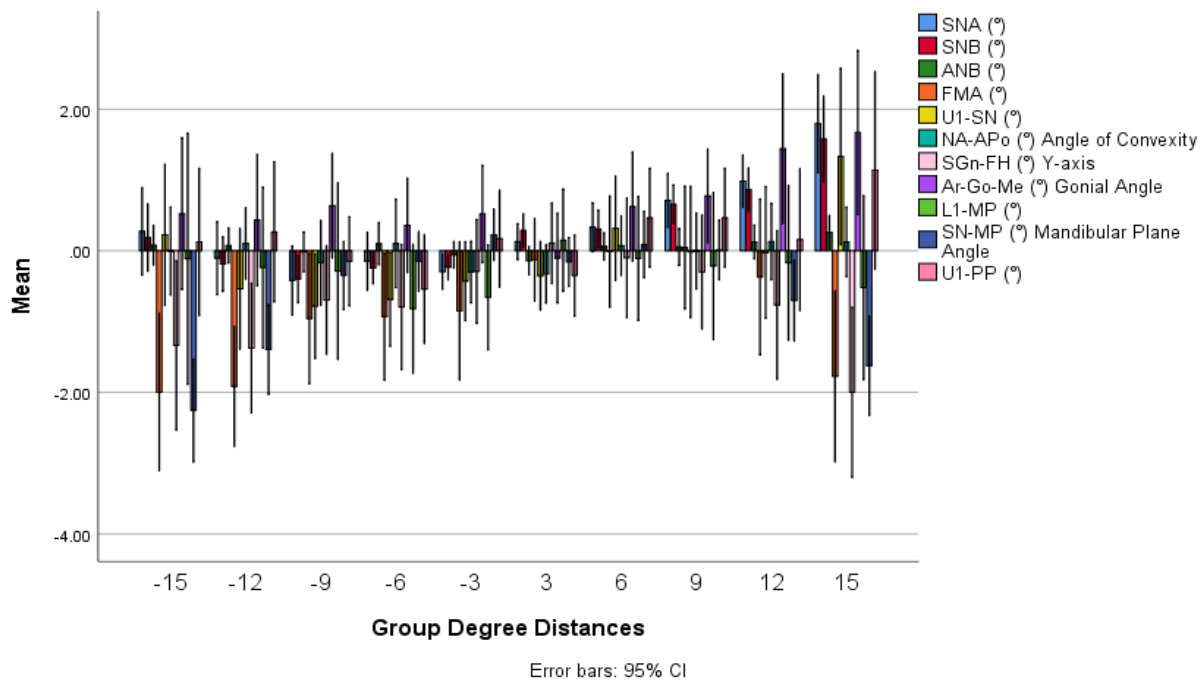


Figure 9 Graph/Bar by group distances-degrees.

TABLE IV

DISTANCES (+/-) FROM 0° WITH AVERAGE STATISTICALLY SIGNIFICANT MEAN

DIFFERENCES

(+) Degrees		3	6	9	12	15
Linear Measurements	Vertical		N-Me	N-Me S-Go	N-Me	N-Me S-Go
	Horizontal					Go-Me
Angular Measurements		SNB	SNB	SNA SNB Ar-Go-Me	SNA SNB Ar-Go-Me MP-SN	SNA SNB ANB FMA U1-SN SGn-FH Ar-Go-Me M-SNP
(-) Degrees		-3	-6	-9	-12	-15
Linear Measurements	Vertical		N-Me	N-Me S-Go	N-Me S-Go	N-Me S-Go
	Horizontal			S-N	S-N Go-Me	Go-Me ANS-PNS
Angular Measurements		SNA SNB	SNB FMA U1-SN	SNB FMA U1-SN	FMA SGn-FH MP-SN	FMA SGn-FH MP-SN

TABLE V

95% CONFIDENCE INTERVAL OF THE DIFFERENCE

Angular	Degrees				95% Confidence Interval of the Difference		6			95% Confidence Interval of the Difference		15			95% Confidence Interval of the Difference	
	N	Mean	Std. Deviation	Sig. (2-tailed)	Lower	Upper	Mean	Std. Deviation	Sig. (2-tailed)	Lower	Upper	Mean	Std. Deviation	Sig. (2-tailed)	Lower	Upper
SNA	24	0.1292	0.60540	0.307	-0.1265	0.3848	0.3333	0.81862	0.058	-0.0123	0.6790	1.7958	1.64356	0.000	1.1018	2.4898
SNB	24	0.2875	0.55350	0.018	0.0538	0.5212	0.3042	0.64030	0.029	0.0338	0.5745	1.5792	1.42858	0.000	0.9759	2.1824
ANB	24	-0.1417	0.47632	0.159	-0.3428	0.0595	0.0625	0.45855	0.511	-0.1311	0.2561	0.2583	0.56792	0.036	0.0185	0.4981
FMA	24	-0.1292	1.38265	0.651	-0.7130	0.4547	-0.0125	1.86205	0.974	-0.7988	0.7738	-1.7750	2.86148	0.006	-2.9833	-0.5667
U1-SN	24	-0.3542	1.14890	0.145	-0.8393	0.1310	0.3167	1.74123	0.382	-0.4186	1.0519	1.3333	2.95144	0.037	0.0870	2.5796
NA-Apo	24	-0.3292	0.97868	0.113	-0.7424	0.0841	0.0708	0.99235	0.730	-0.3482	0.4899	0.1250	1.16218	0.603	-0.3657	0.6157
SGn-FH	24	0.1083	1.35387	0.699	-0.4634	0.6800	-0.1000	2.00326	0.809	-0.9459	0.7459	-2.0000	2.84758	0.002	-3.2024	-0.7976
Ar-Go-Me	24	-0.1042	1.50751	0.738	-0.7407	0.5324	0.6250	1.82977	0.108	-0.1476	1.3976	1.6708	2.74376	0.007	0.5122	2.8294
L1-MP	24	0.1500	1.71414	0.672	-0.5738	0.8738	-0.1083	2.07551	0.800	-0.9847	0.7681	-0.5208	3.08178	0.416	-1.8222	0.7805
SN-MP	24	-0.1583	0.81823	0.353	-0.5038	0.1872	0.0875	1.11016	0.703	-0.3813	0.5563	-1.6250	1.66505	0.000	-2.3281	-0.9219
U1-PP	24	-0.3500	1.36031	0.220	-0.9244	0.2244	0.4667	1.65967	0.182	-0.2341	1.1675	1.1375	3.30689	0.105	-0.2589	2.5339

Angular	Degrees				95% Confidence Interval of the Difference		-6			95% Confidence Interval of the Difference		-15			95% Confidence Interval of the Difference	
	N	Mean	Std. Deviation	Sig. (2-tailed)	Lower	Upper	Mean	Std. Deviation	Sig. (2-tailed)	Lower	Upper	Mean	Std. Deviation	Sig. (2-tailed)	Lower	Upper
SNA	24	-0.2958	0.59453	0.023	-0.5469	-0.0448	-0.1500	0.97043	0.457	-0.5598	0.2598	0.2750	1.46740	0.368	-0.3446	0.8946
SNB	24	-0.2333	0.41668	0.012	-0.4093	-0.0574	-0.2417	0.53966	0.039	-0.4695	-0.0138	0.1875	1.12687	0.423	-0.2883	0.6633
ANB	24	-0.0583	0.44907	0.531	-0.2480	0.1313	0.1000	0.70772	0.496	-0.1988	0.3988	0.0792	0.66003	0.563	-0.1995	0.3579
FMA	24	-0.8500	2.31817	0.086	-1.8289	0.1289	-0.9333	2.12494	0.042	-1.8306	-0.0361	-1.9958	2.63017	0.001	-3.1065	-0.8852
U1-SN	24	-0.4292	1.32287	0.126	-0.9878	0.1294	-0.6875	1.57129	0.043	-1.3510	-0.0240	0.2250	2.36335	0.645	-0.7730	1.2230
NA-Apo	24	-0.3000	1.03083	0.167	-0.7353	0.1353	0.1042	1.47986	0.733	-0.5207	0.7291	-0.0042	1.47338	0.989	-0.6263	0.6180
SGn-FH	24	-0.2917	1.73904	0.420	-1.0260	0.4427	-0.7958	2.09564	0.076	-1.6807	0.0891	-1.3375	2.83607	0.030	-2.5351	-0.1399
Ar-Go-Me	24	0.5208	1.62828	0.131	-0.1667	1.2084	0.3583	1.57891	0.278	-0.3084	1.0251	0.5250	2.54272	0.322	-0.5487	1.5987
L1-MP	24	-0.6583	1.75299	0.079	-1.3986	0.0819	-0.8208	2.16152	0.076	-1.7336	0.0919	-0.1125	4.20355	0.897	-1.8875	1.6625
SN-MP	24	0.2250	0.85935	0.212	-0.1379	0.5879	-0.1500	0.99957	0.470	-0.5721	0.2721	-2.2583	1.72120	0.000	-2.9851	-1.5315
U1-PP	24	0.1708	1.61796	0.610	-0.5124	0.8540	-0.5417	1.81848	0.158	-1.3095	0.2262	-0.1250	2.46458	0.806	-0.9157	1.1657

Linear	Degrees				95% Confidence Interval of the Difference		6			95% Confidence Interval of the Difference		15			95% Confidence Interval of the Difference	
	N	Mean	Std. Deviation	Sig. (2-tailed)	Lower	Upper	Mean	Std. Deviation	Sig. (2-tailed)	Lower	Upper	Mean	Std. Deviation	Sig. (2-tailed)	Lower	Upper
S-N	24	-0.0458	0.45776	0.628	-0.2391	0.1475	-0.0958	0.47866	0.337	-0.2980	0.1063	-0.2583	1.24897	0.321	-0.7857	0.2691
Go-Me	24	0.1333	1.75020	0.712	-0.6057	0.8724	-0.4958	1.94232	0.224	-1.3160	0.3243	-1.2917	3.06011	0.050	-2.5838	0.0005
ANS-PNS	24	-0.0167	1.15105	0.944	-0.5027	0.4694	-0.2042	1.28316	0.444	-0.7460	0.3377	-0.5958	2.71060	0.293	-1.7404	0.5488
N-Me	24	-0.0667	0.96173	0.737	-0.4728	0.3394	-0.4042	0.96300	0.051	-0.8108	0.0025	-3.8958	1.84213	0.000	-4.6737	-3.1180
S-Go	24	0.1042	1.09484	0.646	-0.3581	0.5665	-0.1583	1.39873	0.585	-0.7490	0.4323	-0.9208	1.93053	0.029	-1.7360	-0.1056

Linear	Degrees				95% Confidence Interval of the Difference		-6			95% Confidence Interval of the Difference		-15			95% Confidence Interval of the Difference	
	N	Mean	Std. Deviation	Sig. (2-tailed)	Lower	Upper	Mean	Std. Deviation	Sig. (2-tailed)	Lower	Upper	Mean	Std. Deviation	Sig. (2-tailed)	Lower	Upper
S-N	24	0.1208	0.52002	0.267	-0.0988	0.3404	0.2375	0.58741	0.060	-0.0105	0.4855	0.3667	0.96173	0.075	-0.0394	0.7728
Go-Me	24	-0.2000	1.68342	0.566	-0.9108	0.5108	-0.4708	2.27758	0.322	-1.4326	0.4909	-2.1750	3.28279	0.004	-3.5612	-0.7888
ANS-PNS	24	-0.1292	1.40449	0.657	-0.7222	0.4639	-0.3125	1.28919	0.247	-0.8569	0.2319	-1.2208	1.78690	0.003	-1.9754	-0.4663
N-Me	24	-0.1167	0.97252	0.562	-0.5273	0.2940	-0.9542	1.08907	0.000	-1.4140	-0.4943	-4.8958	1.99553	0.000	-5.7385	-4.0532
S-Go	24	-0.2250	1.26706	0.393	-0.7600	0.3100	-0.4833	1.43335	0.112	-1.0886	0.1219	-1.4708	2.19178	0.003	-2.3963	-0.5453

TABLE VICONSIDERING ± 0.5 ($^{\circ}$) DISTANCE OF CLINICAL SIGNIFICANCE

Degrees (+)	3	6	15
Angular Measurement	SNB	SNB	ANB
Degrees (-)	-3		
Angular Measurement	SNA SNB		

4.3 **Output Results**

4.3.1 **Angular Measurement Variables**

Three of the angular variables: NA-Apo, L1-MP, and U1-PP, out of the eleven angular variables, the mean deviation calculated between the mean on any of the study distances in consideration and the reference mean from the distance of zero (0°) were not statistically significant, (Table II, III, IV, V).

ANB, out of the eleven angular variables, the mean deviation calculated between the mean of the study distances in consideration and the reference mean from the distance of zero (0°) were not statistically significant, except on the $+15^\circ$. Although the mean deviations were statistically significant on $+15^\circ$, the deviations were determined to be not clinically significant, (Table II, III, IV, V).

SNA, out of the eleven angular variables, the mean deviation calculated between the mean of the study distances in consideration and the reference mean from the distance of zero (0°) were not statistically significant, except on the $+15^\circ$, $+12^\circ$, $+9^\circ$, and -3° . Although the mean deviations were statistically significant on -3° , the deviations were determined to be not clinically relevant, (Table II, III, IV, V).

SNB, out of the eleven angular variables, the mean deviation calculated between the mean of any of the study distances in consideration and the reference mean from the distance of zero (0°) were not statistically significant, except on the $+15^\circ$, $+12^\circ$, $+9^\circ$, $+6^\circ$, $+3^\circ$, -3° , -6° , -9° . Although the mean deviations were statistically significant on $+3^\circ$, -3° , the deviations were determined to be not clinically relevant, (Table II, III, IV, V).

FMA, out of the eleven angular variables, the mean deviation calculated between the mean of any of the study distances in consideration and the reference mean from the distance of zero (0°) were not statistically significant, except on the $+15^\circ$, -6° , -9° , -12° , and -15° , (Table II, III, IV, V).

U1-SN, out of the eleven angular variables, the mean deviation calculated between the mean of any of the study distances in consideration and the reference mean from the distance of zero (0°) were not statistically significant, except on the $+15^\circ$, -6° , and -9° , (Table II, III, IV, V).

SGn-FH, out of the eleven angular variables, the mean deviation calculated between the mean of any of the study distances in consideration and the reference mean from the distance of zero (0°) were not statistically significant, except on the $+15^\circ$, -12° , and -15° , (Table II, III, IV, V).

Ar-Go-Me, out of the eleven angular variables, the mean deviation calculated between the mean of any of the study distances in consideration and the reference mean from the distance of zero (0°) were not statistically significant, except on the $+15^\circ$, $+12^\circ$, and $+9^\circ$, (Table II, III, IV, V).

SN-MP, out of the eleven angular variables, the mean deviation calculated between the mean of any of the study distances in consideration and the reference mean from the distance of zero (0°) were not statistically significant, except on the $+15^\circ$, $+12^\circ$, -12° , and -15° , (Table II, III, IV, V).

4.3.2 **Linear Measurement Variables**

S-N, out of the five linear variables, the mean deviation calculated between the mean of any of the study distances in consideration and the reference mean from the distance of zero (0°) were not statistically significant, except on the -9° , and -12° , (Table II, III, IV, V).

Go-Me, out of the five linear variables, the mean deviation calculated between the mean of any of the study distances in consideration and the reference mean from the distance of zero (0°) were not statistically significant, except on the -12° , and -15° , (Table II, III, IV, V).

ANS-PNS, out of the five linear variables, the mean deviation calculated between the mean of any of the study distances in consideration and the reference mean from the distance of zero (0°) were not statistically significant, except on the -15° , (Table II, III, IV, V).

N-Me, out of the five linear variables, the mean deviation calculated between the mean of any of the study distances in consideration and the reference mean from the distance of zero (0°) were not statistically significant, except on the $+15^\circ$, $+12^\circ$, $+9^\circ$, -6° , and -9° , -12° , -15° , (Table II, III, IV, V).

S-Go, out of the five linear variables, the mean deviation calculated between the mean of any of the study distances in consideration and the reference mean from the distance of zero (0°) were not statistically significant, except on the $+15^\circ$, $+9^\circ$, -9° , and -15° , (Table II, III, IV, V).

Angular measurements ANB, NA-APo, Ar-Go-Me, L1-MP, and U1-PP did not indicate statistically significant mean differences in any of the negative distances, p -values >0.05 (Table II). Angular variables NA-Apo, L1-MP, and U1-PP did not indicate statistically significant mean differences in any of the distances from 0° , p -values >0.05 (Table II).

The distance 3° from 0° indicated statistically significant mean differences, p -values <0.05 , only on the angular variables SNB (positive and negative distances) and SNA (negative distance) (Table II, IV).

For the purpose of this study, considering less than $\pm 0.5^\circ$ clinically acceptable, the variable SNB at 3° in both positive and negative distances from 0° are not clinically significant with the mean difference, SD, and 95% confidence interval of the difference showing values as: (+0.29; -0.23), (0.55; 0.42), and 95% C.I. ranging from: (-0.41 to +0.52); respectively (Table V). In this case, SNB does not show clinically significant mean differences at the distance $\pm 3^\circ$ from 0° (Table VI). The variable SNA at 3° in the negative distance from 0° are not clinically significant with the mean difference, SD, and 95% confidence interval of the difference showing values as: (-0.30), (+0.59), and 95% C.I. ranging from: (-0.55 to -0.04); respectively (Table V). SNA does not show clinically significant mean differences at distance -3° from 0° (Table VI).

Based on these results, the null hypothesis was accepted for three of the angular variables: NA-Apo, L1-MP, and U1-PP, for all the distances, $\pm 3^\circ$ through $\pm 15^\circ$, p -values >0.05 .

The null hypothesis was accepted for most of the variables on $\pm 3^\circ$, $p\text{-value} > 0.05$, except for SNB $\pm 3^\circ$, and SNA -3° , $p\text{-values} < 0.05$. Although these deviations were determined to be not clinically relevant.

The null hypothesis was accepted for the variable ANB, $p\text{-value} > 0.05$, except for ANB $+15$, $p\text{-value} < 0.05$. Although this deviation was determined to be not clinically relevant.

The null hypothesis was rejected for many of the variables in the cephalometric measurements when the skull is rotated $\pm 6^\circ$ through $\pm 15^\circ$, $p\text{-value} < 0.05$.

V. DISCUSSION

5.1 **Relation to Other Studies**

Cephalometric radiographs are operator technique sensitive and when the patient's head is improperly positioned within head holding device, distortion is evident (Ahlqvist, Eliasson, and Welander 1986; Baumrind and Frantz 1971; Bergersen 1980; Forsberg, Burstone, and Hanley 1984; Ghafari, Cater, and Shofer 1995; Hsiao, Chang, and Liu 1997). Others authors have stated that due to positioning errors of the head, cephalometric analysis of linear and angular measurements can vary (Tng et al. 1993), thus the analysis has technical limitations and can render measurements inaccurate. Our study assessed for variability between the different degrees of head rotation along the sagittal axis.

5.1.1 **Landmarking**

During this study, the principle investigator noticed difficulty landmarking cephalometric radiographs that had greater than $\pm 9^\circ$ of skull rotation. The amount of magnification, distortion and ill-aligned bilateral landmarks made anatomical landmark allocation challenging. Bilateral structures were situated on opposite sides of the rotational axis hence landmarks moved in opposite directions when the skull was rotated. Thus, the resultant image can either increase or decrease in superimposition of landmarks. Some bilateral landmarks were nearly 10-25mm apart, making the process of bisecting the difference and selecting the midpoint between the two structures difficult. An example of an ideal skull position and an example of these ill-positioned bilateral structure at -15° are illustrated in Figure 9 where right and left Orbitales are 19mm apart, Gonions are 23.5mm apart, Condylions are 25.4mm apart, and Porions are 18.0mm apart.

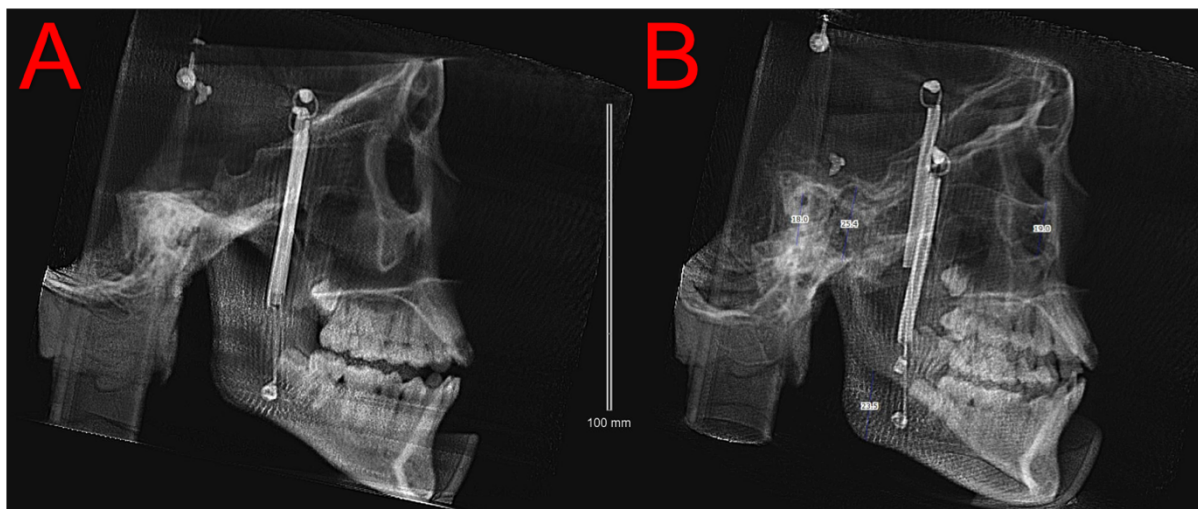


Figure 10. A: Ideal Skull Position, B: Skull at -15° Rotation.

According to Baumrind and Franz, certain anatomical landmarks, such as Condylion, Basion, Orbitale, ANS, and PNS are potentially more prone to error because of overlapping structures over the landmarks being identified (Baumrind & Frantz, 1971). It has also been previously reported that identification of Porion can have accuracy and precision problems (Y. J. Chen et al. 2000). The identification of landmarks along a gradual curve, such as Pogonion, Menton, Gnathion, Gonion, A point, and B point rather than a point on an edge is more difficult to pinpoint and errors are proportionately larger (Baumrind and Frantz 1971). Likewise, radiographic quality can affect identification of landmarks such as Pogonion, Condylion, Orbitale, Anterior Nasal Spine, B point, Pogonion, Gonion, and Glabella (Gravely and Benzies 1974).

Some authors have argued that landmark identification errors of less than 1 mm are unlikely to be of clinical significance (Y. J. Chen et al. 2004; McClure et al. 2005). Thus, landmark errors of 1.5mm should be avoided whereas landmarks with errors 2.5mm or greater should

certainly be avoided (Major et al. 1996). In our study, Go-Me, N-Me, S-Go, SNA, SNB, FMA, SGn-FH, Ar-Go-Me, and MP-SN show measurement error in both linear and angular measurements and have the landmarks Gonion, Menton, A Point, B Point, and Gnathion in common, which are known to be associated with landmark errors as mentioned above (Baumrind 1971). To help reduce landmark identification errors for ambiguous and superimposed structures, digital processing was facilitated via Dolphin 3D® software in an attempt to enhance image contrast. Authors have previously demonstrated that radiographic films can be digitally enhanced to achieve better contrast and density so anatomical structures can be visually improved and better discerned. (Ishida et al. 1984; Macri and Wenzel 1993).

5.1.2 **Linear Measurements**

Our study found that horizontal linear measurements S-N and ANS-PNS are not statistically significant in any of the positive distances, p -values > 0.05 . This is either likely due to the fact that the midsagittal landmarks used to obtain the measurement are near the sagittal axis of rotation or because both sella and nasion landmarks are on the same side of the axis of rotation thus are affected less. However, ANS-PNS was statistically significant at -15° due to distortion. Both S-N and ANS-PNS are the most reliable linear measurements in the positive distances. The horizontal linear measurement Go-Me was statistically significant at -15° , -12° , $+15^\circ$. Gonion is a bilateral landmark, and the mandibular length could either be a measurement in the vertical dimension, horizontal dimension, or a resultant of both depending on the mandibular plane angle; the higher the angle the more vertical the mandible. Thus, linear measurements that have a vertical component are affected more when rotated about the sagittal axis due to the rotation itself. The error in the vertical linear measurements N-Me and S-Go at -15° decreased as the skull rotated away from the film, then increased as the skull rotated towards the X-ray source at $+15^\circ$.

Landmarks in the mandible are also vertically farther from the central ray and structurally bilateral, which may be associated with linear measurement error. The vertical linear measurements N-Me and S-Go did not indicate statistically significant mean differences at $\pm 3^\circ$ from 0° . In this study, we have seen that vertical linear measurements have greater measurement errors. Similarly, Yoon et al. found that this resulted because the closer the head rotates towards the film, the image decreases, and that the rotation itself causes the decrease of images (Yoon 2001).

The other factors affecting N-Me and S-Go are when random errors are introduced due to landmarks having unclear definitions and no reference to head position. It has been suggested that Menton, Gonion, and Gnathion landmarks are ambiguous and that some landmark definitions are unclear and are imprecise (Savage, Showfety, and Yancey 1987). Menton is defined as the most inferior point of the chin, Gonion is defined as the most inferior and posterior point on the mandibular angle, and Gnathion is defined as the most anterior and inferior point of the mandibular symphysis. When improper positioning of the head occurs during exposure of a cephalogram, these landmarks become unclear and imprecise, and thus introduce random measurement errors. Figure 9B illustrates an example of how a landmark such as Menton can be difficult to identify when the most inferior point of the mandibular chin is not easily identified.

5.1.3 **Angular Measurements**

SNA and SNB have an increasing upward trend of measurement error as the skulls rotate towards $+15^\circ$, which seems to be due to superimposition of anatomical structures, magnification, and distortion rendering landmark identification of A Point and B Point difficult. SNB shows errors in its angular measurement as early as $\pm 3^\circ$ of skull rotation and SNA shows angular measurement errors at -3° of skull rotation. With skull rotation, the overlap of B Point with incisor

root eminences and landmark position along the gradual concavity of the mandibular symphysis make consistent landmarking a challenge. Therefore, as skull rotation moved towards $+15^\circ$, the greater the magnification and overlap of structures, thus the greater the angular measurement error.

The angular measurements NA-Apo, L1-MP, and U1-PP did not indicate statistically significant mean differences in any of the positive or negative distances, $p\text{-values} > 0.05$. As the skull was tilted at various degrees of rotation, NA-Apo appears to change by similar rates in a proportional manner, having minimal effect on its angular measurement. Similarly, the palatal plane and its associated angle, U1-PP, is in close proximity to the sagittal axis of rotation and the landmarks are on the midsagittal plane, thus there was a minimal effect on the angular measurement (Gaddam et al. 2015; Yoon 2001). The effects on the angular measurement ANB were similar to NA-Apo, L1-MP, and U1-PP and did not indicate statistically significant mean differences in any of the positive or negative distances ($p\text{-values} > 0.05$) with the exception of $+15^\circ$ which is likely due to the increase in the object to film distance introducing significant magnification and distortion. In our study we found that angular measurements NA-Apo, L1-MP, and U1-PP were the most reliable angular measurements and variable ANB is generally reliable in the A-P dimension.

L1-MP is defined as the angle between a line through the long axis of the lower incisor and the mandibular plane. As the mandible rotates about the sagittal axis, the angular measure of L1-MP experiences similar rates of change and seems to have a proportionate relationship. Similar to the variable S-N, L1-MP points are all on the same side of the rotational axis and thus affected less when rotated. We found that identification of the lower incisor apex and incisal tip, or the long axis of the incisors was possible via digital enhancing. Durão et al. established that not all the

landmarks are reproducible (Durão et al. 2015). Condylion, Gnathion, Orbitale, and Anterior Nasal Spine were considered the least reliable, and the lower incisor border was the most consistent (Durão et al. 2015). Angular measurement U1-SN showed statistically significant mean differences at $+15^\circ$, -6° , and -9° (p -values >0.05) which may be due to the overlapping of neighboring incisor tips and the nearby large canine roots making the task of landmarking and tracing inevitably erroneous. However, at -12° and -15° , the operator found that some rotations can actually cause a superimposed structure to be in better position for convenient anatomical landmark identification.

The angular measurement error of FMA gradually increased as the skull rotated in both the positive and negative direction towards $\pm 15^\circ$. This change in angle measurement is thought to be due to the skull rotation itself. As the skull rotated towards the film or towards the X-ray source, the angle decreased. Similarly, angular measurements MP-SN and SGn-FH resulted in an increased error trend towards $\pm 15^\circ$ and it is also thought that this resulted due to the skull rotation itself, overall seeing a decreasing in the angular measurement as the skull moved toward the film or towards the X-ray source.

Ar-Go-Me did not indicate statistically significant mean differences in any of the negative distances (p -values >0.05) but statistically significant mean differences were found at $+9^\circ$, $+12^\circ$, and $+15^\circ$ (p -values <0.05). Articulare is defined as the junctional point between the inferior surface of the cranial base and the posterior ascending rami of the mandibular border and thus is not an anatomical landmark. Figure 10A represents an ideally positioned skull. At skull rotations $+9^\circ$ to $+15^\circ$, the right and left mandibular condyles manifest separately as seen in Figure 10B and were

found to be unreliable and unclear due to magnification, differences between right and left sides, and superimposition of structures.

In general, our study showed that skull rotations in the positive direction had greater angular measurement errors. According to Malkoc et al., depending on the direction of rotation, different planes have different magnifications in different ratios (Malkoc et al. 2005).

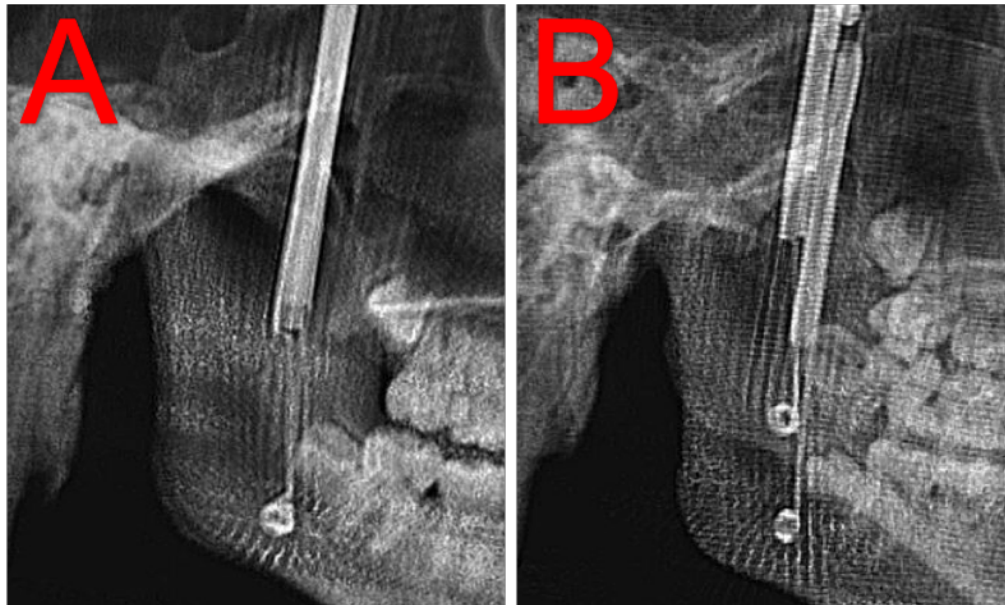


Figure 11. A: Condyles in Ideal Skull Position. B: Condyles in +15° Skull Position.

5.1.4 General Trend Observed in Cephalometric Measurement Errors

Cephalograms of different head rotations were compared to the ideal (0°) cephalogram. A delta (Δ) was obtained by subtracting the cephalometric measurements obtained from the ideal (0°) cephalogram from the cephalometric measurements obtained at various degrees of skull

rotation. Figure 8 illustrates the general trend of cephalometric measurement errors at various degrees of skull orientation. The following represents trends observed from the (-) direction to the (+) direction:

Horizontal Linear Measurements

- S-N: Gradual descending trend
- Go-Me: Ascending then descending trend
- ANS-PNS: Ascending then descending trend

Vertical Linear Measurements

- N-Me: Ascending then descending trend
- S-Go: Ascending then descending trend

Angular Measurements

- SNA: Gradual ascending trend
- SNB: Gradual ascending trend
- ANB: Flat delta trend
- FMA: Ascending then descending trend
- U1-SN: Ascending trend
- NA-Apo: Flat trend
- SGn-FH: Ascending then descending trend
- Ar-Go-Me: Ascending trend
- L1-MP: Flat trend
- MP-SN: Ascending then descending trend
- U1-PP: Ascending trend

5.1.6 **Clinical Relevance and Application**

Linear and angular measurement errors caused by head rotation about the sagittal axis, may lead to diagnostic and interpretation errors during the analysis of lateral cephalometric radiographs. Therefore, during exposure of cephalometric radiographs, the patient's head should be positioned as ideally as possible within the head holding device without any rotations (Figure 11). One must also consider the fact that there is no bilateral symmetry in the face or body and because of the variability among individuals, the ear rods which are symmetrically constructed may iatrogenically induce an unwanted head rotation. Therefore, the operator must be aware of such problems and adjust the head position appropriately so the ear rods do not interfere with the position of the head keeping the interpupillary line parallel to the floor (Salzmann 1964).

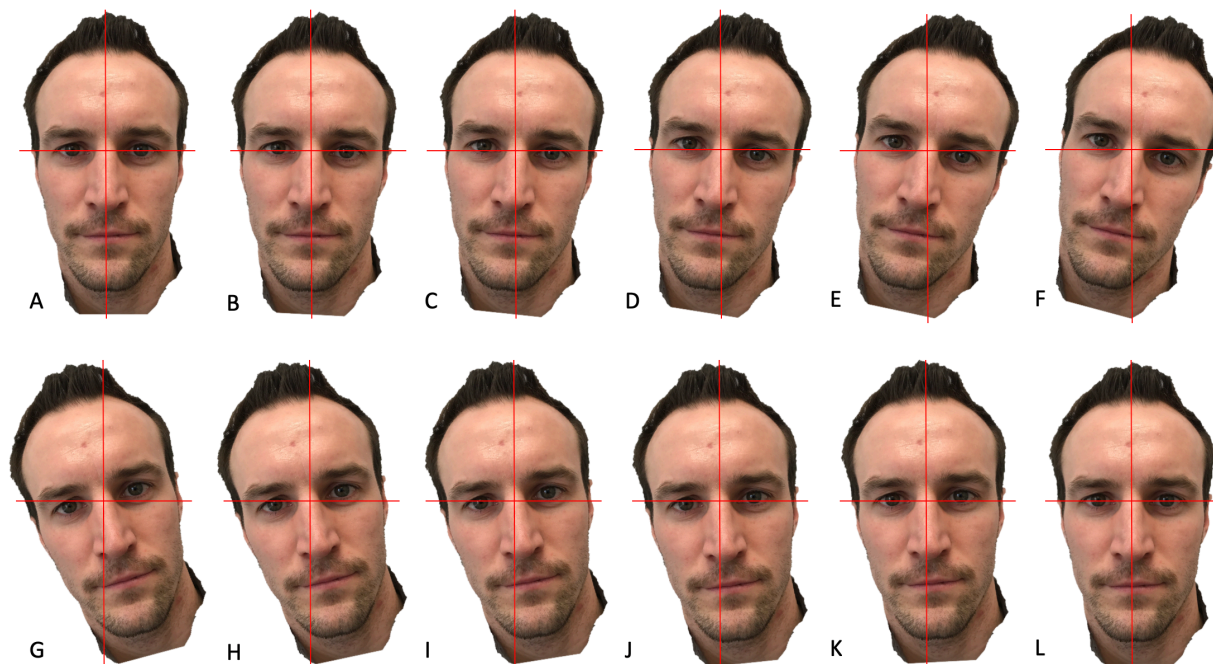


Figure 12. Examples of head rotations when viewed from the front 0° (A), 3° (B), 6° (C), 9° (D), 12° (E), 15° (F), -15° (G), -12° (H), -9° (I), -6° (J), -3° (K), 0° (L)

The current study found that head rotations of greater than $\pm 6^\circ$ have a negative impact on cephalometric measurements and the measurements will not be accurate. Thus, in a clinical setting with head rotations of $\pm 6^\circ$ or greater, a retake of the lateral cephalogram may be warranted. Cephalometric measurements that were found reliable at $+3^\circ$ of head rotations are the following: S-N, Go-Me, ANS-PNS, N-Me, S-Go, SNA, ANB, FMA, U1-SN, NA-APo, SGn-FH, Ar-Go-Me, L1-MP, MP-SN, and U1-PP and for -3° are: S-N, Go-Me, ANS-PNS, N-Me, S-Go, ANB, FMA, U1-SN, NA-APo, SGn-FH, Ar-Go-Me, L1-MP, MP-SN, and U1-PP. Cephalometric measurements found reliable at $+6^\circ$ are: S-N, Go-Me, ANS-PNS, S-Go, SNA, ANB, FMA, U1-SN, NA-APo, SGn-FH, Ar-Go-Me, L1-MP, MP-SN, and U1-PP and for -6° are: S-N, Go-Me, ANS-PNS, S-Go, SNA, ANB, NA-APo, SGn-FH, Ar-Go-Me, L1-MP, MP-SN, and U1-PP.

Angular variables SNB at $\pm 3^\circ$ and SNA at -3° indicated statistically significant mean differences, however, it does not show clinical significance. Therefore, head rotations of $\pm 3^\circ$ may be considered clinically acceptable although angular measurements SNA and SNB should be considered less reliable. Some cephalometric measurements at head rotations of $\pm 6^\circ$ are still reliable, however, we recommend being cautious as some variables in question may be unreliable as shown in this study and a re-take of the cephalometric radiograph may be necessary.

CBCT can significantly improve treatment planning and diagnosis (Carlson et al. 2014) in orthodontic cases. Aside from better accuracy, CBCT images can be reoriented to produce a reconstructed lateral cephalogram with optimal skull orientation (Moshiri et al. 2007). The option to position the skull in an ideal head position can have a positive impact on the accuracy of cephalometric measurements. However, there is higher radiation dose in CBCT over 2D lateral cephalograms thus limiting its use to impaction, skeletal asymmetry, and craniofacial abnormalities (Signorelli et al. 2016). Therefore, when deciding which modality to choose, one should use the modality that answers the clinical questions in mind through the principles of ALARA (as low as reasonably achievable) (Carlson et al. 2014).

In order for orthodontic treatment and growth to be analyzed via cephalometric radiographs, the patient should be positioned consistently to have validity. If consistent methodologic approaches or standardization cannot be processed, further development of head positioner devices is warranted.

5.2 **Limitations of the Current Study**

The conclusions of this study are based on available dry human skulls and not living subjects. The benefits of dental radiology are not in doubt and has greatly enhanced dental practice. However, the benefits come with a price and for the current study exposing a live patient to radiation repeatedly strictly for research purposes was not ethical. Thus, this current study resulted in a small sample size.

Identification of cephalometric landmarks was challenging especially when structures were overlapped and rotated, obscuring the image. Outlines of the cranium are relatively easy to identify because of the high contrast, whereas structures within the cranium are often unclear and indistinct because of superimposed anatomic details (Midtgård, Björk, and Linder-Aronson 1974). Baumrind and Frantz have concluded that the probability of placing landmarks correctly in an ideally positioned skull is 44% (Baumrind and Frantz 1971). Therefore, it has been suggested that landmark identification errors may be considered the major source of error in cephalometrics analysis (Baumrind and Frantz 1971; Midtgård, Björk, and Linder-Aronson 1974; Richardson 1966). Many other factors exist that affect the identification of landmarks such as the quality of the radiograph. Some authors have stated that quality of the radiograph is of the utmost importance (McWilliam and Welander 1978). Some studies have used metal balls (Gaddam et al. 2015; Yoon 2001) or tantalum implants (Spolyar 1987) that help to reduce landmark errors, however, our study focused on real life clinical situations.

Furthermore, a major limitation in this study is that cephalometric measurement values were used for analysis rather than landmark coordinates. Future studies could use landmark coordinates to see if the landmarks move in a predictable direction upon rotation.

VI. CONCLUSION

When the skull is in the ideal position of zero degrees within the head holding device, cephalometric measurements can be useful in orthodontic diagnosis, treatment planning, studying treatment progress, and in assessing treatment outcome. However, the patient's skull can be positioned incorrectly during cephalometric radiograph exposure which can significantly affect landmark allocation, introduce magnification and distortion, and alter measurements obtained thereafter. One of the many benefits of 3D CBCT over conventional 2D lateral cephalometric radiographs is the ability to take the 3D volumetric data, reorient the skull to ideal position and reconstruct a lateral cephalogram. When stabilization of the skull in an ideal position is difficult to obtain during exposure of a conventional 2D cephalometric radiograph, CBCT may be an ideal choice of modality.

In our study, there is an increase in measurement error as the skull is rotated along the sagittal axis from ideal position (0°) towards $\pm 15^\circ$. Specifically, measurements at head rotations of greater than $\pm 6^\circ$ are not all reliable and the operator should consider repositioning the patient's head to the ideal position for re-exposure. Generally, angular measurements of lateral cephalometric radiographs were more reliable than linear measurements. The most reliable measurement in the positive direction are S-N, ANS-PNS, and in the negative distances are ANB and Ar-Go-Me. ANB is the most reliable angular measurement in the A-P dimension in both positive and negative directions. The most reliable angular measurements in both positive and negative distances were NA-Apo, L1-MP and U1-PP. Linear measurements S-N, Go-Me, ANS-PNS, N-Me, S-Go, and angular measurements ANB, FMA, U1-SN, NA-APo, SGn-FH, Ar-Go-Me, L1-MP, MP-SN, and U1-PP are reliable at $\pm 3^\circ$ changes in head position. If lateral

cephalometric analysis is to be regarded as a valid technique in establishing quantifiable and reliable data measurements, ideal head positioning should be a priority.

One must also consider that although a patient may be positioned correctly, magnification, landmark identification errors, distortion, and quality of the radiograph are still potential factors that could also have an effect on cephalometric analysis, thus interpretation of the radiograph can vary and not truly reflect the condition of the patient. It appears that changes in the head orientation may affect the location of landmarks and thus the resultant angular and linear measurements obtained. Having a good understanding of these potential sources of error are critical and landmark identification on rotated cephalometric radiographs must be approached with caution.

CITED LITERATURE

- Ahlqvist, Jan, Stina Eliasson, and U Welanders. 1986. "The Effect of Projection Error on Cephalometric Length Measurements." *European Journal of Orthodontics* 8 (September): 141–48. <https://doi.org/10.1093/ejo/8.3.141>.
- Baumrind, Sheldon. 1971. "The Reliability of Head Film Measurements" 60 (2): 17.
- Baumrind, Sheldon, and Robert C. Frantz. 1971. "The Reliability of Head Film Measurements: 1. Landmark Identification." *American Journal of Orthodontics* 60 (2): 111–27. [https://doi.org/10.1016/0002-9416\(71\)90028-5](https://doi.org/10.1016/0002-9416(71)90028-5).
- Bergersen, E. O. 1980. "Enlargement and Distortion in Cephalometric Radiography: Compensation Tables for Linear Measurements." *The Angle Orthodontist* 50 (3): 230–44. [https://doi.org/10.1043/0003-3219\(1980\)050<0230:EADICR>2.0.CO;2](https://doi.org/10.1043/0003-3219(1980)050<0230:EADICR>2.0.CO;2).
- Carlson, Sean K., John Graham, James Mah, Aaron Molen, David E. Paquette, and Juan-Carlos Quintero. 2014. "Let the Truth about CBCT Be Known." *American Journal of Orthodontics and Dentofacial Orthopedics* 145 (4): 418–19. <https://doi.org/10.1016/j.ajodo.2014.01.014>.
- Chen, Y. J., S. K. Chen, H. F. Chang, and K. C. Chen. 2000. "Comparison of Landmark Identification in Traditional versus Computer-Aided Digital Cephalometry." *The Angle Orthodontist* 70 (5): 387–92. [https://doi.org/10.1043/0003-3219\(2000\)070<0387:COLIIT>2.0.CO;2](https://doi.org/10.1043/0003-3219(2000)070<0387:COLIIT>2.0.CO;2).
- Chen, Y.J., S.K. Chen, H.W. Huang, C.C. Yao, and H.F. Chang. 2004. "Reliability of Landmark Identification in Cephalometric Radiography Acquired by a Storage Phosphor Imaging System." *Dento Maxillo Facial Radiology* 33 (5): 301–6. <https://doi.org/10.1259/dmfr/85147715>.
- Dibbets, Jos M. H., and Kai Nolte. 2002. "Effect of Magnification on Lateral Cephalometric Studies." *American Journal of Orthodontics and Dentofacial Orthopedics* 122 (2): 196–201. <https://doi.org/10.1067/mod.2002.125565>.
- Downs, William B. 1948. "Variations in Facial Relationships: Their Significance in Treatment and Prognosis." *American Journal of Orthodontics* 34 (10): 812–40. [https://doi.org/10.1016/0002-9416\(48\)90015-3](https://doi.org/10.1016/0002-9416(48)90015-3).
- Downs, Williams B. 1952. "The Role of Cephalometrics in Orthodontic Case Analysis and Diagnosis." *American Journal of Orthodontics* 38 (3): 162–82. [https://doi.org/10.1016/0002-9416\(52\)90106-1](https://doi.org/10.1016/0002-9416(52)90106-1).
- Durão, Ana Paula Reis, Aline Morosolli, Pisha Pittayapat, Napat Bolstad, Afonso P. Ferreira, and Reinhilde Jacobs. 2015. "Cephalometric Landmark Variability among Orthodontists and Dentomaxillofacial Radiologists: A Comparative Study." *Imaging Science in Dentistry* 45 (4): 213–20. <https://doi.org/10.5624/isd.2015.45.4.213>.

- Forsberg, Clifton T., Charles J. Burstone, and Kevin J. Hanley. 1984. "Diagnosis and Treatment Planning of Skeletal Asymmetry with the Submental-Vertical Radiograph." *American Journal of Orthodontics* 85 (3): 224–37. [https://doi.org/10.1016/0002-9416\(84\)90062-9](https://doi.org/10.1016/0002-9416(84)90062-9).
- Gaddam, Rajkumar, H C Shashikumar, N K Lokesh, T Suma, Siddarth Arya, and G S Shwetha. 2015. "Assessment of Image Distortion from Head Rotation in Lateral Cephalometry." *Journal of International Oral Health : JIOH* 7 (6): 35–40.
- Ghafari, Joseph, Paul E. Cater, and Frances S. Shofer. 1995. "Effect of Film-Object Distance on Posteroanterior Cephalometric Measurements: Suggestions for Standardized Cephalometric Methods." *American Journal of Orthodontics and Dentofacial Orthopedics* 108 (1): 30–37. [https://doi.org/10.1016/S0889-5406\(95\)70063-3](https://doi.org/10.1016/S0889-5406(95)70063-3).
- Goldberg, M A, M Pivovarov, W W Mayo-Smith, M P Bhalla, J G Blickman, R T Bramson, G W Boland, H J Llewellyn, and E Halpern. 1994. "Application of Wavelet Compression to Digitized Radiographs." *American Journal of Roentgenology* 163 (2): 463–68. <https://doi.org/10.2214/ajr.163.2.8037051>.
- Gravelly, J. F., and P. M. Benzies. 1974. "The Clinical Significance of Tracing Error in Cephalometry." *British Journal of Orthodontics* 1 (3): 95–101.
- Hatton, M. E., and R. M. Grainger. 1958. "Reliability of Measurements from Cephalo Grams at the Burlington Orthodontic Research Centre." *Journal of Dental Research* 37 (5): 853–59.
- Hsiao, T. H., H. P. Chang, and K. M. Liu. 1997. "A Method of Magnification Correction for Posteroanterior Radiographic Cephalometry." *The Angle Orthodontist* 67 (2): 137–42. [https://doi.org/10.1043/0003-3219\(1997\)067<0137:AMOMCF>2.3.CO;2](https://doi.org/10.1043/0003-3219(1997)067<0137:AMOMCF>2.3.CO;2).
- Ishida, M., K. Doi, L. N. Loo, C. E. Metz, and J. L. Lehr. 1984. "Digital Image Processing: Effect on Detectability of Simulated Low-Contrast Radiographic Patterns." *Radiology* 150 (2): 569–75. <https://doi.org/10.1148/radiology.150.2.6691118>.
- Jacobson, A. 1975. "The 'Wits' Appraisal of Jaw Disharmony." *American Journal of Orthodontics* 67 (2): 125–38. [https://doi.org/10.1016/0002-9416\(75\)90065-2](https://doi.org/10.1016/0002-9416(75)90065-2).
- Jacobson, A. 1976. "Application of the 'Wits' Appraisal." *American Journal of Orthodontics and Dentofacial Orthopedics* 70 (2): 179–89. [https://doi.org/10.1016/S0002-9416\(76\)90318-3](https://doi.org/10.1016/S0002-9416(76)90318-3).
- Kumar, V., J. B. Ludlow, A. Mol, and L. Cevidanes. 2007. "Comparison of Conventional and Cone Beam CT Synthesized Cephalograms." *Dento Maxillo Facial Radiology* 36 (5): 263–69. <https://doi.org/10.1259/dmfr/98032356>.
- Kumar, Vandana, John Ludlow, Lucia Helena Soares Cevidanes, and André Mol. 2008. "In Vivo Comparison of Conventional and Cone Beam CT Synthesized Cephalograms." *The Angle Orthodontist* 78 (5): 873–79. <https://doi.org/10.2319/082907-399.1>.

- Larheim, T.A., and S. Eggen. 1979. "Determination of Tooth Length with a Standardized Paralleling Technique and Calibrated Radiographic Measuring Film." *Oral Surgery, Oral Medicine, Oral Pathology* 48 (4): 374–78. [https://doi.org/10.1016/0030-4220\(79\)90038-0](https://doi.org/10.1016/0030-4220(79)90038-0).
- MacMahon, H., K. Doi, S. Sanada, S. M. Montner, M. L. Giger, C. E. Metz, N. Nakamori, F. F. Yin, X. W. Xu, and H. Yonekawa. 1991. "Data Compression: Effect on Diagnostic Accuracy in Digital Chest Radiography." *Radiology* 178 (1): 175–79. <https://doi.org/10.1148/radiology.178.1.1984299>.
- Macri, Vincenzo, and Ann Wenzel. 1993. "Reliability of Landmark Recording on Film and Digital Lateral Cephalograms." *Eur J Orthod* 15 (3): 137–48.
- Major, P. W., D. E. Johnson, K. L. Hesse, and K. E. Glover. 1996. "Effect of Head Orientation on Posterior Anterior Cephalometric Landmark Identification." *The Angle Orthodontist* 66 (1): 51–60. [https://doi.org/10.1043/0003-3219\(1996\)066<0051:EOHOOP>2.3.CO;2](https://doi.org/10.1043/0003-3219(1996)066<0051:EOHOOP>2.3.CO;2).
- Malkoc, Siddik, Zafer Sari, Serdar Usumez, and Alp Erdin Koyuturk. 2005. "The Effect of Head Rotation on Cephalometric Radiographs." *European Journal of Orthodontics* 27 (3): 315–21. <https://doi.org/10.1093/ejo/cjh098>.
- McClure, Scott R., P. Lionel Sadowsky, André Ferreira, and Alex Jacobson. 2005. "Reliability of Digital Versus Conventional Cephalometric Radiology: A Comparative Evaluation of Landmark Identification Error." *Seminars in Orthodontics* 11 (2): 98–110. <https://doi.org/10.1053/j.sodo.2005.04.002>.
- McNamara, James A. 1984. "A Method of Cephalometric Evaluation." *American Journal of Orthodontics and Dentofacial Orthopedics* 86 (6): 449–69. [https://doi.org/10.1016/S0002-9416\(84\)90352-X](https://doi.org/10.1016/S0002-9416(84)90352-X).
- McWilliam, J. S., and U. Welander. 1978. "The Effect of Image Quality on the Identification of Cephalometric Landmarks." *The Angle Orthodontist* 48 (1): 49–56.
- Midtgård, Jacob, Gunnar Björk, and Sten Linder-Aronson. 1974. "Reproducibility of Cephalometric Landmarks and Errors of Measurements of Cephalometric Cranial Distances." *The Angle Orthodontist* 44 (1): 56–61. [https://doi.org/10.1043/0003-3219\(1974\)044<0056:ROCLAE>2.0.CO;2](https://doi.org/10.1043/0003-3219(1974)044<0056:ROCLAE>2.0.CO;2).
- Moshiri, Mazyar, William C. Scarfe, Michael L. Hilgers, James P. Scheetz, Anibal M. Silveira, and Allan G. Farman. 2007. "Accuracy of Linear Measurements from Imaging Plate and Lateral Cephalometric Images Derived from Cone-Beam Computed Tomography." *American Journal of Orthodontics and Dentofacial Orthopedics* 132 (4): 550–60. <https://doi.org/10.1016/j.ajodo.2006.09.046>.
- Park, Chang-Seo, Jae-Kyu Park, Huijun Kim, Sang-Sun Han, Ho-Gul Jeong, and Hyok Park. 2012. "Comparison of Conventional Lateral Cephalograms with Corresponding CBCT Radiographs." *Imaging Science in Dentistry* 42 (4): 201–5. <https://doi.org/10.5624/isd.2012.42.4.201>.

- Resnik, Randolph R., and Carl E. Misch. 2015. *Dental Implant Prosthetics*. Second. Mosby.
- Richardson, Andrew. 1966. "An Investigation into the Reproducibility of Some Points, Planes, and Lines Used in Cephalometric Analysis." *American Journal of Orthodontics* 52 (9): 637–51. [https://doi.org/10.1016/0002-9416\(66\)90212-0](https://doi.org/10.1016/0002-9416(66)90212-0).
- Rino Neto, José, João Batista de Paiva, Gilberto Vilanova Queiroz, Miguel Ferragut Attizzani, and Hiroshi Miasiro Junior. 2013. "Evaluation of Radiographic Magnification in Lateral Cephalograms Obtained with Different X-Ray Devices: Experimental Study in Human Dry Skull." *Dental Press Journal of Orthodontics* 18 (2): 17e1–7. <https://doi.org/10.1590/S2176-94512013000200005>.
- Salzmann, J. A. 1964. "Limitations of Roentgenographic Cephalometrics." *American Journal of Orthodontics* 50 (3): 169–88. [https://doi.org/10.1016/0002-9416\(64\)90189-7](https://doi.org/10.1016/0002-9416(64)90189-7).
- Savage, Anthony W., Kevin J. Showfety, and John Yancey. 1987. "Repeated Measures Analysis of Geometrically Constructed and Directly Determined Cephalometric Points." *American Journal of Orthodontics and Dentofacial Orthopedics* 91 (4): 295–99. [https://doi.org/10.1016/0889-5406\(87\)90169-7](https://doi.org/10.1016/0889-5406(87)90169-7).
- Signorelli, Luca, Raphael Patcas, Timo Peltomäki, and Marc Schätzle. 2016. "Radiation Dose of Cone-Beam Computed Tomography Compared to Conventional Radiographs in Orthodontics." *Journal of Orofacial Orthopedics / Fortschritte Der Kieferorthopädie* 77 (1): 9–15. <https://doi.org/10.1007/s00056-015-0002-4>.
- Spolyar, John L. 1987. "Head Positioning Error in Cephalometric Radiography." *The Angle Orthodontist* 57 (1): 77–88. [https://doi.org/10.1043/0003-3219\(1987\)057<0077:HPEICR>2.0.CO;2](https://doi.org/10.1043/0003-3219(1987)057<0077:HPEICR>2.0.CO;2).
- Stabrun, A. E., and K. Danielsen. 1982. "Precision in Cephalometric Landmark Identification." *European Journal of Orthodontics* 4 (3): 185–96.
- Steiner, Cecil C. 1953. "Cephalometrics for You and Me." *American Journal of Orthodontics* 39 (10): 729–55. [https://doi.org/10.1016/0002-9416\(53\)90082-7](https://doi.org/10.1016/0002-9416(53)90082-7).
- Steiner, Cecil C. 1960. "The Use of Cephalometrics as an Aid to Planning and Assessing Orthodontic Treatment: Report of a Case." *American Journal of Orthodontics* 46 (10): 721–35. [https://doi.org/10.1016/0002-9416\(60\)90145-7](https://doi.org/10.1016/0002-9416(60)90145-7).
- Tng, Tony T. H., Tommy C. K. Chan, Michael S. Cooke, and Urban Hägg. 1993. "Effect of Head Posture on Cephalometric Sagittal Angular Measures." *American Journal of Orthodontics and Dentofacial Orthopedics* 104 (4): 337–41. [https://doi.org/10.1016/S0889-5406\(05\)81330-7](https://doi.org/10.1016/S0889-5406(05)81330-7).
- Tweed, C. H. 1946. "The Frankfort-Mandibular Plane Angle in Orthodontic Diagnosis, Classification, Treatment Planning, and Prognosis." *American Journal of Orthodontics and Oral Surgery* 32 (April): 175–230.

- Tweed, Charles H. 1953. "Evolutionary Trends in Orthodontics, Past, Present, and Future."
American Journal of Orthodontics 39 (2): 81–108. [https://doi.org/10.1016/0002-9416\(53\)90014-1](https://doi.org/10.1016/0002-9416(53)90014-1).
- Weems, RA, and Alex Jacobson. 1995. *Radiographic Cephalometry : From Basics to Videoimaging / Edited by Alexander Jacobson*. Quintessence.
- Yoon, Young-Jooh. 2001. "Effect of Head Rotation on Lateral Cephalometric Radiographs."
Angle Orthodontist 71 (5): 8.

APPENDICES

APPENDIX A



Notice of Determination of Human Subject Research

August 6, 2018

Kan Tsunoda, DMD, DC
Orthodontics
Phone: (630) 723-4944

RE: **Protocol # 2018-0914**
The Effect of Head Posture on Lateral Cephalometric Measurements

Sponsor: None
IP#: Not applicable
Grant/Contract No: Not applicable
Grant/Contract Title: Not applicable

The UIC Office for the Protection of Research Subjects received your "Determination of Whether an Activity Represents Human Subjects Research" application, and has determined that this activity **DOES NOT meet the definition of human subject research** as defined by 45 CFR 46.102(f).

Specifically, the activity involves UIC student residents analyzing and collecting data from iCat CBCT images of each skull and then statistical analysis will be performed. Each lateral cephalometric image extracted from the iCat CBCT will be landmarked and analyzed in Dolphin Imaging and Tx STUDIO. Measurements will be documented in an Excel spreadsheet and SPSS.

You may conduct your activity without further submission to the IRB.

If this activity is used in conjunction with any other research involving human subjects or if it is modified in any way, it must be re-reviewed by OPRS staff.

APPENDIX B

CEPHALOMETRIC RADIOGRAPHS

Skull 1

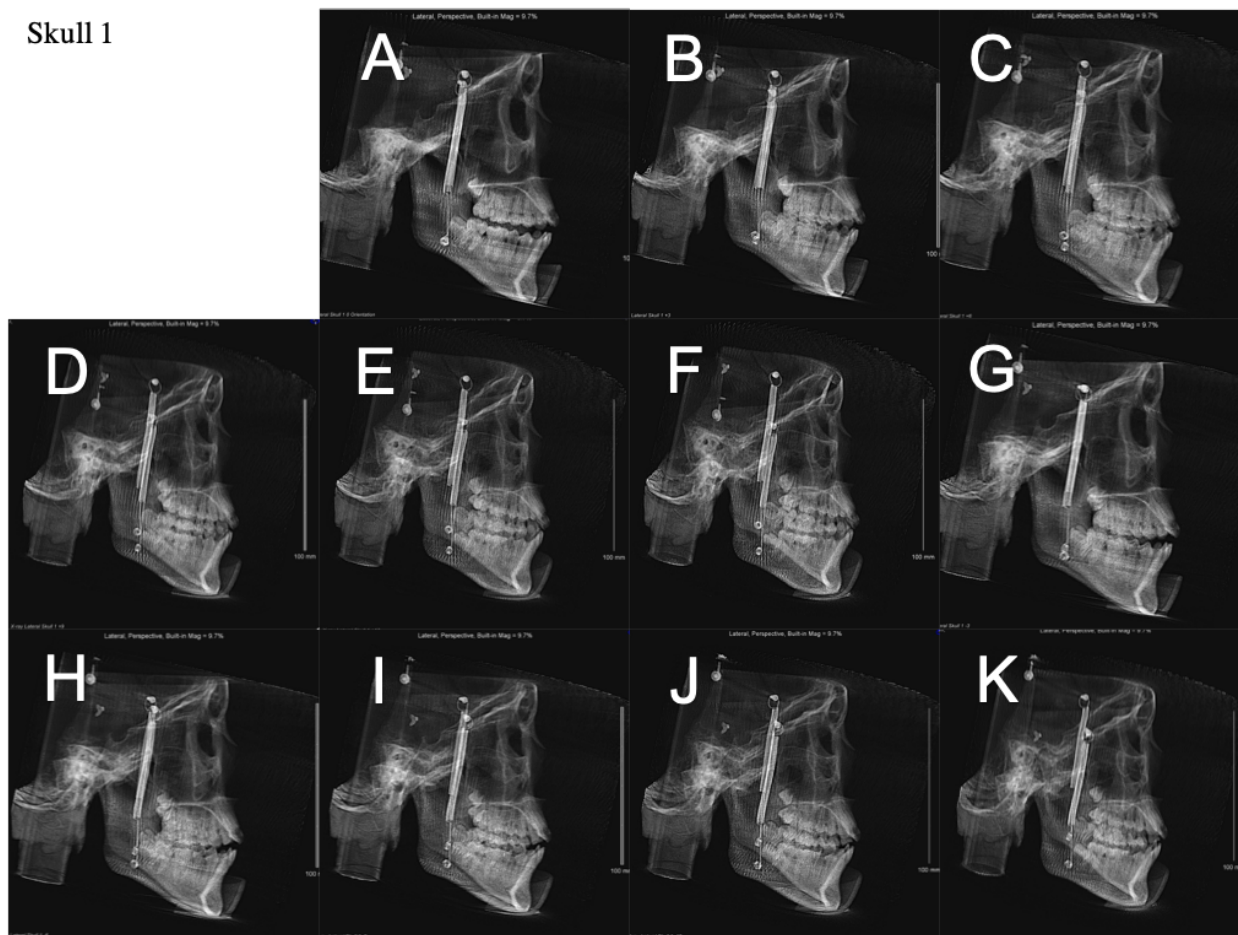


Figure 11. Skull 1. Cephalometric radiographs taken under 0° (A), 3° (B), 6° (C), 9° (D), 12° (E), 15° (F), -3° (G), -6° (H), -9° (I), -12° (J), -15° (K)

APPENDIX B (continued)

CEPHALOMETRIC RADIOGRAPHS (continued)

Skull 2

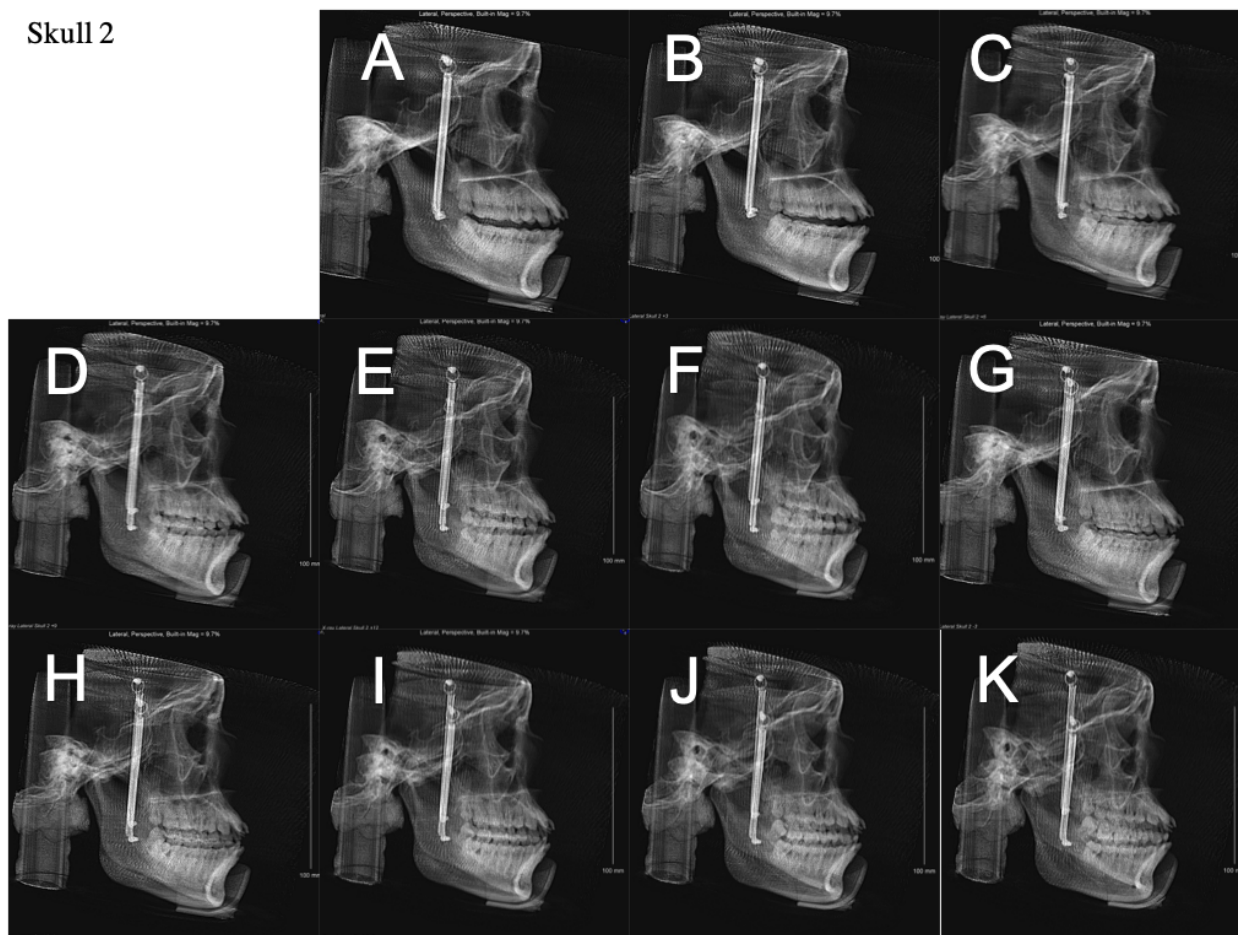


Figure 13. Skull 2. Cephalometric radiographs taken under 0° (A), 3° (B), 6° (C), 9° (D), 12° (E), 15° (F), -3° (G), -6° (H), -9° (I), -12° (J), -15° (K)

APPENDIX B (continued)

CEPHALOMETRIC RADIOGRAPHS (continued)

Skull 3

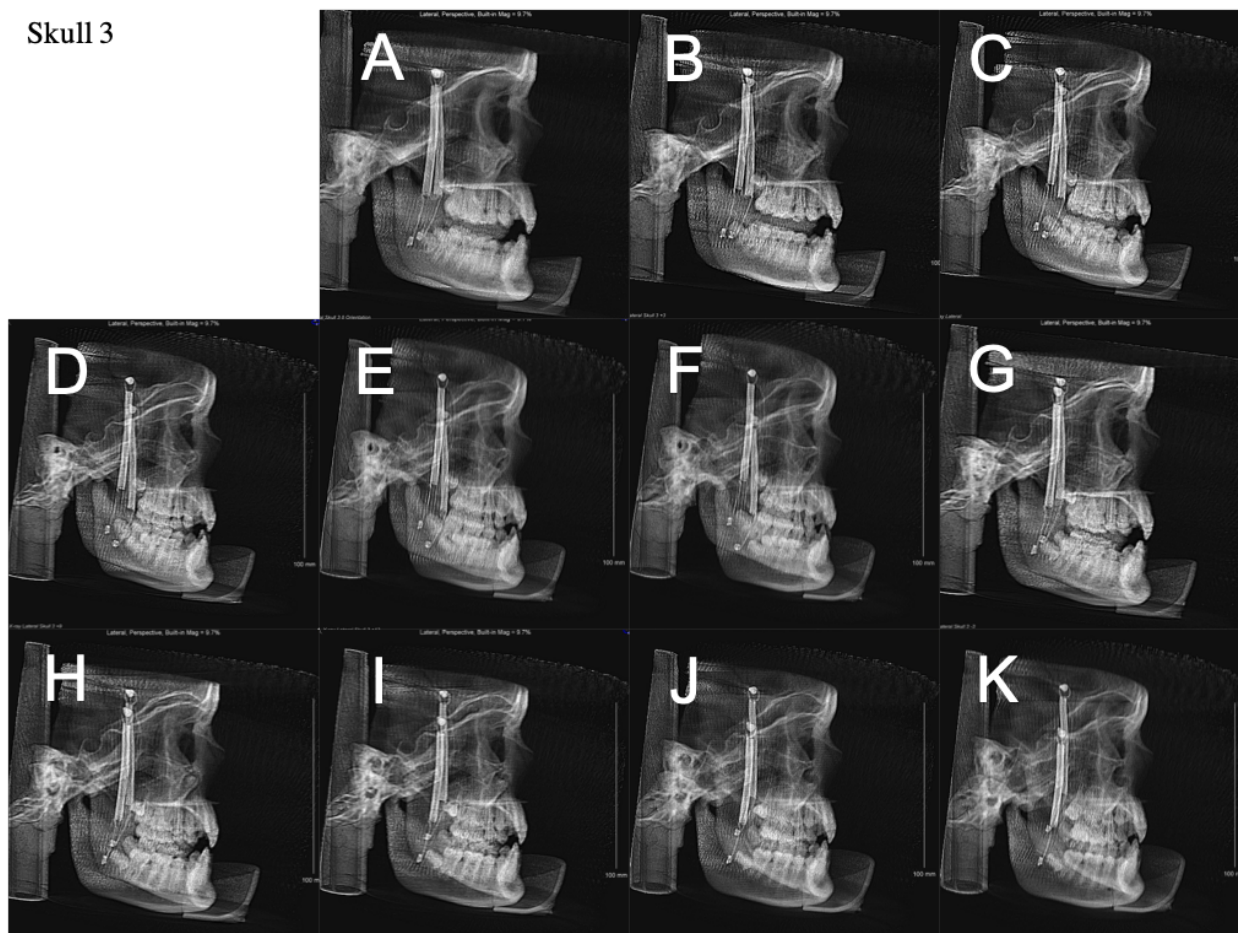


Figure 14. Skull 3. Cephalometric radiographs taken under 0° (A), 3° (B), 6° (C), 9° (D), 12° (E), 15° (F), -3° (G), -6° (H), -9° (I), -12° (J), -15° (K)

APPENDIX B (continued)

CEPHALOMETRIC RADIOGRAPHS (continued)

Skull 4

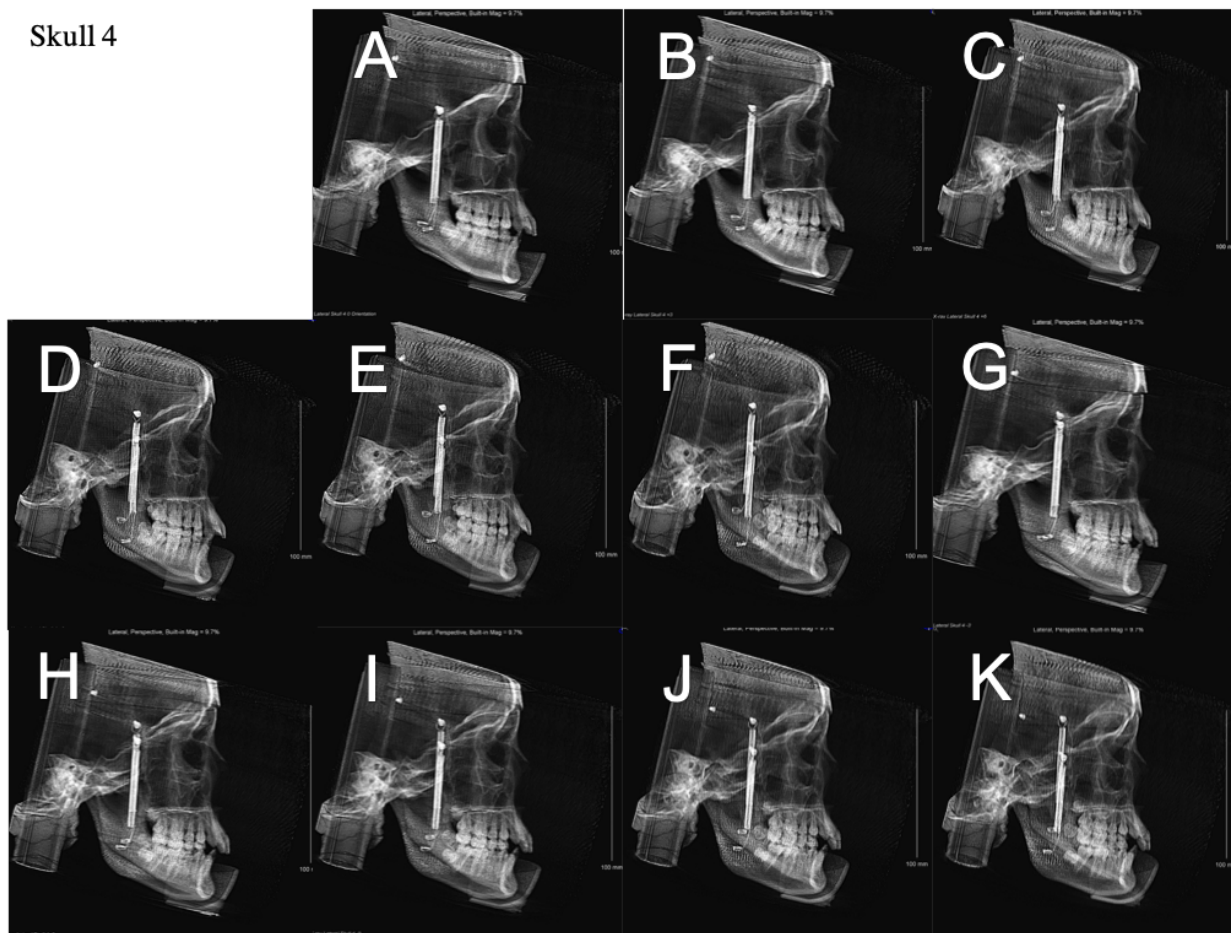


Figure 15. Skull 4. Cephalometric radiographs taken under 0° (A), 3° (B), 6° (C), 9° (D), 12° (E), 15° (F), -3° (G), -6° (H), -9° (I), -12° (J), -15° (K)

APPENDIX B (continued)

CEPHALOMETRIC RADIOGRAPHS (continued)

Skull 5

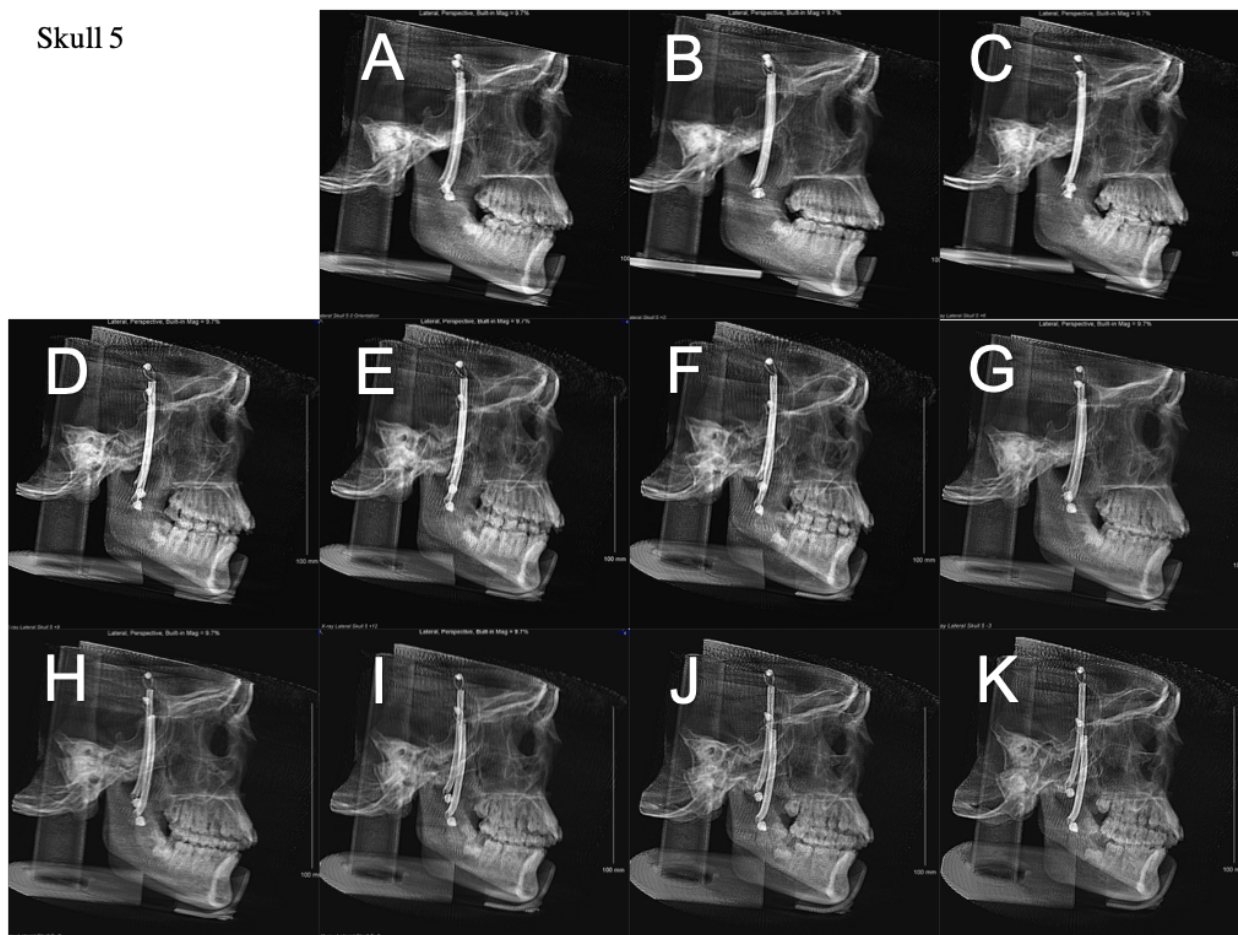


Figure 16. Skull 5. Cephalometric radiographs taken under 0° (A), 3° (B), 6° (C), 9° (D), 12° (E), 15° (F), -3° (G), -6° (H), -9° (I), -12° (J), -15° (K)

APPENDIX B (continued)

CEPHALOMETRIC RADIOGRAPHS (continued)

Skull 6

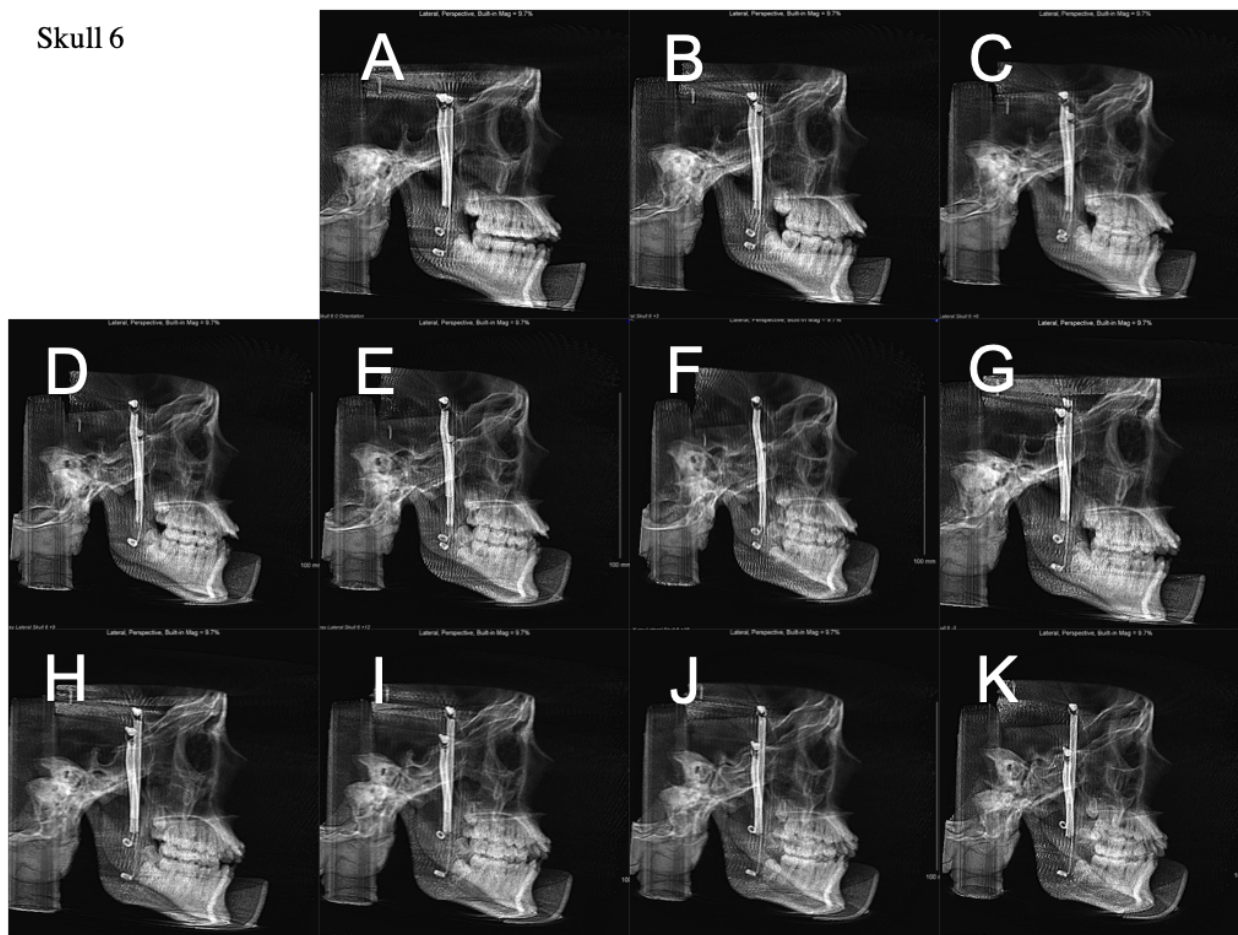


Figure 17. Skull 6. Cephalometric radiographs taken under 0° (A), 3° (B), 6° (C), 9° (D), 12° (E), 15° (F), -3° (G), -6° (H), -9° (I), -12° (J), -15° (K)

APPENDIX B (continued)

CEPHALOMETRIC RADIOGRAPHS (continued)

Skull 7

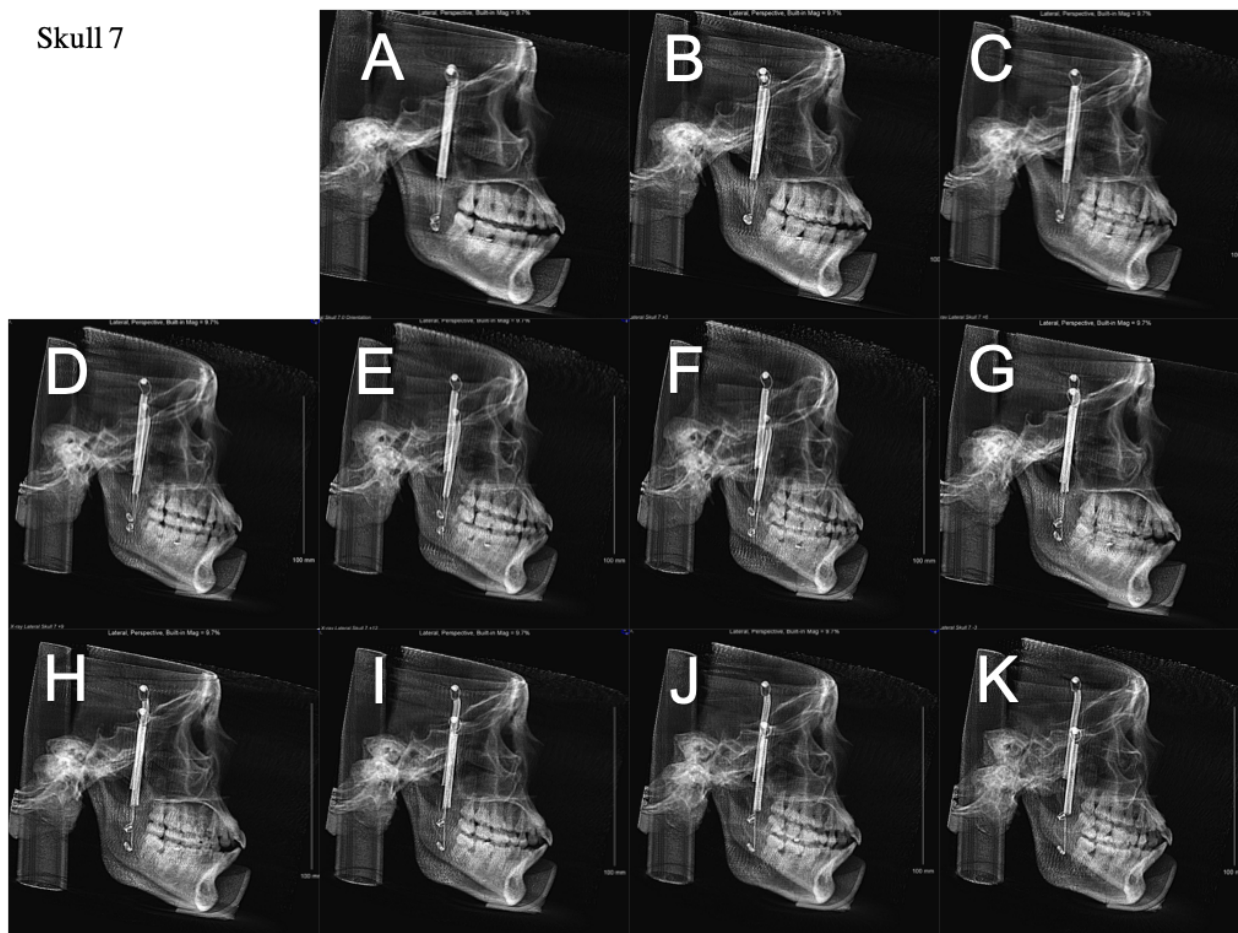


Figure 18. Skull 7. Cephalometric radiographs taken under 0° (A), 3° (B), 6° (C), 9° (D), 12° (E), 15° (F), -3° (G), -6° (H), -9° (I), -12° (J), -15° (K)

APPENDIX B (continued)

CEPHALOMETRIC RADIOGRAPHS (continued)

Skull 8

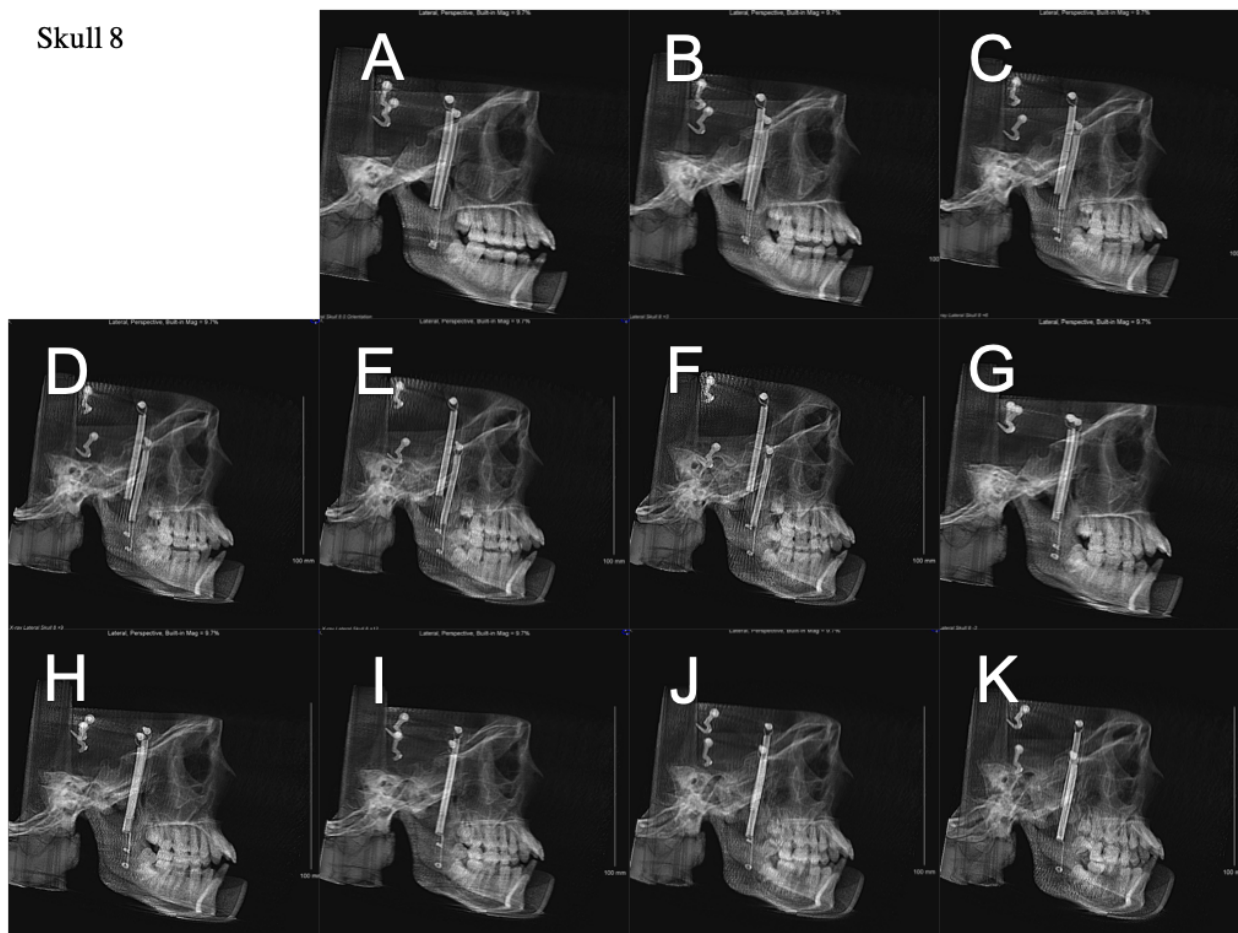


Figure 19. Skull 8. Cephalometric radiographs taken under 0° (A), 3° (B), 6° (C), 9° (D), 12° (E), 15° (F), -3° (G), -6° (H), -9° (I), -12° (J), -15° (K)

APPENDIX B (continued)

CEPHALOMETRIC RADIOGRAPHS (continued)

Skull 9

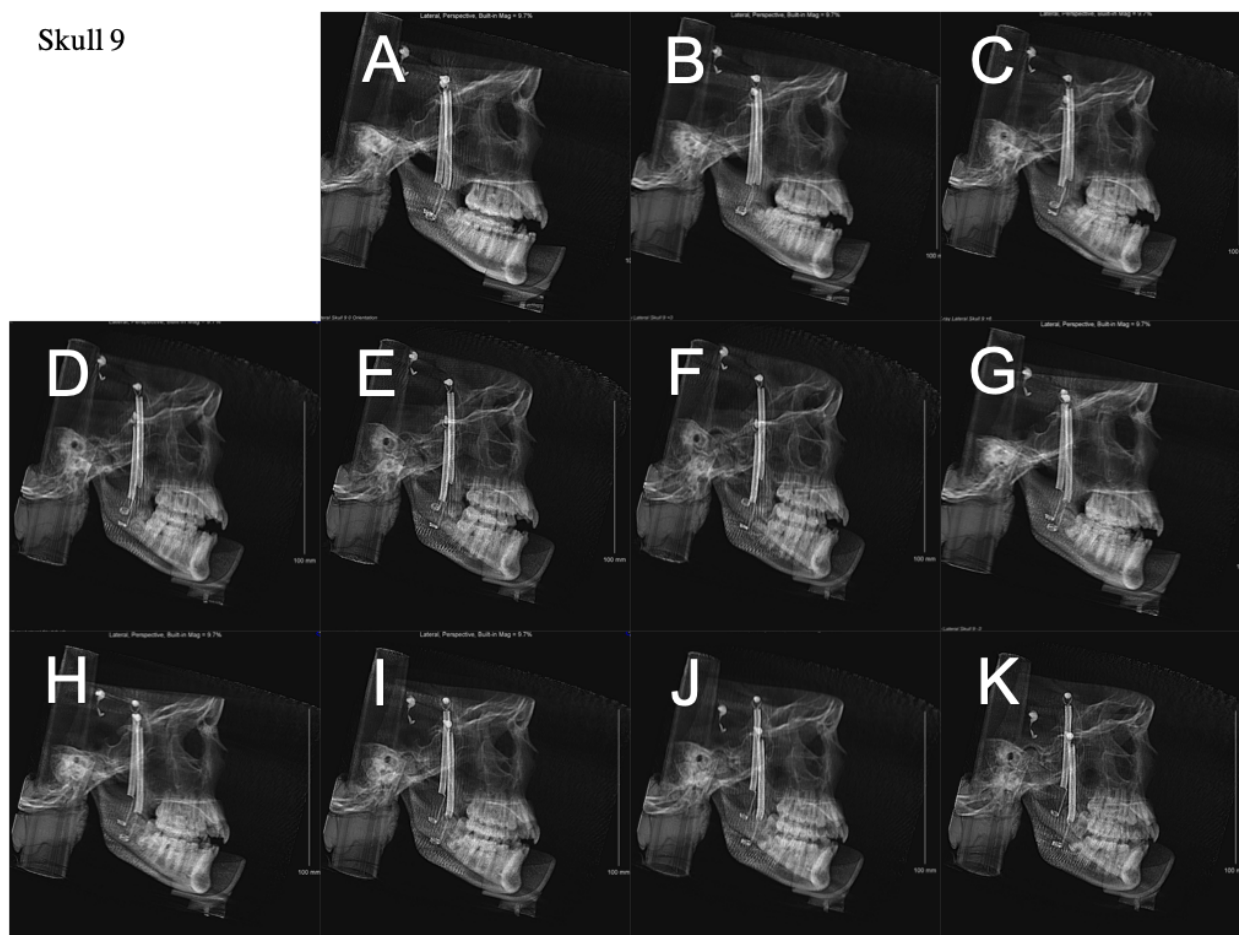


Figure 20. Skull 9. Cephalometric radiographs taken under 0° (A), 3° (B), 6° (C), 9° (D), 12° (E), 15° (F), -3° (G), -6° (H), -9° (I), -12° (J), -15° (K)

APPENDIX B (continued)

CEPHALOMETRIC RADIOGRAPHS (continued)

Skull 10

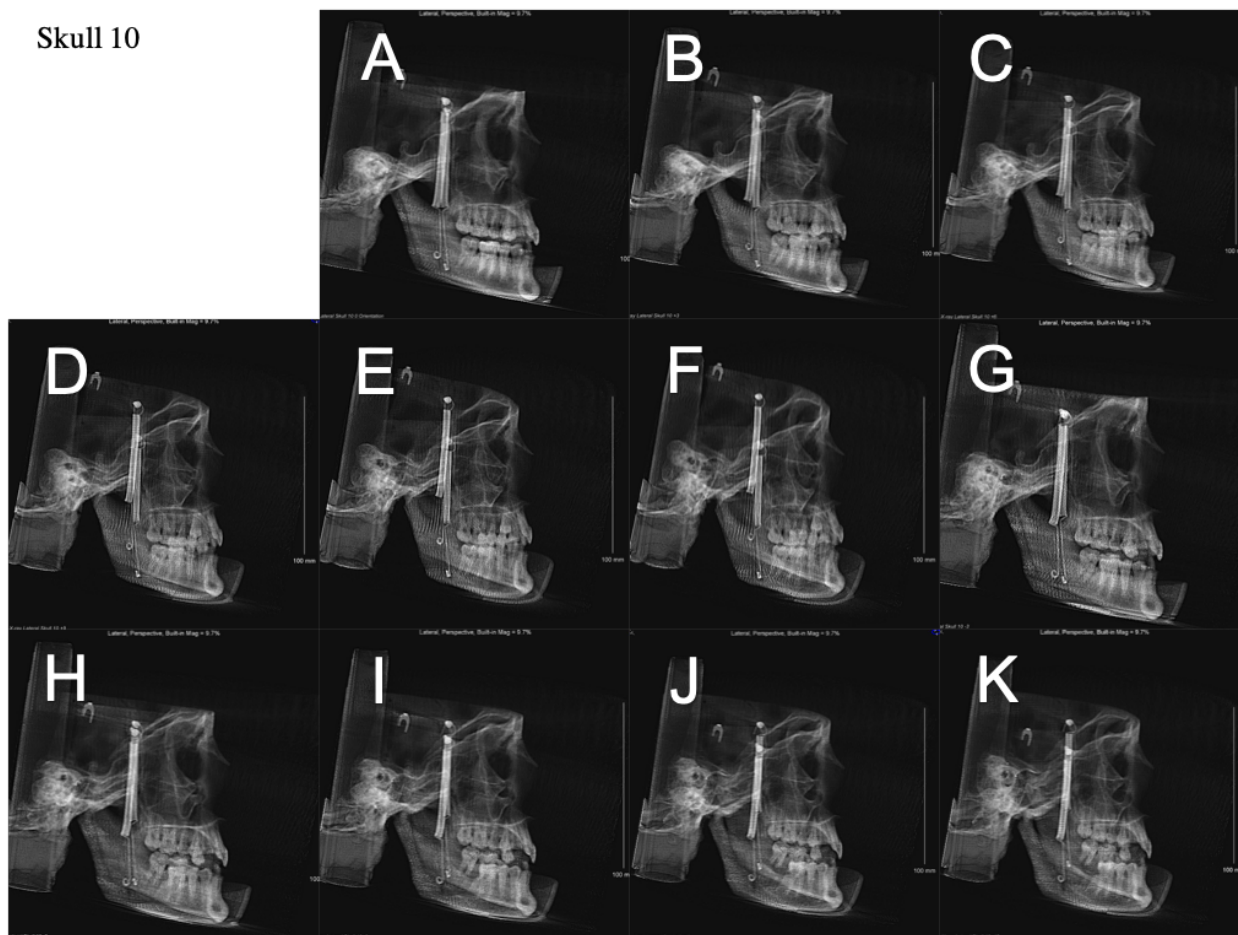


Figure 21. Skull 10. Cephalometric radiographs taken under 0° (A), 3° (B), 6° (C), 9° (D), 12° (E), 15° (F), -3° (G), -6° (H), -9° (I), -12° (J), -15° (K)

APPENDIX B (continued)

CEPHALOMETRIC RADIOGRAPHS (continued)

Skull 11

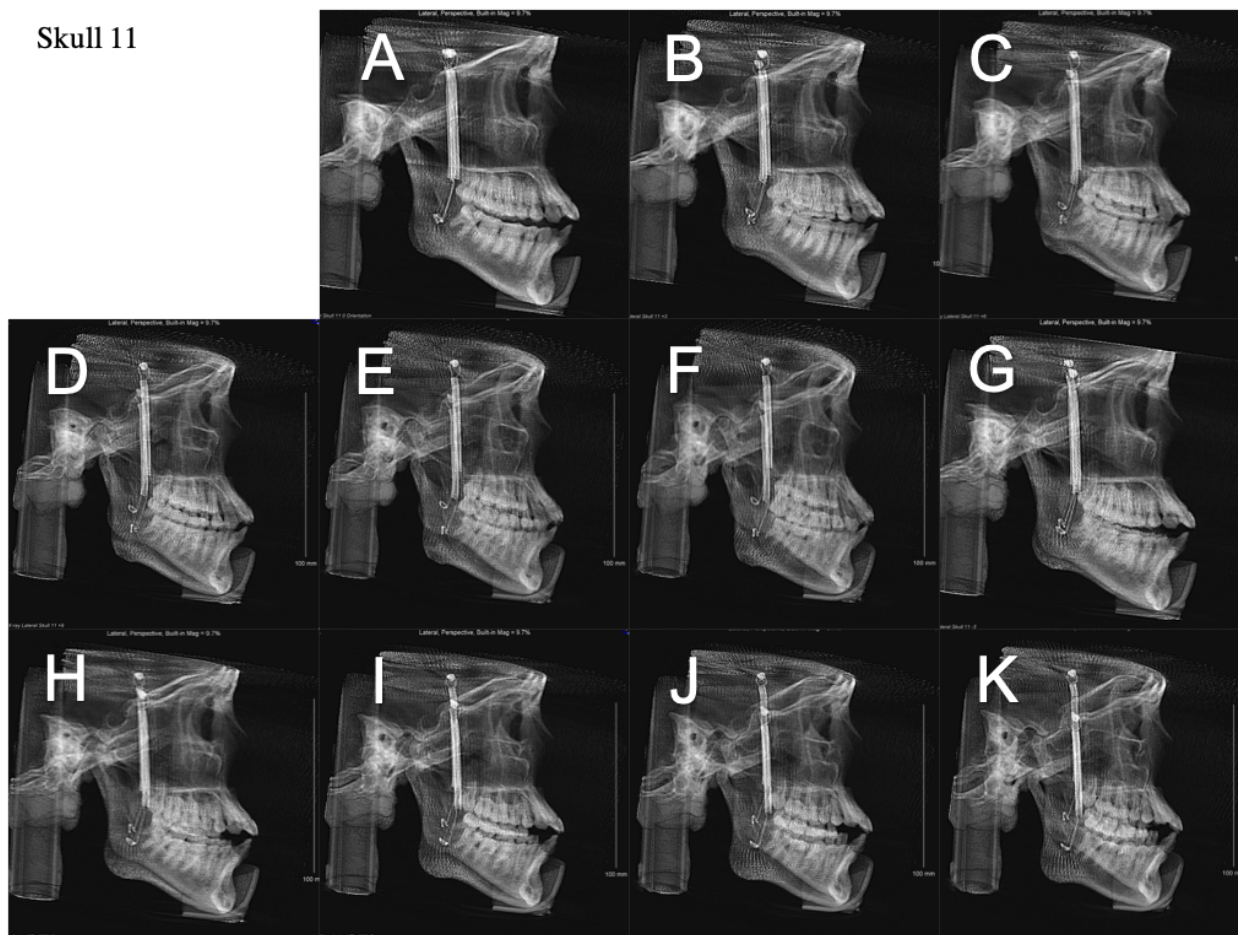


Figure 22. Skull 11. Cephalometric radiographs taken under 0° (A), 3° (B), 6° (C), 9° (D), 12° (E), 15° (F), -3° (G), -6° (H), -9° (I), -12° (J), -15° (K)

APPENDIX B (continued)

CEPHALOMETRIC RADIOGRAPHS (continued)

Skull 12

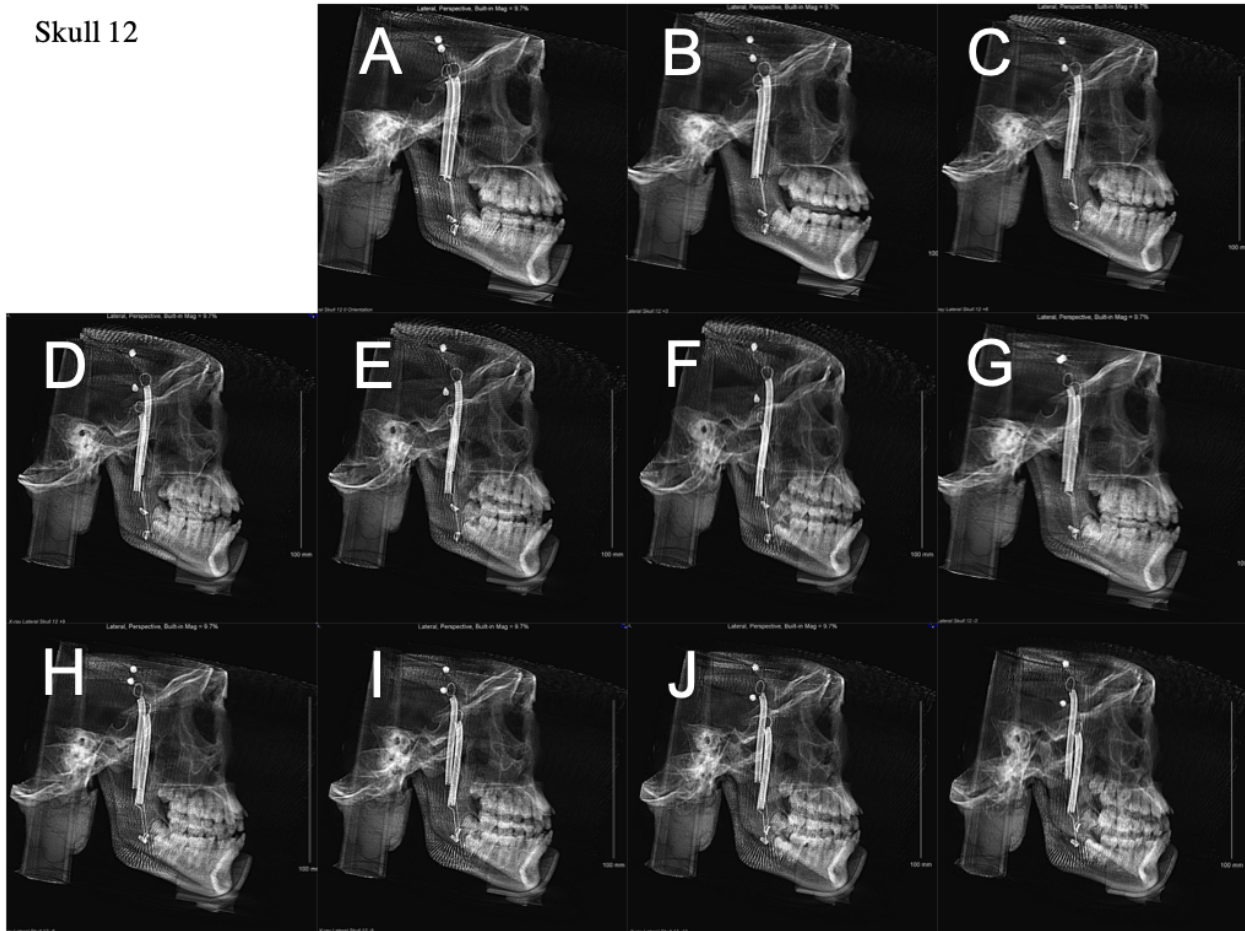


Figure 23. Skull 12. Cephalometric radiographs taken under 0° (A), 3° (B), 6° (C), 9° (D), 12° (E), 15° (F), -3° (G), -6° (H), -9° (I), -12° (J), -15° (K)

APPENDIX B (continued)

CEPHALOMETRIC RADIOGRAPHS (continued)

Skull 13

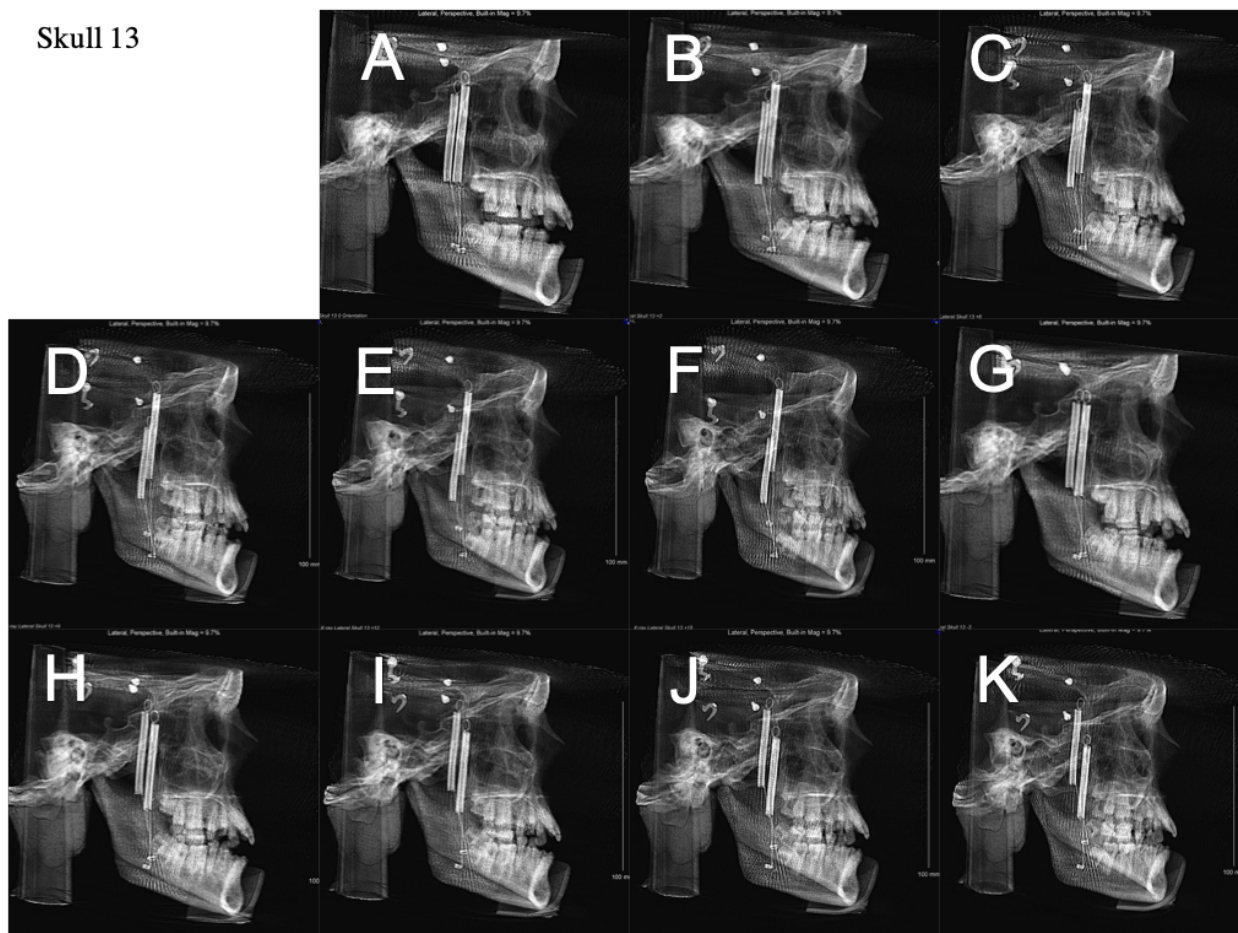


Figure 24. Skull 13. Cephalometric radiographs taken under 0° (A), 3° (B), 6° (C), 9° (D), 12° (E), 15° (F), -3° (G), -6° (H), -9° (I), -12° (J), -15° (K)

APPENDIX B (continued)

CEPHALOMETRIC RADIOGRAPHS (continued)

Skull 14

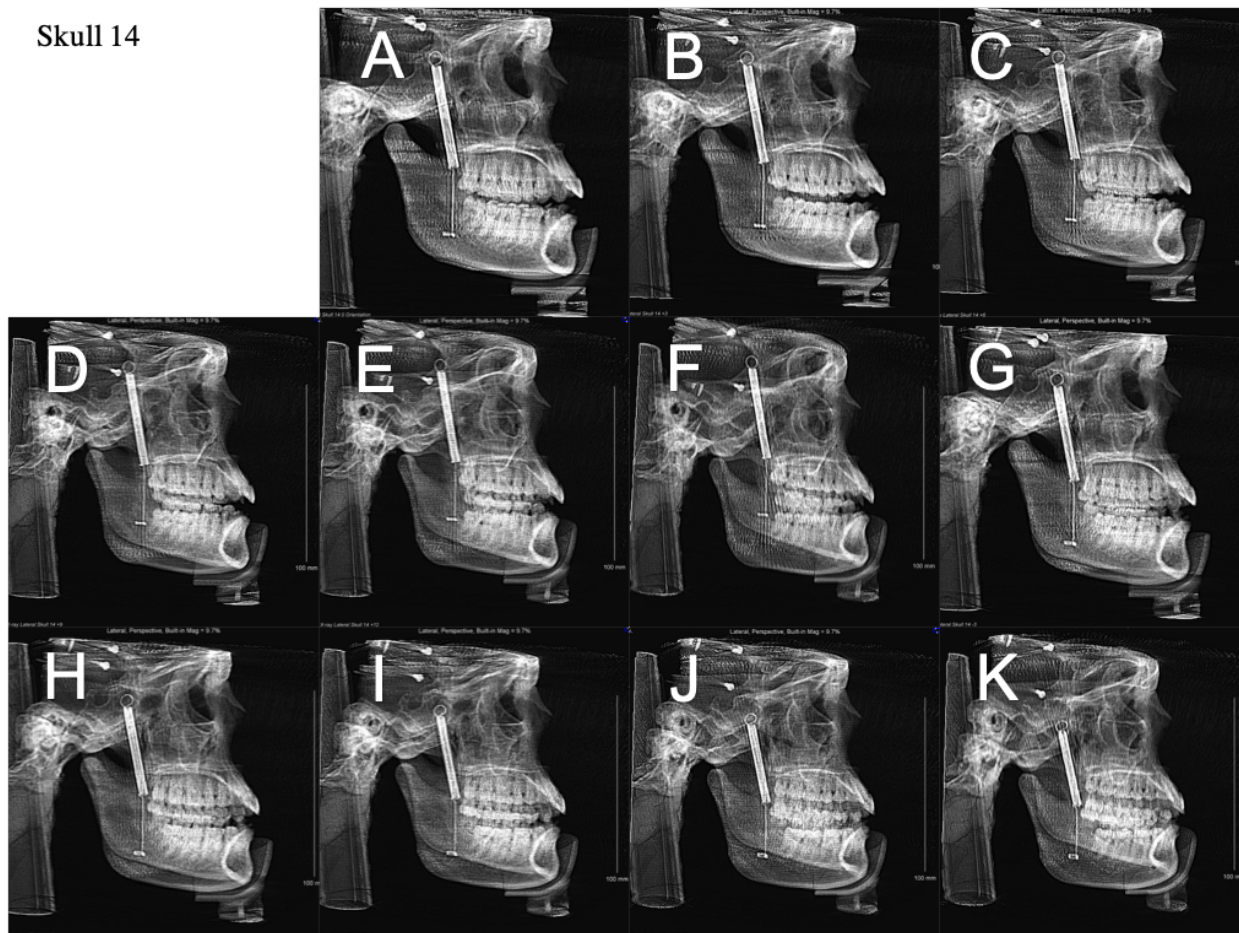


Figure 25. Skull 14. Cephalometric radiographs taken under 0° (A), 3° (B), 6° (C), 9° (D), 12° (E), 15° (F), -3° (G), -6° (H), -9° (I), -12° (J), -15° (K)

APPENDIX B (continued)

CEPHALOMETRIC RADIOGRAPHS (continued)

Skull 15

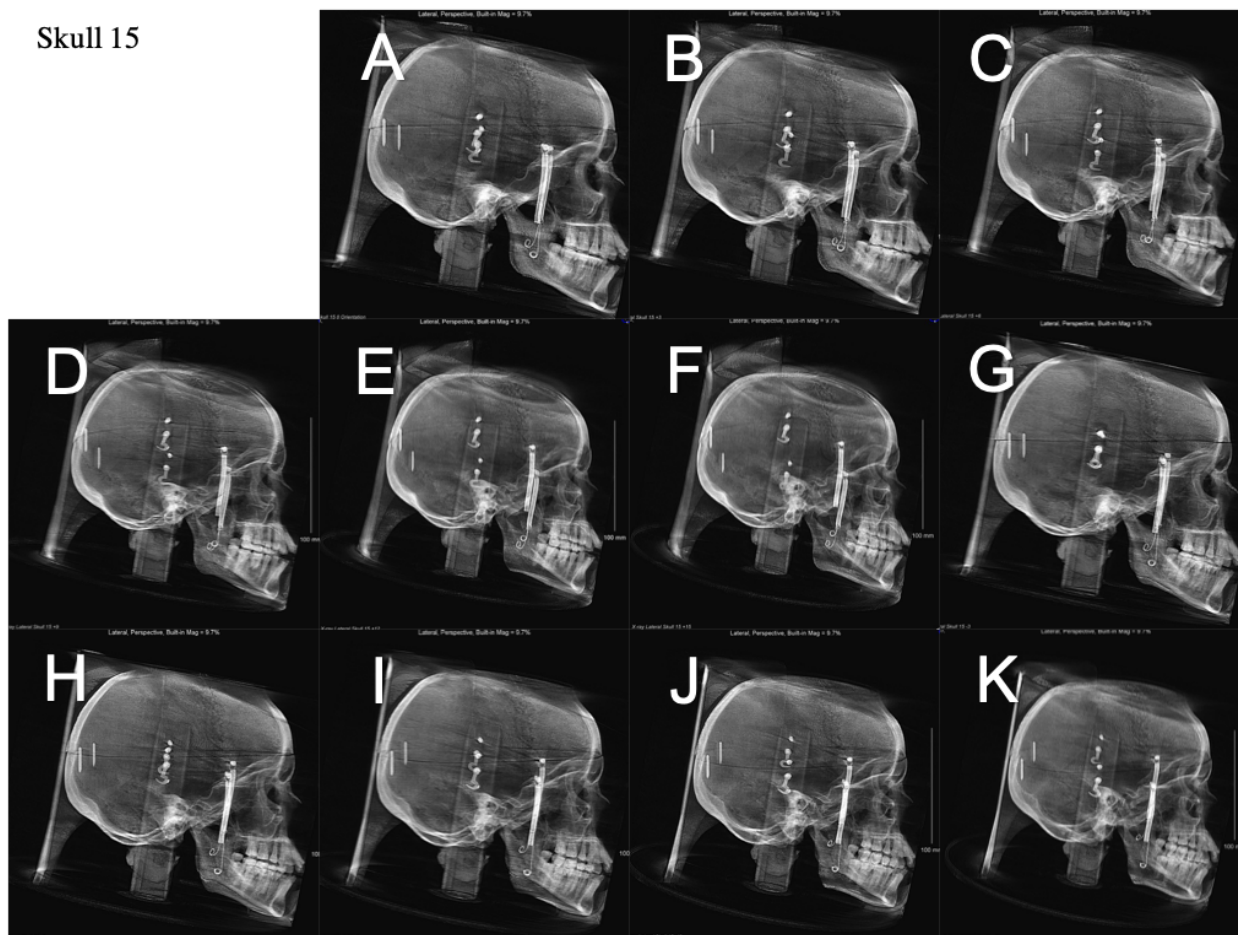


Figure 26. Skull 15. Cephalometric radiographs taken under 0° (A), 3° (B), 6° (C), 9° (D), 12° (E), 15° (F), -3° (G), -6° (H), -9° (I), -12° (J), -15° (K)

APPENDIX B (continued)

CEPHALOMETRIC RADIOGRAPHS (continued)

Skull 16

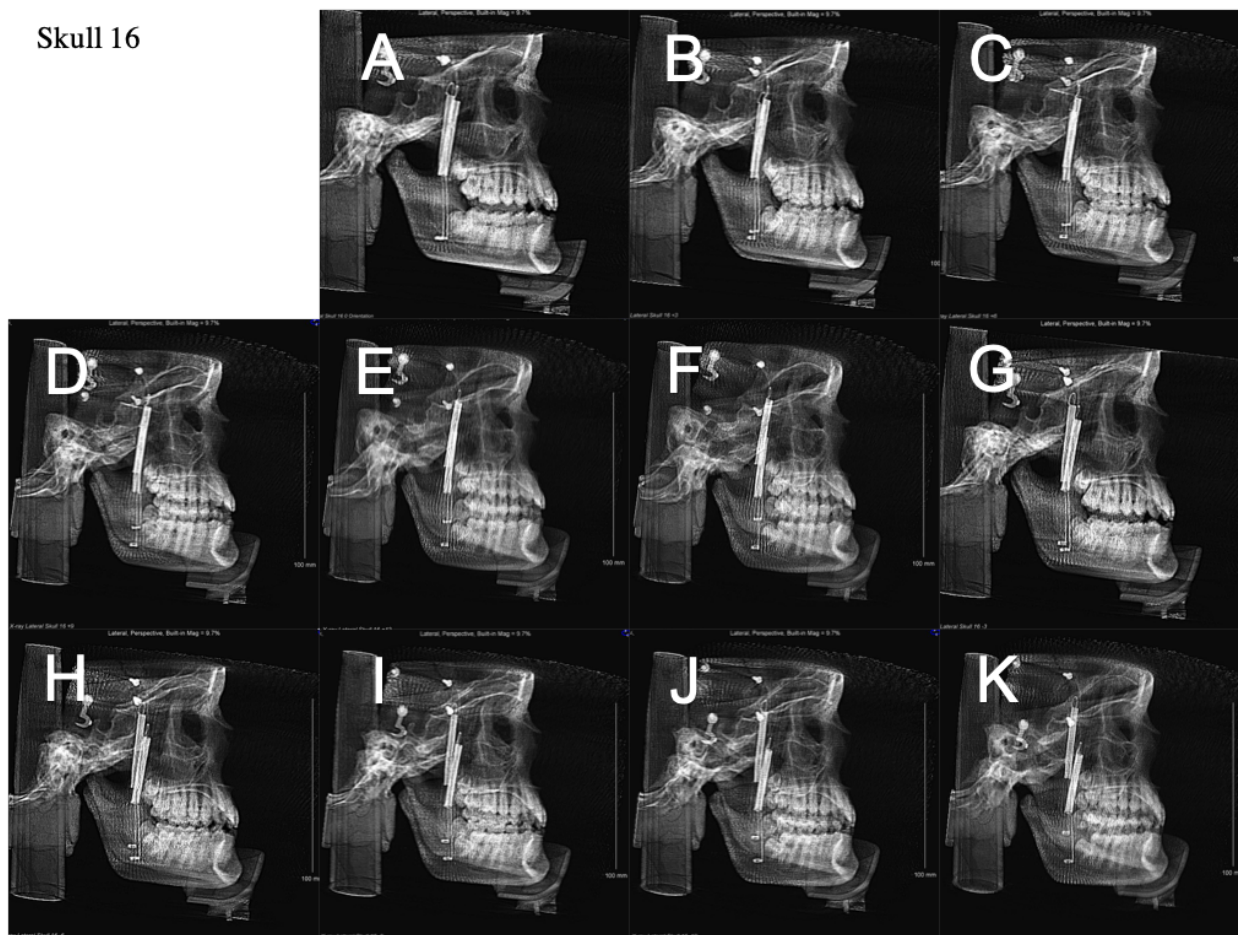


Figure 27. Skull 16. Cephalometric radiographs taken under 0° (A), 3° (B), 6° (C), 9° (D), 12° (E), 15° (F), -3° (G), -6° (H), -9° (I), -12° (J), -15° (K)

APPENDIX B (continued)

CEPHALOMETRIC RADIOGRAPHS (continued)

Skull 17

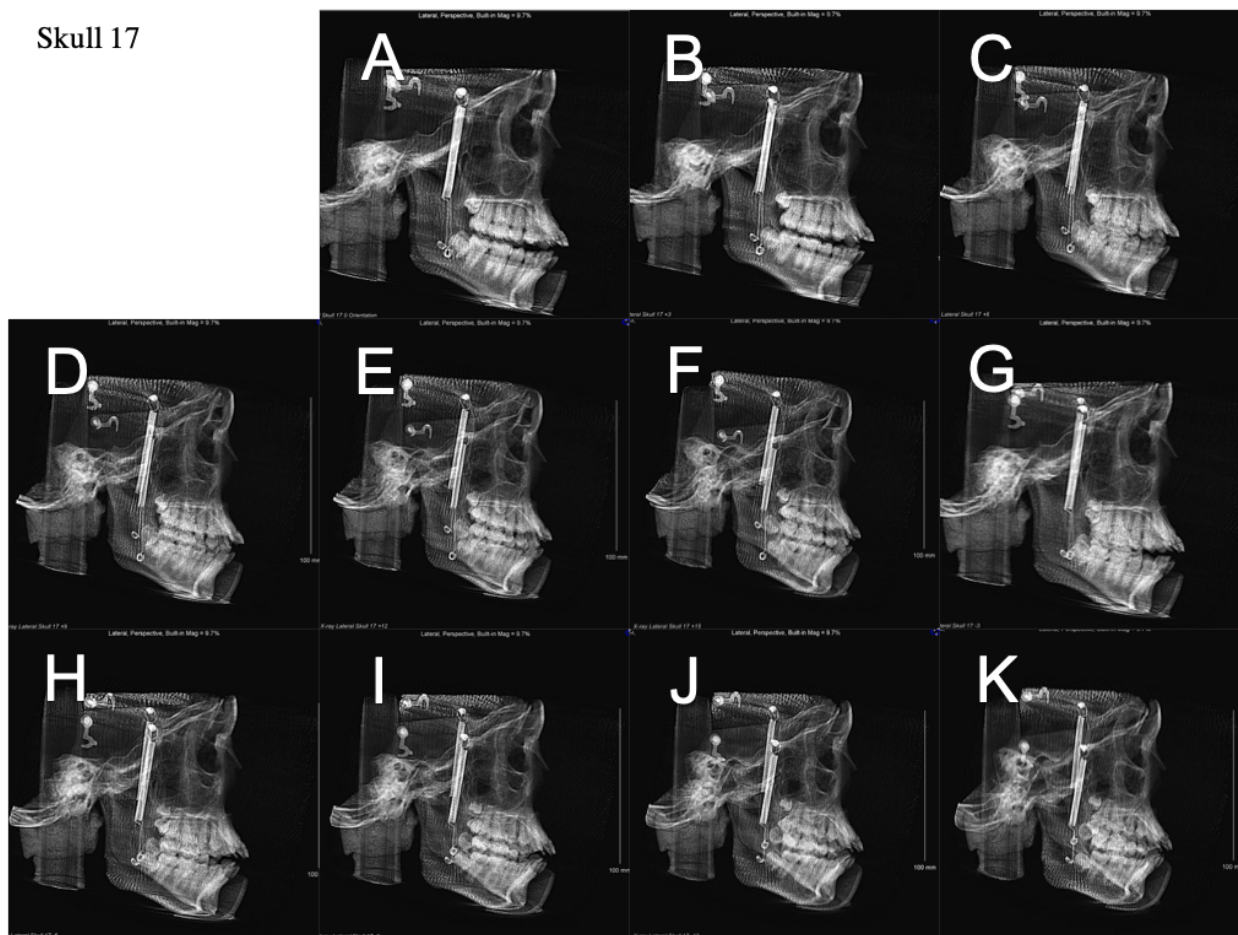


Figure 28. Skull 17. Cephalometric radiographs taken under 0° (A), 3° (B), 6° (C), 9° (D), 12° (E), 15° (F), -3° (G), -6° (H), -9° (I), -12° (J), -15° (K)

APPENDIX B (continued)

CEPHALOMETRIC RADIOGRAPHS (continued)

Skull 18

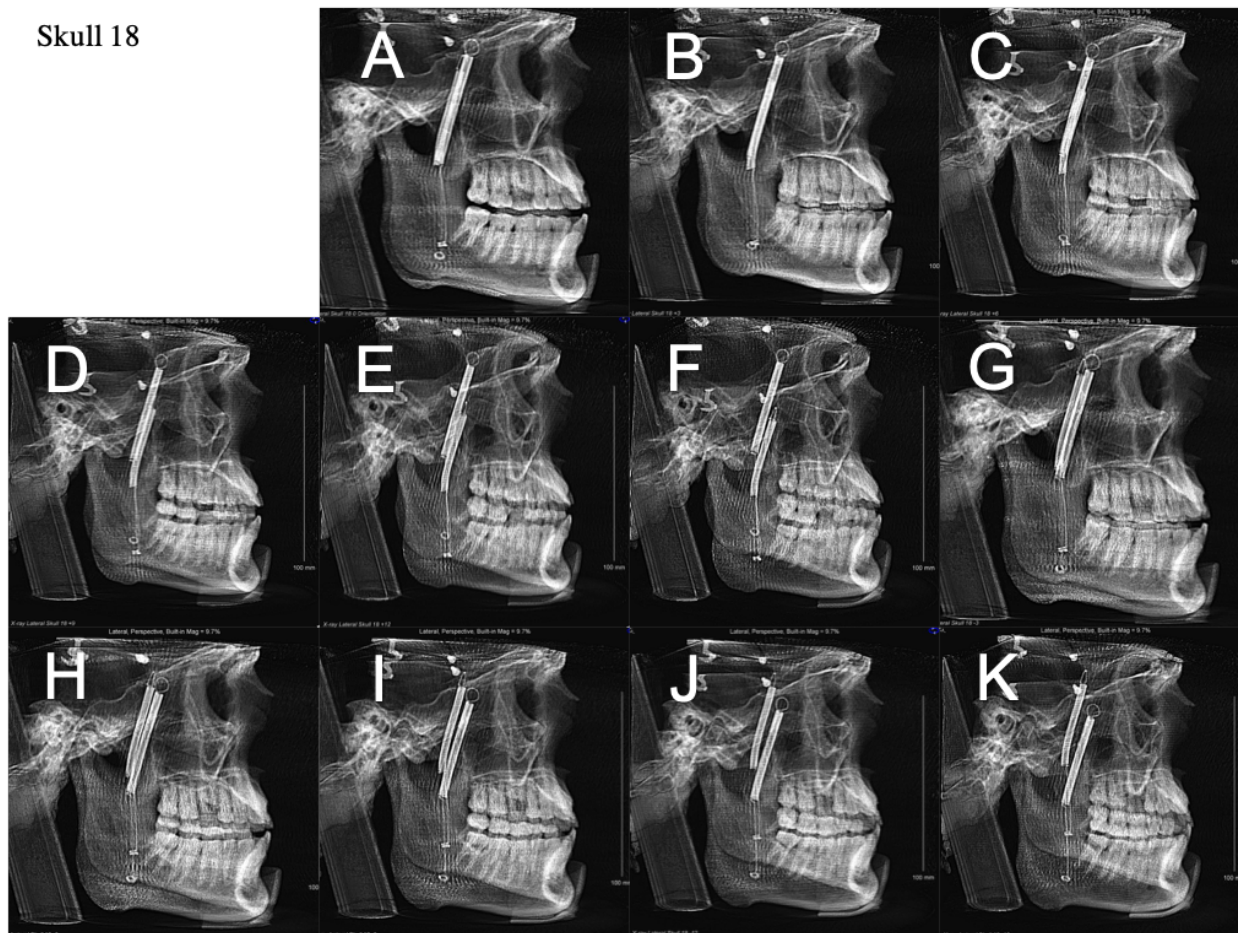


Figure 29. Skull 18. Cephalometric radiographs taken under 0° (A), 3° (B), 6° (C), 9° (D), 12° (E), 15° (F), -3° (G), -6° (H), -9° (I), -12° (J), -15° (K)

APPENDIX B (continued)

CEPHALOMETRIC RADIOGRAPHS (continued)

Skull 19

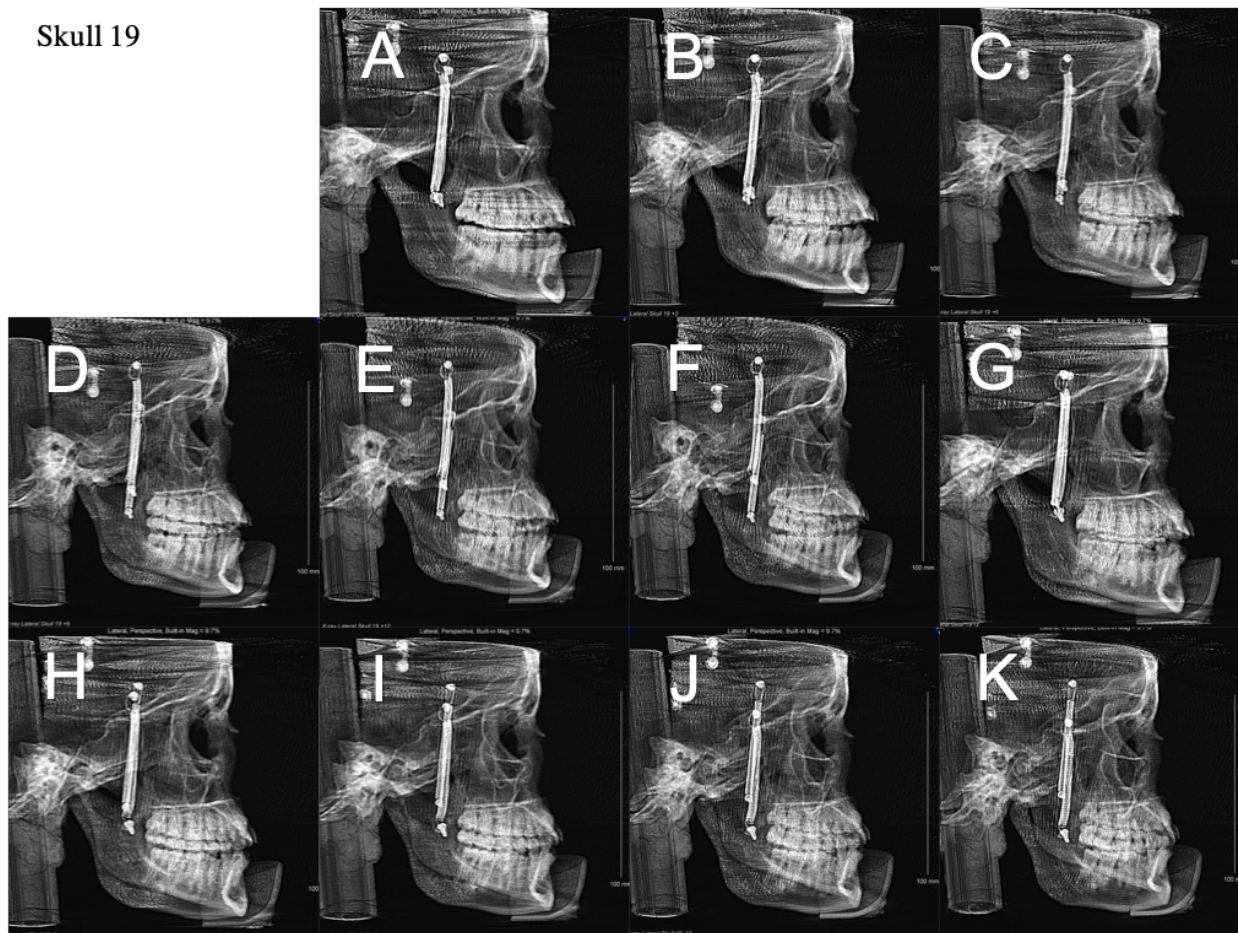


Figure 30. Skull 19. Cephalometric radiographs taken under 0° (A), 3° (B), 6° (C), 9° (D), 12° (E), 15° (F), -3° (G), -6° (H), -9° (I), -12° (J), -15° (K)

APPENDIX B (continued)

CEPHALOMETRIC RADIOGRAPHS (continued)

Skull 20

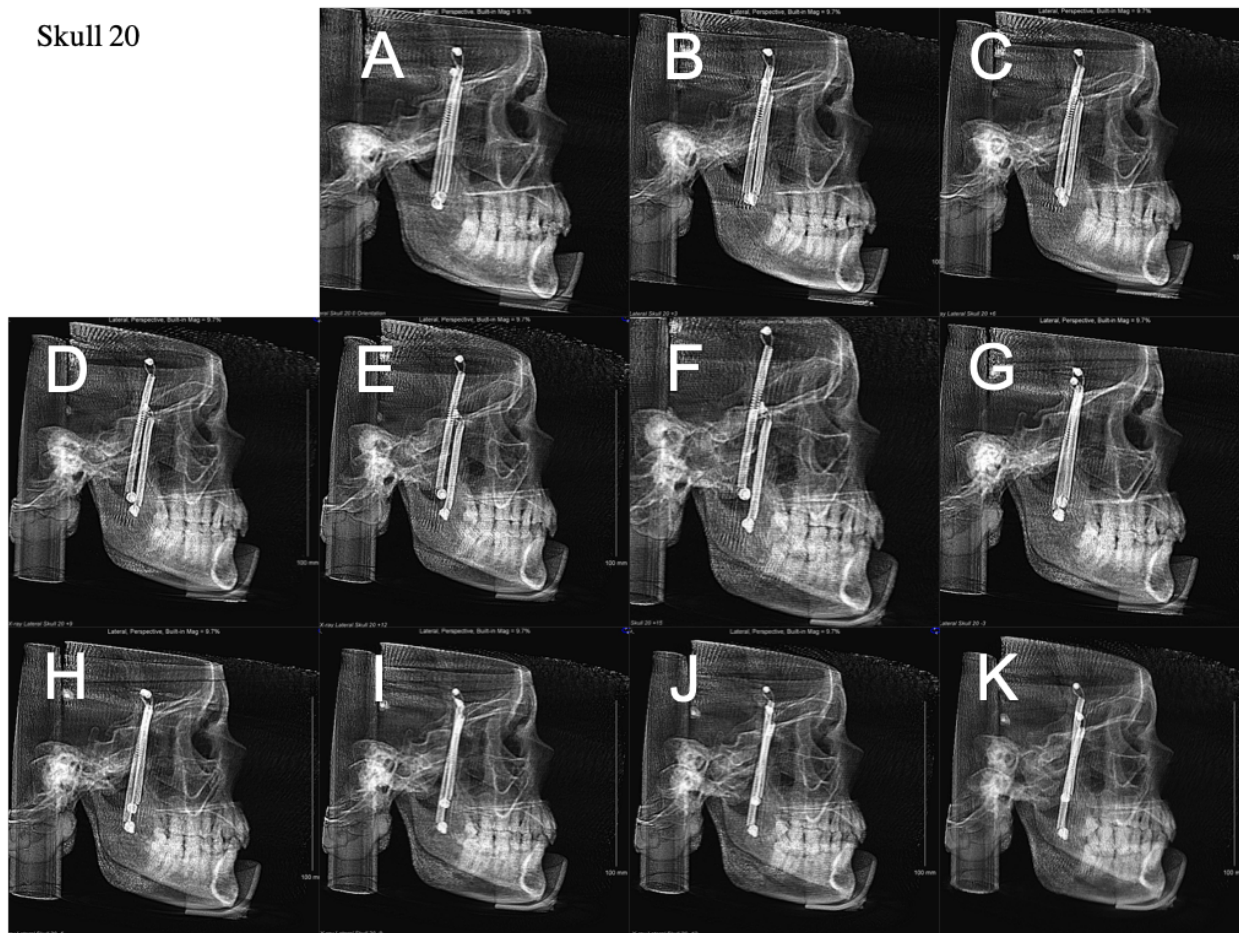


Figure 31. Skull 20. Cephalometric radiographs taken under 0° (A), 3° (B), 6° (C), 9° (D), 12° (E), 15° (F), -3° (G), -6° (H), -9° (I), -12° (J), -15° (K)

APPENDIX B (continued)

CEPHALOMETRIC RADIOGRAPHS (continued)

Skull 21

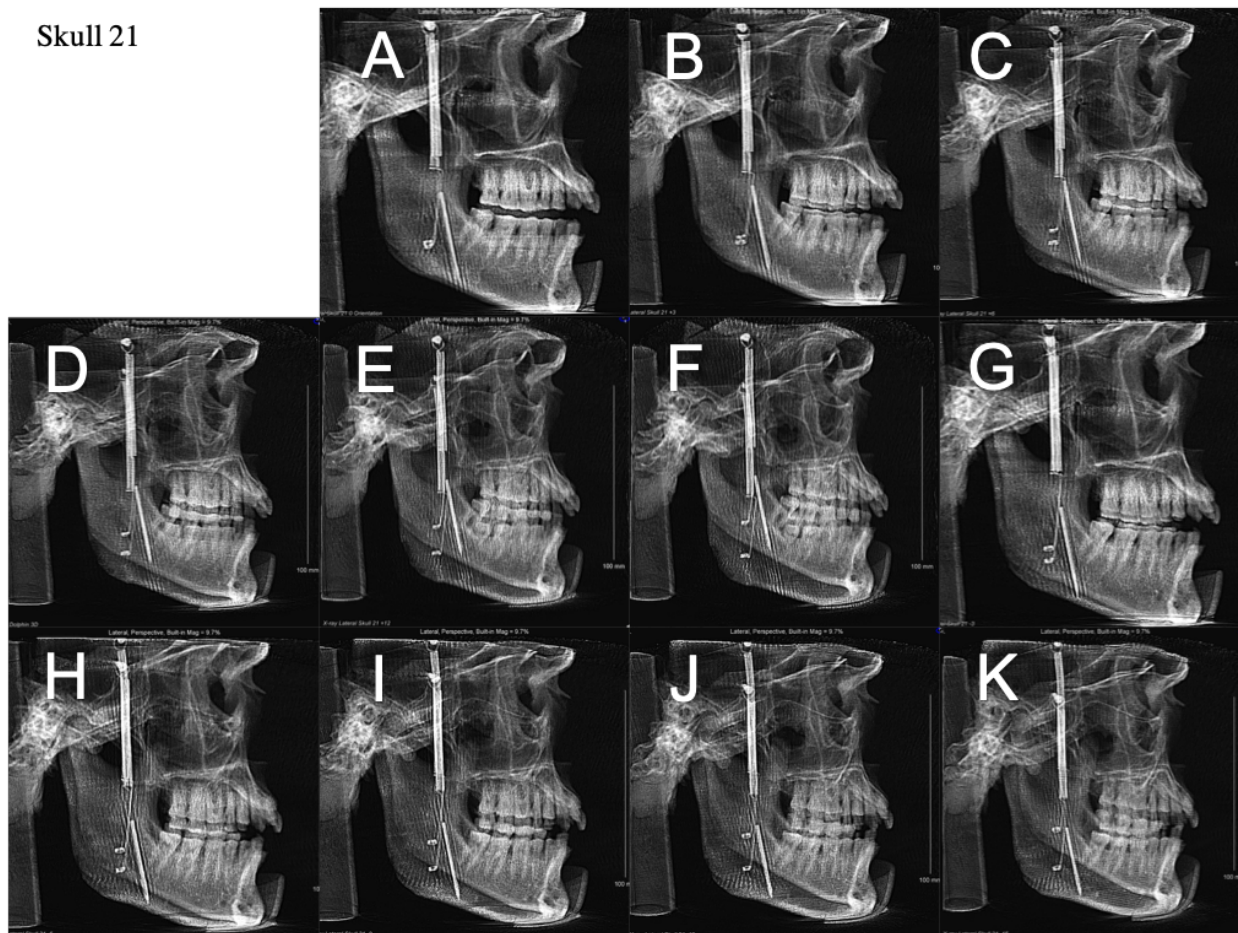


Figure 32. Skull 21. Cephalometric radiographs taken under 0° (A), 3° (B), 6° (C), 9° (D), 12° (E), 15° (F), -3° (G), -6° (H), -9° (I), -12° (J), -15° (K)

APPENDIX B (continued)

CEPHALOMETRIC RADIOGRAPHS (continued)

Skull 22

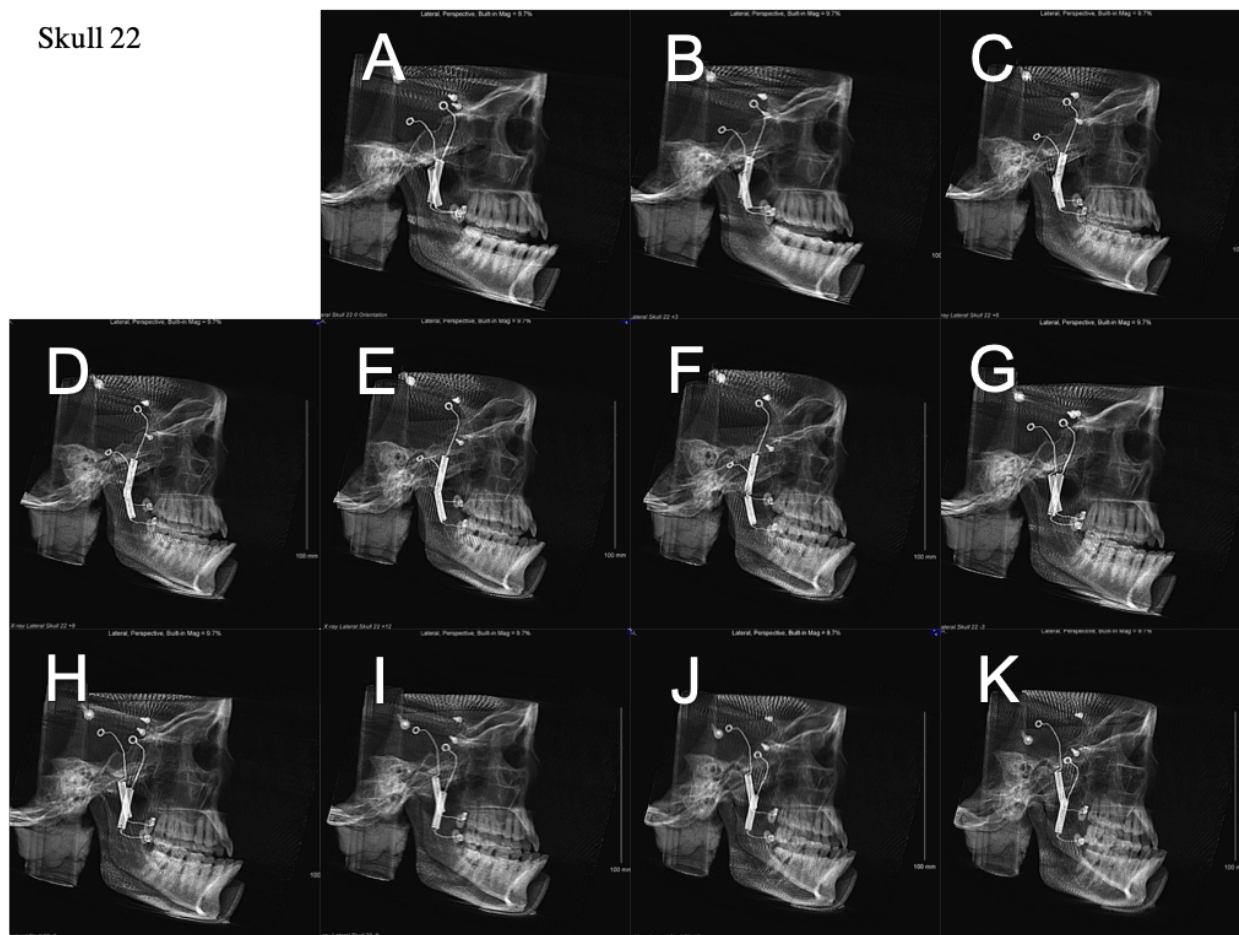


Figure 33. Skull 22. Cephalometric radiographs taken under 0° (A), 3° (B), 6° (C), 9° (D), 12° (E), 15° (F), -3° (G), -6° (H), -9° (I), -12° (J), -15° (K)

APPENDIX B (continued)

CEPHALOMETRIC RADIOGRAPHS (continued)

Skull 23

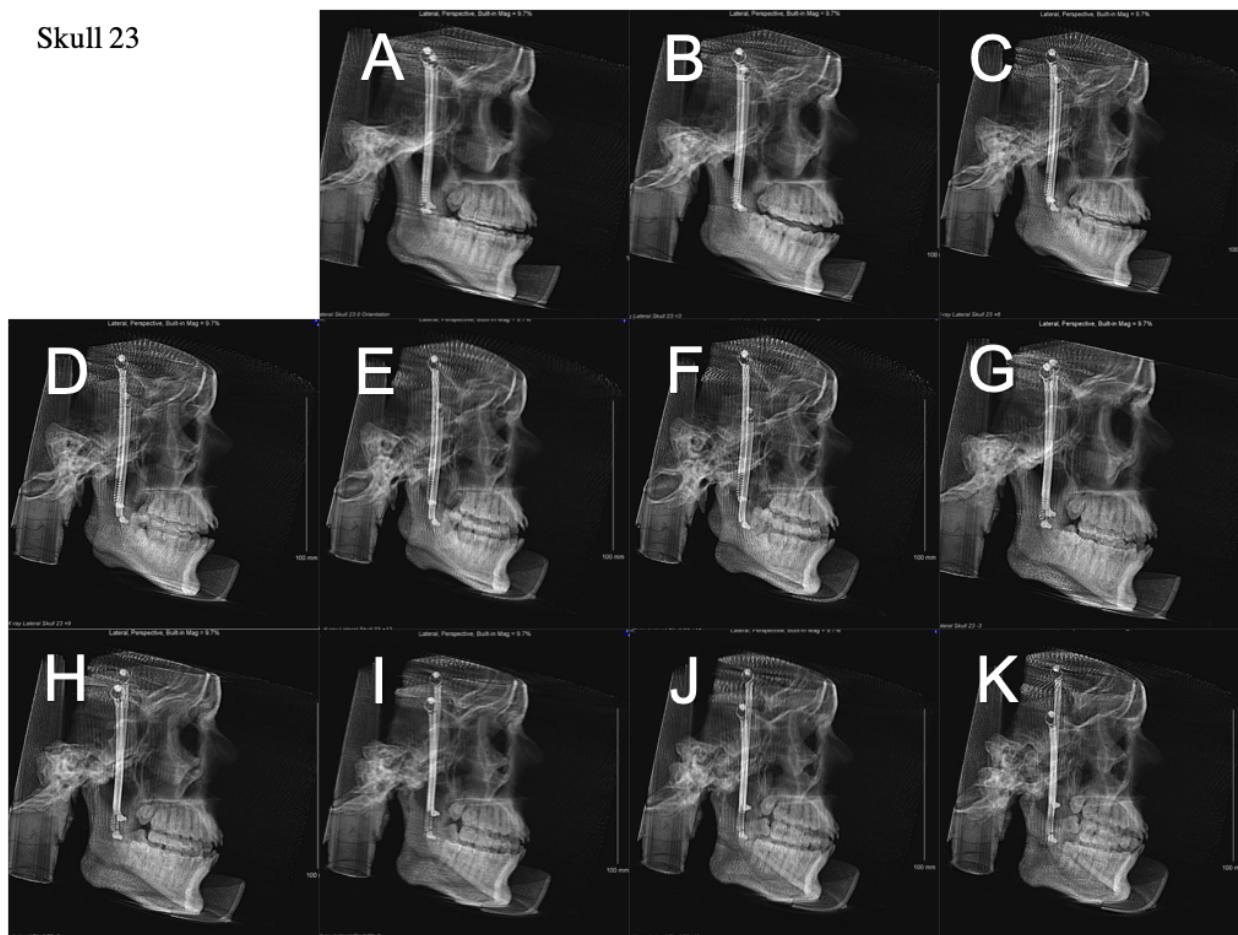


Figure 34. Skull 23. Cephalometric radiographs taken under 0° (A), 3° (B), 6° (C), 9° (D), 12° (E), 15° (F), -3° (G), -6° (H), -9° (I), -12° (J), -15° (K)

APPENDIX B (continued)

CEPHALOMETRIC RADIOGRAPHS (continued)

Skull 24

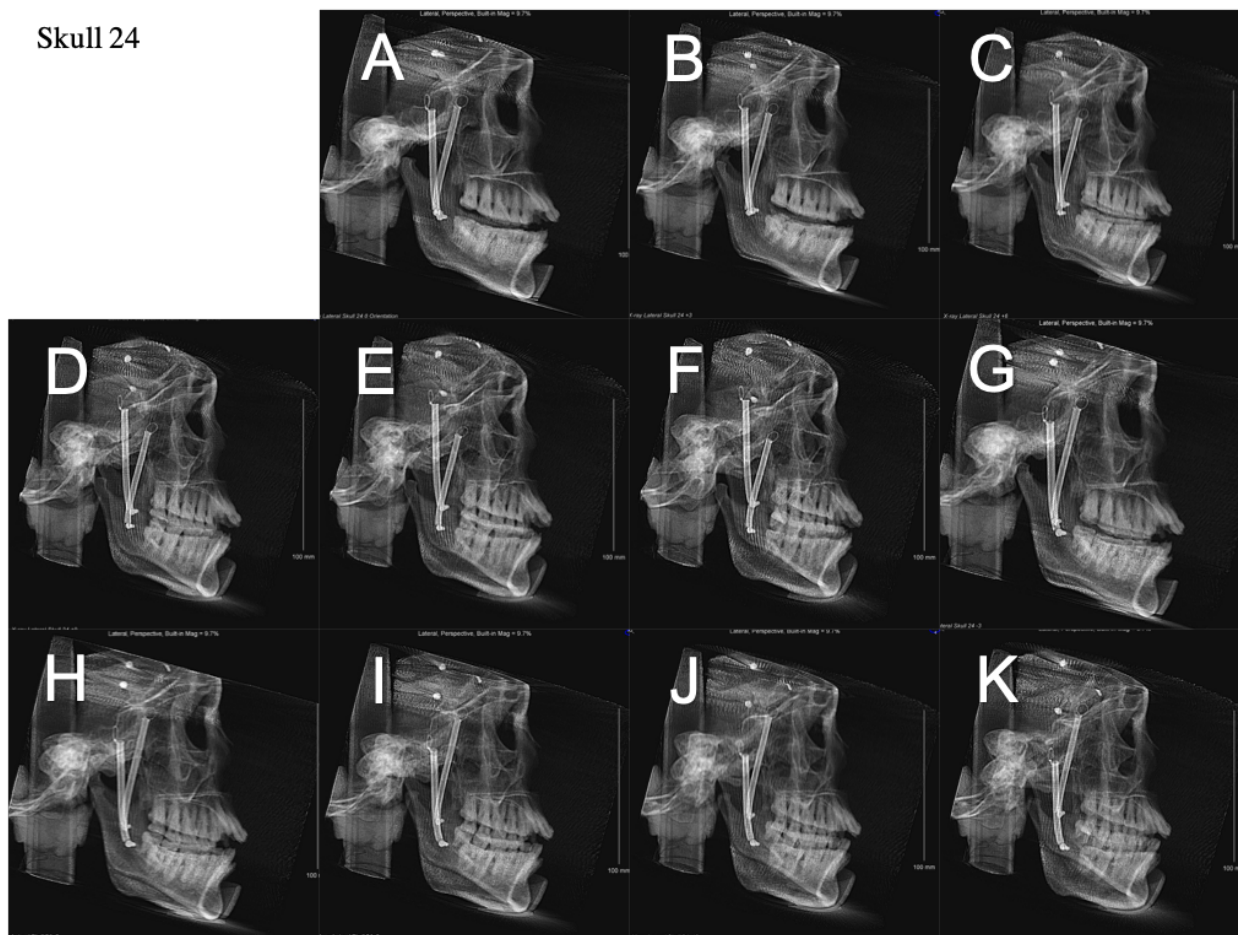


Figure 35. Skull 24. Cephalometric radiographs taken under 0° (A), 3° (B), 6° (C), 9° (D), 12° (E), 15° (F), -3° (G), -6° (H), -9° (I), -12° (J), -15° (K)

APPENDIX C

TABLE VII

RAW DATA. DELTA BETWEEN ANGULATED SKULL VS IDEAL SKULL POSITION (Δ)

Skull #	-15															
	SNA	SNB	ANB	FMA	U1-SN	NA-APo	SGn-FH	Ar-Go-Me	L1-MP	MP-SN	N-Me	Go-Me	S-Go	S-N	ANS-PNS	U1-PP
1	2.4	2.2	0.1	3.3	0.5	-0.6	4.7	-0.7	3.4	-4.2	-5.9	-5.5	1.9	-1.3	-1.9	-3.8
2	-1.2	-0.1	-1	2.2	1.2	-0.8	3.3	-1.2	6.9	-1.8	-6.2	-3.9	-2.7	-0.4	1.9	0.5
3	1.4	1.8	-0.4	-1.8	3.3	-1.1	-4	0.3	-2.7	-0.5	-5.5	3.1	-4.9	0.3	-3.1	1.1
4	-2.1	-1.7	-0.4	-1.6	-5.5	-1.4	-2.9	1.5	-0.6	1.2	-3	-1.6	-3.8	1	0.5	-4.7
5	-0.3	-0.3	0	1.2	-1.6	0.6	2.7	0.7	-2	-3.3	-4.9	-4.8	0.1	1.4	-1.3	-1.8
6	-2.5	-1.6	-0.9	-4.6	-2.8	-0.9	-2.7	-0.2	1.2	-2.4	-4.8	-2.1	-1.9	0.8	-0.6	-1
7	0.7	0.7	0.1	-2.5	-1.4	-0.1	-0.3	-1.7	-4.5	-4.8	-6.4	-2.6	-0.3	1.1	-0.8	-3
8	0.6	-0.1	0.8	-3	-2.3	1.8	-2.7	5	-1.5	-1.7	-4.2	-6.1	0.1	0.4	-1.4	0.1
9	0.6	-0.4	1	1.8	0.3	1.4	1.6	5.7	3.5	-1.4	-3.5	-5.5	0.7	1.2	-1.3	0.2
10	1.1	1.8	-0.7	0.8	0.7	-1.4	1.4	1.8	0.2	-1.6	-3	-1	-0.3	-2.4	-0.2	0.7
11	-1.8	-1.1	-0.7	0.2	-0.1	-2.6	3.2	-1.1	-1.9	-4.1	-7.2	-6.7	-0.2	0.5	-0.5	0.2
12	0.8	0.7	0.2	-3	2.8	0.1	-0.6	-0.3	-1.1	-4	-3.8	-1.8	1.2	-0.3	-0.8	-0.7
13	-1.6	-0.5	-1.1	-2.3	3	-3.4	-2.4	1.3	-0.3	-2.2	-6	-2.4	-2.4	2	0	5.2
14	1.6	0.2	1.4	-3.1	-2.1	2.3	-2	1.4	1.9	-2.6	-4.7	-3.5	-0.7	0.3	-3	-1.4
15	-1.4	-1.4	-0.1	-6	3.1	-1.1	-5	-1	-1.2	-1.5	-3.1	-0.2	-1.5	0.2	-1.9	-0.4
16	0.2	-0.2	0.4	-1.1	1.9	0.4	-2.1	1.1	-3.9	0.3	-1.6	2.2	-2.2	0.6	-3	3.5
17	2.7	1.8	0.8	-2.2	-3	2.5	-0.7	0.3	0.4	-4.2	-3.3	-4	2.3	1	0.2	-2.3
18	0	-0.2	0.2	-3.7	3.8	-0.5	-4.2	-1.5	0.2	-1.3	-7.4	5.3	-5.9	0.6	-3.1	4.7
19	0.9	0.5	0.3	-6.9	2.2	1.4	-3.7	-5.7	12	-6.2	-9.9	-3.5	-3	1	1.9	3.1
20	0.2	0.3	-0.1	-2	-1.3	0.1	-1.3	-1.5	-7.6	-3	-7.2	0.4	-3.7	0.5	-5.9	-1.5
21	1.3	0.8	0.5	-5.1	-1.6	0.9	-5.5	2.2	2.2	-1.4	-6.5	-2.7	-3.1	-0.1	0.4	0.2
22	1.2	0.9	0.3	-1.9	1.8	0.5	-1.7	5.5	-7.5	-1.9	-4.2	-9.2	1.3	0.2	-1.6	1.3
23	2.5	1.5	0.9	0.7	3.1	1.7	-0.2	2.1	4.2	-1.3	-4.6	2.1	-3.1	-1.1	-1.1	2.6
24	-0.7	-1.1	0.3	-5.7	-2.6	0.1	-6	0.6	-1	-0.3	-3.6	-0.2	-3.2	1.3	-0.5	-1.8

APPENDIX C (continued)

TABLE VII. (continued)

RAW DATA. DELTA BETWEEN ANGULATED SKULL VS IDEAL SKULL POSITION (Δ)

Skull #	-12															
	SNA	SNB	ANB	FMA	U1-SN	NA-Apo	SGn-FH	Ar-Go-Me	L1-MP	MP-SN	N-Me	Go-Me	S-Go	S-N	ANS-PNS	U1-PP
1	1.5	1.1	0.3	1.4	-2.2	0.3	1.4	2.4	1.3	-1.4	-2.6	-2.8	0.7	-0.6	-2.6	-3.7
2	-1.3	-0.6	-0.7	0.9	-0.9	-0.5	1.3	-0.7	5.9	-0.7	-4.9	-1.9	-3.4	0.4	1.9	-1.3
3	-0.5	0	-0.5	-0.1	1.5	-1.6	-3.1	3.1	-3	2	-2.1	0.5	-4.1	1.2	-4.5	2.9
4	-1.6	-2	0.4	-1.3	-3.7	0.5	-2.7	2.1	-0.5	1.7	-2.2	-1	-3.7	0.7	1.7	-2.4
5	-0.6	-0.3	-0.2	-0.7	-0.8	-0.3	0.2	3.1	-2	-1.8	-2.8	-3.9	0.6	0.6	1.5	-0.4
6	-2.2	-1.8	-0.5	-0.4	0	-0.2	0.5	1.9	-0.7	-0.8	-2	-1.6	-0.7	1.3	0.5	1.8
7	0.2	0.4	-0.1	-2.2	-0.1	0.2	-2	5.2	-5.9	-1.3	-3.2	-5.2	1.2	0.3	-1.2	-0.6
8	0.3	0.1	0.3	-3.2	-3.3	1.2	-1.6	4	0.2	-2.8	-3.1	-7.2	2.3	0.5	-1.9	-1.3
9	1	-0.2	1.1	2.2	-1.5	1.9	2.4	6.1	0.3	-0.8	-0.7	-7.1	3.7	0.5	-1.1	-1.3
10	0.5	0.2	0.3	1.3	-0.7	0.2	0.6	0.4	2.5	0	-2.2	-1.2	-1.4	-0.3	3.1	0.1
11	-1.5	-1.2	-0.3	1.6	0	-1.7	4	-2.4	-3.2	-2.9	-4.7	-4.7	0.1	0.6	-2.3	0.7
12	0.4	0.3	0	-3.1	1.6	0.5	-0.5	-2	-0.2	-3.5	-4	-3.4	1	-0.5	1.3	1.3
13	-1.7	-0.7	-1	-1.2	3.8	-2.6	-2.1	0.9	-1	0.1	-2.3	1.2	-2.9	1.3	0.6	5.5
14	1	-0.1	1.1	-2.5	-1.3	1.5	-1.1	0.3	0.6	-2.7	-4.4	-4.1	-0.3	0.2	-3.1	1.6
15	-1.6	-1.7	0.1	-5.9	2.4	-0.1	-3.2	-5.3	-1.3	-2.4	-1.8	1.9	-0.1	0.1	-1.2	4.8
16	-0.1	-0.1	0	-3.7	-2.9	0.3	-2.7	-0.3	-2.5	-2.1	-2.8	-1.2	-0.1	0.9	-2.4	-2.1
17	2.1	1.7	0.4	-2.7	-1	1.6	-2	0.9	-0.8	-3	-3.7	-3	0.4	0.6	1.1	0
18	-0.7	0.3	-1	-2.3	4.2	-2.2	-1.5	-0.3	3.4	-2.6	-5.5	-1.3	-1.9	1.1	-2.1	5.3
19	0.3	-0.3	0.6	-7.6	-2	1.5	-3.9	-5.9	9.7	-5.4	-7.6	-5.1	-1.1	0.4	0.3	-0.5
20	-0.9	-0.5	-0.4	-3.4	-1.8	-0.7	-2.7	-2.5	-3.5	-1.9	-4.2	-0.3	-2.2	0.9	-3.1	-0.7
21	1.9	1.1	0.7	-2.5	-1	1.3	-4	2.6	2.9	-0.2	-3.6	1.9	-3.3	0.3	0.6	-0.7
22	0.3	0.2	0.1	-3.5	0	0.2	-3.5	3.1	-6.4	-0.8	-2.9	-6.8	0.4	0.3	-1.3	-1.1
23	1.5	0.6	0.9	-4.9	-1.8	0.7	-4	-2.2	4.1	-3.4	-6.1	0.8	-2.5	0.1	-4	-1.2
24	-0.8	-1	0.2	-2.6	-1.4	0.5	-2.8	-1.1	-2.6	0.2	-2.1	0.3	-2.6	0.9	2	-2.3

APPENDIX C (continued)

TABLE VII. (continued)

RAW DATA. DELTA BETWEEN ANGULATED SKULL VS IDEAL SKULL POSITION (Δ)

Skull #	-9															
	SNA	SNB	ANB	FMA	U1-SN	NA-APo	SGn-FH	Ar-Go-Me	L1-MP	MP-SN	N-Me	Go-Me	S-Go	S-N	ANS-PNS	U1-PP
1	0.4	0	0.4	0.1	-6.4	1	0.5	0.3	2.9	-0.1	0.3	-0.5	0.8	-0.9	-1.1	-7.5
2	0.9	0.8	0.1	2.5	-0.6	0.3	2.5	2.8	1.8	-1	-1.8	-5.2	1.1	0.8	1.2	-1.2
3	1	0.7	0.2	-1.1	1.7	0.5	-2.6	0.1	0	0.7	-1	0.6	-1.9	0.7	-1.9	1.4
4	-0.9	-1	0	-1.7	-5.7	0.5	-2.2	-0.6	0.4	0.8	-1.3	-1.2	-1.7	0.2	0.3	-5.1
5	-2.9	-1	-1.8	0.9	-1.8	-3.2	1.6	3	-3.5	-1	-2.1	-3.9	0.1	0.9	-0.3	-0.7
6	-2.5	-1.3	-1.2	-0.8	-0.8	-2.6	0.5	-1.1	-0.7	-1.8	-3.8	-1.2	-2.2	0.8	0.3	0.3
7	0.1	0.9	-0.7	-4.9	0.5	-1.5	-6.3	0	-6.3	0.2	-2.5	5	-4.6	0	-0.3	0.1
8	-0.2	-0.9	0.8	0.5	-1.7	1.5	0.2	5.8	0.4	0.4	-1.1	-4.4	0.3	0.1	-0.3	1.2
9	-1.6	-1.5	-0.1	2.5	-0.7	-1	1.9	3.5	0.8	0.9	0.3	-3	0.5	1.3	-1.2	-0.6
10	-1.4	-1.1	-0.3	1.9	-0.4	-0.6	0.5	-0.2	0	2	-0.5	1	-3	0.4	3.2	2.2
11	-1.3	-0.7	-0.6	0.2	0.1	-1.7	0.2	0.5	-3.6	-0.1	-1.7	0.4	-1.7	0.1	-1.6	0.9
12	0.8	0.5	0.3	2.8	2.9	0	3.1	-1	-2.3	-0.8	-0.8	2.6	-1	-0.9	-0.7	0.3
13	-1.5	-0.7	-0.8	-3	1	-2.3	-2.4	1	-0.1	-1	-3.2	-3.2	-0.8	0.3	0.5	1.9
14	0	-0.8	0.8	-1.1	-2.6	0.4	-1.1	2.4	8	-0.2	-1.5	-3.5	-0.3	0.2	-1.1	-1.2
15	-1.8	-2	0.2	-3	0.6	-0.7	-2.6	1.4	-3.3	0.3	0.1	-1.9	0.4	0.7	1.6	2.3
16	-0.2	-0.2	0	0.9	-1.1	0.2	0.4	0.8	-3.2	0	-1.6	0.1	-1.5	0.7	-2.7	-0.7
17	1.5	1	0.5	-1.6	-4.3	1.9	-1.1	3	-0.9	-1.9	-3.1	-3.9	0.6	0	-1.9	-2.8
18	-1.2	-0.4	-0.8	-3.3	0.9	-1.9	-2.4	-1.1	2.8	-1.8	-2.9	0.1	-0.7	1.5	-1.9	1.6
19	0.9	0.2	0.7	-4.8	-2.5	1.8	-2.7	-2	5.1	-3.5	-5.4	-5.8	-0.5	0.3	-0.3	-1.5
20	-0.4	-0.6	0.2	-5.4	-1.6	0.1	-5.7	-0.4	-3.6	-0.3	-2.3	0.8	-2.1	0.8	-3.1	-0.5
21	0.3	-0.1	0.3	-2.5	-0.7	0.7	-3	0.9	-0.2	0.1	-1.7	0.3	-1.6	0.2	0.6	-0.1
22	0.2	-0.2	0.5	0.4	1.2	1.2	-0.7	4	-3.1	0.4	-2.4	-5.7	-0.8	1.1	3.6	-0.6
23	0.3	-0.5	0.8	-1.9	-2.7	1.2	-1.6	0	1.9	-0.3	-2.4	1.2	-2.2	-1	0.1	-2.4
24	-0.6	-0.7	0.1	-1	-0.1	0.1	-0.7	-2.8	-1.2	-0.4	-0.7	4	-2.3	1.2	1.7	0.1

APPENDIX C (continued)

TABLE VII. (continued)

RAW DATA. DELTA BETWEEN ANGULATED SKULL VS IDEAL SKULL POSITION (Δ)

Skull #	-6															
	SNA	SNB	ANB	FMA	U1-SN	NA-APo	SGn-FH	Ar-Go-Me	L1-MP	MP-SN	N-Me	Go-Me	S-Go	S-N	ANS-PNS	U1-PP
1	2	0.3	1.6	1.4	-0.9	3	1.9	-2.3	1.7	-0.4	-0.2	1.6	-0.1	-1.3	-0.7	-3.2
2	-0.4	0.4	-0.8	0.5	2.4	-1.1	0.8	-0.8	4.7	-1	-2.6	-2.7	-0.6	0.4	-0.2	1.7
3	-0.4	0.1	-0.5	-1.1	1.6	-1.2	-2.6	0	-1.1	1.5	0.5	0.3	-1.3	0.6	-2.6	2.5
4	-0.7	-0.6	-0.1	-3	-3.8	-0.4	-2.6	-0.4	0.7	-0.3	-0.1	-2.6	1.2	0.3	0.7	-3.2
5	-1.8	-1	-0.8	2.8	0.6	-1.8	3.1	2.8	-0.9	-0.5	-0.5	-3.3	0.9	1.4	-1.4	2.4
6	-0.8	-0.5	-0.2	0.1	-3	-0.4	-0.3	-0.5	-4.4	-0.4	-3.4	1.6	-4	0.9	0.4	-3.8
7	0	0.3	-0.2	-3.6	0	-0.7	-4.2	-0.2	-0.8	0.4	-0.3	2.2	-1.4	0.1	-0.7	-0.1
8	-0.6	-0.4	-0.2	-0.8	-4.9	-0.1	-0.8	5.1	-4	-0.3	-1.3	-5.1	1.1	0.5	-1.7	-2.9
9	0.5	-0.8	1.3	2.1	-1.4	1.6	1.8	2.4	0.7	0.1	-1.3	-3.8	0.2	0.9	-0.2	-1.7
10	-1.2	-1.1	-0.1	-0.3	-2.1	-0.7	-1.6	1.3	0.2	2.3	1	0.2	-1.6	0.1	1.3	-0.5
11	-0.6	-0.6	0	0.1	-0.5	-0.3	0	-0.4	-4.4	0.3	-0.6	2.1	-1.7	-0.1	-0.9	0
12	0.9	0.6	0.3	2.5	1	1	3.9	-1.9	-0.2	-1.9	-1.6	-0.4	0.6	-0.8	1.1	-0.3
13	-2	-0.7	-1.3	0.1	-0.4	-3	-0.5	1.4	-1.9	0.4	-0.3	0.3	-0.9	1.1	-0.7	1
14	-0.1	-0.9	0.8	-0.2	-0.4	0.5	-0.2	4	-3.7	0	-1	-4.9	0.4	0.1	-0.6	0.2
15	-0.9	-0.7	-0.2	-5.5	4.4	-1.2	-4	-0.1	-0.3	-1.7	-0.3	-2.9	2.4	0.4	-0.3	5.4
16	-0.4	-0.6	0.2	-1.1	-1.9	0.3	-2.3	1.6	-3.6	1.5	0.1	1	-1.7	0.2	-5.6	-0.6
17	1.6	0.8	0.9	1.5	-4.4	2.4	1.8	2.7	-1.7	-0.8	-1.2	-3	1.1	-0.4	0.8	-3.7
18	-0.2	-0.2	0	-1.6	-0.8	-0.6	-1.6	-0.6	4.6	-0.5	-2.6	1.1	-1.9	0.1	-0.5	-0.8
19	-0.2	0	-0.2	-3.3	-0.5	0.1	-2	-1	5.3	-1.7	-2.9	-2.9	-0.5	0.1	0.5	0.5
20	-0.9	-0.3	-0.6	-2.6	-2.1	-1.3	-3.4	-1	-0.7	0.5	-1	2.4	-2.3	0.7	-0.7	-0.9
21	1	0.2	0.8	-2.2	-0.4	1.8	-2.5	-1.5	-1.3	0.1	-0.3	4.2	-1.7	0.2	0.8	0.2
22	0.6	-0.4	1	-1.2	-0.4	2.6	-0.9	2.7	-2.3	-0.1	-1.3	-5.5	0.7	0.2	2.3	-0.8
23	0.5	-0.2	0.7	-5.6	-1.7	1.3	-4.8	0.7	0.4	-1	-1.5	0.2	-0.4	-0.4	0	-1.6
24	0.5	0.5	0	-1.8	0.1	0.7	-2.1	0.6	-3.7	-0.1	-0.2	0.6	-0.1	0.4	-0.4	-0.8

APPENDIX C (continued)

TABLE VII. (continued)

RAW DATA. DELTA BETWEEN ANGULATED SKULL VS IDEAL SKULL POSITION (Δ)

Skull #	-3															
	SNA	SNB	ANB	FMA	U1-SN	NA-APo	SGn-FH	Ar-Go-Me	L1-MP	MP-SN	N-Me	Go-Me	S-Go	S-N	ANS-PNS	U1-PP
1	0.5	-0.2	0.6	-0.4	-3.5	0.9	-0.3	-1.2	2.1	0.4	1.5	1	0.7	-0.8	0.4	-4
2	0.5	0.3	0.2	1.5	1.7	0	1.2	-0.1	-0.9	-0.3	-1.4	0	-1	0	-0.9	0.5
3	-0.2	-0.4	0.2	-2.3	1.3	-0.4	-2.5	-3.1	-0.2	0.2	-0.8	0.2	-1.2	0.1	-4	1.4
4	-0.6	-0.6	0	-3.1	-2.3	-0.3	-3.7	1.1	5.9	1	0.1	-1.5	-0.5	0	0.7	-1.5
5	-1.9	-0.1	-1.8	-0.2	-2.7	-3.4	0.4	2.4	-2.1	-1	-0.1	-2.8	1.8	0.5	1.1	-1.7
6	-0.2	-0.3	0.1	0.7	-0.3	0.6	1.7	0.7	-2.4	-1.2	-1.8	-2.6	0.4	0.4	0.7	-1
7	-0.2	0.1	-0.2	-1.5	1.1	-0.5	-1.2	0.1	-1.5	-0.2	0.4	1	0.2	0	0.9	1.1
8	-0.4	-0.2	-0.1	-1.6	-4.4	0.6	-0.9	2.6	-4.6	-0.8	-0.8	-2.9	1.2	0.2	-1.4	-3.3
9	-1.1	-0.8	-0.3	-1.1	0.6	-1.1	-1.1	3.4	-0.2	0.1	-1	-5.5	1.2	0.7	-1.6	0.2
10	-1.1	-0.4	-0.7	2.3	-0.3	-1.7	0.9	-2	-1.3	2.2	1.3	5.8	-3	-0.5	1.7	1.2
11	-0.5	-0.3	-0.3	2.9	-0.3	-1.4	2.5	0.9	-1.9	0.4	-0.5	0	-0.9	-0.1	-2.1	0.1
12	0	-0.1	0.1	0.7	3.6	-0.2	1.4	-1.2	-1	-0.3	-0.1	1.5	-0.3	-1.3	1.2	2
13	-0.6	-0.3	-0.2	0.5	0.2	-0.1	0.1	-0.1	-1.2	0.5	-0.2	-0.9	-0.6	0.6	0.8	1.7
14	0	0.1	-0.1	0.7	0.7	-0.6	1	2.6	-0.5	-0.3	1.1	-2.6	2.2	-0.2	-0.7	1.2
15	-0.7	-0.3	-0.4	-9	5.6	-0.9	-8.3	0.4	0.3	-0.8	1.6	1.6	1.9	0.5	-0.5	6.4
16	-0.4	-0.6	0.1	-2	-0.5	-0.7	-2.8	0.2	-2.3	1.1	0.1	0	-0.9	-0.2	-3.3	-0.4
17	1.1	0.7	0.4	5.2	3.6	1.5	4.2	3.5	-3.6	0.6	-0.4	-1.7	0.1	0	-0.6	3.9
18	-1.3	-1	-0.4	-1.8	-2	-1.6	-2.4	0.5	1.9	0.6	-0.5	1.1	-1.5	1	1.4	-1.3
19	-0.3	-0.7	0.4	-1.2	0.5	0.5	-1.4	-1.4	4.5	0.1	-1.7	-0.1	-1.9	0.4	1.1	1.9
20	-0.8	0.5	-1.3	0.5	-0.8	-2.8	-0.4	-1.1	-2.2	-0.4	-0.7	0.9	-0.5	1.9	-2.6	-1.2
21	0.6	0.3	0.4	0.6	-1.9	0.8	-0.9	1.5	-1.4	1.4	0.9	2.2	-1.3	0.2	0.1	-1.4
22	-0.6	-0.6	0.1	-0.2	0.1	0	-1.2	2.6	-2.8	1.4	0.4	-2.9	-0.1	0.5	0.6	-0.2
23	0.4	-0.1	0.5	-2.1	-1.8	0.9	-1.8	1.5	2	-0.5	-1	-0.4	-0.3	-0.2	-0.5	-1.6
24	-0.3	-0.6	0.3	1.1	-0.5	0.7	0.5	0.7	-4.4	1.2	0.8	1.8	-1.1	0.2	1.6	0.1

APPENDIX C (continued)

TABLE VII. (continued)

RAW DATA. DIFFERENCE BETWEEN ANGULATED SKULL VS IDEAL SKULL
POSITION (Δ)

Skull #	3															
	SNA	SNB	ANB	FMA	U1-SN	NA-APo	SGn-FH	Ar-Go-Me	L1-MP	MP-SN	N-Me	Go-Me	S-Go	S-N	ANS-PNS	U1-PP
1	-0.5	-0.8	0.3	-1	-2.4	0	-0.2	-0.3	-0.3	-0.5	0.8	-1.2	1.7	0.1	-0.4	-2.8
2	-0.4	0.9	-1.3	2.4	-1.7	-2.3	2.6	-0.3	-1.2	-0.8	-0.6	-0.2	1.4	-0.2	0.5	-2.8
3	1.2	1.1	0.2	-0.4	-0.1	0.1	0.6	0.8	0.8	-1.9	-1.8	-5.5	1.5	-0.3	-1.8	0
4	0	0	0	-1.5	0.2	0.3	-1	-1	2.3	0.1	0.8	-0.5	0.7	-0.6	-0.1	0.6
5	0.7	0.9	-0.2	0	0.1	0.6	0.3	0.4	0.6	-0.5	0.6	0.9	0.9	-0.4	-1	-0.3
6	-0.2	0.3	-0.5	-2.1	0.3	-0.7	-0.5	-1.5	-0.2	-1.8	-0.5	-0.5	1.1	0	1.6	0.8
7	0.7	1.1	-0.2	2.9	0.4	-0.5	2.3	0.6	-3.1	0.3	0.5	2.5	-0.6	-0.4	-1.4	-1.4
8	0.2	0.7	-0.4	-1.2	1.7	-0.7	-0.4	-3.2	2.4	-1.4	-0.2	2.4	0.4	0	2.8	2.8
9	-0.1	-0.7	0.6	-2	0.3	0.1	-2.1	2.2	4.9	0.3	-0.2	-4.1	1.2	0.3	1.1	1.1
10	-0.6	0.2	-0.8	0	-0.2	-1.4	-0.6	-1.4	-1.1	1.2	1.2	3	-1.1	-0.7	0.8	0.4
11	0.1	0	0.1	2.9	-1.5	-0.5	2.9	2.3	1.1	-0.3	-2	-3.5	0.1	-0.5	-1.3	-2.4
12	0.4	0.1	0.3	0.1	0.1	0	0.4	-1.7	2	-0.4	-0.3	2.3	-0.9	-0.6	2	0.2
13	-1.1	0	-1.1	1.2	-0.5	-2.6	0.4	-1.1	1.3	0.3	0.1	2	-1.3	1.2	-1	0.6
14	0	0.1	-0.1	-2.3	-0.9	-0.3	-2.4	-0.1	1.8	0.1	-0.2	-0.7	-0.1	-0.3	-1.2	-1.5
15	0.2	0.2	-0.1	-3.8	4	-0.5	-4.3	1.9	1.1	0.4	1.5	-0.9	1.4	0.2	0.6	4.6
16	-0.6	-0.1	-0.4	0.8	-1.6	-0.9	0.4	0.1	3.5	0.3	-1.1	-2.2	-0.9	0	-0.7	-0.2
17	1.3	0.9	0.4	1.4	0.6	1.5	0.8	3.7	-3.4	0.1	0.4	-2.8	1.5	0.5	0	1
18	-0.4	-0.1	-0.3	2	-2.3	-1.4	1.6	0.1	-1.3	0.1	-0.3	1.4	-0.5	0.3	-0.9	-2.4
19	0.8	0.5	0.3	-0.8	0	0.9	-1	1.2	-1	-0.3	-0.7	-1.5	0.4	0.2	2.2	0.4
20	0.2	0.3	-0.1	2.3	-1	-0.2	1.3	-2.8	-3	0.4	0.8	6.7	-2	0.8	1.6	-1.1
21	-0.1	0.4	-0.5	-4.5	-0.4	-1	-4.2	0.5	-0.6	-0.9	-1	-0.3	0.4	0.1	-0.1	-0.1
22	1.1	1.3	-0.2	0.3	2	-0.1	-0.2	-1.8	-2.7	-0.7	-1.4	1.5	-1	-0.1	-0.6	0.4
23	0.1	0	0.1	0.6	-1.7	0.9	0	1.4	2.6	1.2	0.7	-0.1	-0.5	-0.3	-3.2	-2.6
24	0.1	-0.4	0.5	0.2	-0.9	0.8	-0.1	-7.5	1.1	0.9	1.3	10.5	-4.3	-0.4	0.3	-1.7

APPENDIX C (continued)

TABLE VII. (continued)

RAW DATA. DIFFERENCE BETWEEN ANGULATED SKULL VS IDEAL SKULL
POSITION (Δ)

Skull #	6															
	SNA	SNB	ANB	FMA	U1-SN	NA-APo	SGn-FH	Ar-Go-Me	L1-MP	MP-SN	N-Me	Go-Me	S-Go	S-N	ANS-PNS	U1-PP
1	0.6	0.2	0.6	1.3	-4.3	0.5	1.8	-1.1	-3.4	-0.8	0.1	0.6	0.9	-0.5	-0.3	-5.4
2	0.2	0.7	-0.5	-2.5	0.2	-0.4	-1.8	2.7	1.6	-1.2	-1	-5.1	2.2	0.1	0.6	0.8
3	0.2	0.3	0	2.1	-0.3	-0.1	2.8	4.4	0.4	-1.2	-1.8	-6.1	1.1	0.1	-2.4	0.4
4	-0.4	-0.5	0.1	-4.6	1.2	-0.1	-5.6	-2.6	0	1.3	0.5	-52.7	-2.9	0	0.5	1.8
5	0.9	0.5	0.4	4.7	1.7	0.6	4.9	0.1	2.6	-0.7	-0.1	-0.1	0.7	0.1	-1.7	0.4
6	1	0.8	0.2	0.7	2.9	0.2	1.7	1.3	-0.2	-1.9	-1.1	-2.2	1.9	-0.3	1.9	2.3
7	0.3	0.3	0.1	2.4	0.2	0.1	1.6	1.4	-1.6	0.8	0.1	490.3	-0.5	-0.3	-0.1	0.5
8	1.1	1	0.3	0.5	0.8	0.9	0.7	1.2	3	-0.6	-0.2	-1.2	0.9	-0.3	0.6	2.2
9	1.1	0.2	1	-2.8	1.6	1.7	-3.3	2.8	5.5	0.5	-1	-3.3	0.2	-0.1	-0.7	2.7
10	-1.7	-1	-0.7	-1.4	-2	-1.1	-2.4	2.3	2.2	2.5	1.5	0.5	-1.4	-0.4	-1	1.2
11	0.2	0.6	-0.4	5	-0.4	-1.5	4.2	4.4	3.3	0	-2.2	-2.2	-0.7	-0.6	-3	-1.9
12	0.9	0.5	0.4	0.1	0.1	0.7	0.7	-2.4	1.7	-0.8	-1.2	3	-1.6	-1	1.2	0.1
13	-1.2	-0.6	-0.7	0	-2.4	-1.5	-0.7	2.5	-2.2	0.6	-0.2	-2.6	0.2	1.1	0	-0.9
14	-0.1	-0.3	0.3	0.1	-1.2	0.5	-0.7	2.5	-4.5	1.1	-0.6	-1.3	-1.3	0	-2.4	-1.8
15	-0.3	0.2	-0.5	1.3	5	-0.6	1.3	0.2	0.5	-0.3	0.4	-0.8	0.9	0.7	-0.3	5.1
16	-0.3	0	-0.3	1.2	-0.8	-1.2	-0.1	-2.4	1.4	1.1	-1.3	0	-2.3	-0.3	-2.5	0.1
17	1.9	1.9	0	0.6	0.2	0.7	-0.4	2.2	-6.9	-0.5	0.1	0.5	0.8	0.4	0.1	-1
18	0.5	0.8	-0.2	2.6	3.4	-1	2.2	-0.9	-1.4	-0.5	-0.7	2.1	-0.3	0.2	0.7	2.7
19	1	0.4	0.6	-3.3	1.8	1.2	-2.6	-1.8	-4.7	-1.2	-2.1	0	-0.7	-0.1	2.1	2.7
20	-0.1	0.5	-0.6	0.3	-0.8	-1.6	-0.6	-0.7	-2.8	0.4	0.7	2.2	-0.3	0.7	0.5	-1.2
21	1.5	1.2	0.3	-4.4	-0.6	0.5	-5.5	2	0.7	0.4	-0.7	-1.3	-0.3	-0.7	0.7	-0.8
22	0.7	0.4	0.3	-0.4	2.5	0.6	-0.4	2.9	-2.8	-0.3	-0.6	-5.3	2	-0.3	-0.6	2.2
23	0.3	-0.2	0.5	3.2	-2.2	1.8	2.4	0.4	1.4	1.5	0.8	0.4	-0.8	-0.5	0.3	-2.4
24	-0.3	-0.6	0.3	-2.4	0	0.8	-3.6	-0.4	-1.4	1.9	0.9	4	-2.5	-0.3	1.1	-0.6

APPENDIX C (continued)

TABLE VII. (continued)

RAW DATA. DIFFERENCE BETWEEN ANGULATED SKULL VS IDEAL SKULL

POSITION (Δ)

Skull #	9															
	SNA	SNB	ANB	FMA	U1-SN	NA-APo	SGn-FH	Ar-Go-Me	L1-MP	MP-SN	N-Me	Go-Me	S-Go	S-N	ANS-PNS	U1-PP
1	0.9	0.4	0.3	1.4	-2.9	0.3	1.5	-0.5	0	-0.9	-1	-0.2	0.4	-0.3	-1.7	-4.4
2	0.7	0.7	0	2.7	-3.5	0.2	1.4	-0.6	-2.7	1	-0.9	2.8	-2.7	-0.3	0.3	-3.5
3	0.3	0.9	-0.7	-1.9	0.8	-2	-1.6	1.1	-2	-1.6	-2.1	-2.3	0.2	0.1	-1.3	0.3
4	-0.9	-0.5	-0.4	1.6	0.3	-0.7	0.4	0.2	3.9	1.6	-0.1	2.1	-2.8	-0.1	1.1	1.4
5	0.3	0.9	-0.5	4.5	0.7	-1.2	3.9	2.2	3	-0.2	0	-0.7	0.6	0.2	-1.8	1.6
6	1.3	1.2	0	0.1	4.3	0.1	0.4	-0.1	-1.3	-1.6	-1.5	2.8	-1	0	1.6	2.8
7	0.5	0.8	-0.2	0.5	4.4	-1.1	0.1	1.3	-0.5	-0.4	-1.7	-1.4	-0.1	-0.6	0.2	4.4
8	1	0.7	0.4	4	-1.3	0.3	3.5	1.5	4.9	-0.4	-0.6	1.9	-0.5	-0.2	0.5	-0.7
9	1.4	0.5	0.9	-5.6	1.4	1.1	-5.3	6.7	4	-1.2	-2.4	-11.1	4.3	0.1	0.1	0.8
10	0.3	0.8	-0.5	0.6	-0.4	-1.4	-0.8	-1.5	2.5	0.4	-1.7	1.6	-2.4	-0.1	-2.2	1.4
11	1	0.7	0.3	0.6	0.7	-0.3	-0.1	3.7	-0.8	-0.6	-3.3	-1.7	-1.5	-0.3	-1.8	0.1
12	1.2	1.4	-0.2	2.9	1	0	2.6	-0.8	-5.5	-0.6	-0.9	1.9	-1	-0.6	0.5	0.7
13	0.9	0.2	0.8	1.5	-1.2	1.2	0.2	1	0.6	0.2	-1.1	1.3	-1.8	1.4	0.9	0
14	-0.1	-0.5	0.4	1.4	-2.9	0.7	0.1	3.2	-7.6	1.8	-0.7	-2.1	-2	-0.3	-2.7	-1.6
15	0.3	0.6	-0.4	-3.4	9.6	0	-3.4	-1.4	0.3	-0.4	0.3	1.4	0.1	0.3	1.4	10.6
16	-0.5	-0.3	-0.1	-0.5	-1.3	-0.2	-2.4	0.1	0.3	1.9	-1.6	1.1	-3.7	0.1	-2.5	0.2
17	2	1.2	0.8	0.2	-3.9	2	-1.2	1.4	-6	0	-0.5	0.9	-0.7	0.8	-0.8	-4.6
18	1.4	1.7	-0.3	-0.3	3.2	-1	-1.2	0	-0.7	-1.1	-1.8	3.1	-0.8	0.7	-1.3	2.6
19	0.8	0.4	0.5	-3.6	0	0.8	-4.6	0.5	4.7	0.2	-2.7	-1.5	-2.1	0.2	0.2	1.3
20	-0.7	0.9	-1.6	0.5	-1	-3.4	-1	0.7	-3.9	0.7	0	2.7	-1.5	0.5	-2.1	-2.1
21	2.8	1.9	0.9	0	0.9	1.7	-1.5	2.8	-1	0.1	-2.3	-0.9	-1.4	-1.2	2.8	1.3
22	-0.4	0.1	-0.5	-3.7	2.4	-0.2	-3.4	3.6	-0.7	-0.3	-0.3	-4.6	1.7	0.1	-0.9	2.4
23	2.2	1.4	0.8	1.2	-3	1.5	0.2	1.9	1.6	0.4	-0.3	1.5	-0.6	-1.6	-3.7	-5.5
24	0.4	-0.3	0.6	0	2.3	1.5	-1	-1.4	-0.3	1.3	-0.5	4.9	-3.8	-0.9	1.7	3.6

APPENDIX C (continued)

TABLE VII. (continued)

RAW DATA. DIFFERENCE BETWEEN ANGULATED SKULL VS IDEAL SKULL

POSITION (Δ)

Skull #	12															
	SNA	SNB	ANB	FMA	U1-SN	NA-APo	SGn-FH	Ar-Go-Me	L1-MP	MP-SN	N-Me	Go-Me	S-Go	S-N	ANS-PNS	U1-PP
1	1.2	0.5	0.5	2.5	-2.8	0.5	1.7	1.1	-3.2	-0.2	-1.9	-2.9	-0.1	-0.1	-0.3	-3.5
2	1.2	1.1	0.1	4.2	-3.5	0.7	3.4	0.4	-1.3	0.1	-1.7	0.4	-1.7	-0.2	3.3	-3.4
3	1	0.8	0.2	-1.3	1.5	-0.2	-0.9	4.4	0.4	-1.9	-2.7	-4.2	0.9	0.3	0.1	1.3
4	-0.2	-0.2	0	0.4	0.5	-0.4	-1.3	-0.4	3.8	0.9	-1.8	0.8	-3.2	0.9	0.3	1.1
5	1.2	1.6	-0.5	5.3	4	-0.9	5.3	-0.3	3.5	-1.8	-1.3	0.8	0.7	0.3	-1.9	4.3
6	1.1	2.2	-1.1	4.5	4.2	-3	5	1.6	-1.3	-3.1	-2.9	-0.7	1	-0.3	1.5	3.7
7	0.1	-0.1	0.3	-1.3	0.4	-0.1	-1.9	4.7	0	0.1	-2.2	-5.2	0.9	0.2	-4.5	0.6
8	2	1.2	0.9	-2.7	0.4	1.8	-1.6	4	2.8	-2.5	-1.2	-4.4	3.4	-0.1	-1.9	2.5
9	1	0.2	0.8	3.1	0	1.2	2.2	9	6.4	0.4	-2	-8.9	2.4	0	-2.6	1.9
10	1.4	1	0.4	2	0.6	1	1.6	4.4	-0.6	-0.7	-3.3	-2.6	-0.9	-1	-0.6	0.4
11	0.3	0	0.3	3.8	-1.7	-0.7	3.2	4	1.9	-0.8	-6	-4.9	-2.4	-0.6	0.9	-2.3
12	0.9	1.1	-0.2	-0.6	-0.5	-0.4	-0.7	2	-2.7	-1.1	-2.5	-2.3	0.1	-0.6	1.5	-2
13	-0.6	0.1	-0.7	-2.2	-2.5	-1.6	-3.6	0.1	-3.2	0.4	-2.4	0.9	-3.1	1	-0.9	-0.4
14	1.2	0.5	0.7	1.1	-2.8	1.2	-0.9	3.2	-6.8	1.5	-2.7	-0.9	-3.7	-1.2	-4.1	-0.5
15	1.1	1.2	-0.1	-4.2	6.6	0.3	-4	-2.6	-1	-1.3	-1.4	1.3	-0.3	-0.4	-1.2	8.6
16	0.1	0.1	0	-3.1	0.2	0.2	-3.7	-0.1	2.3	-0.1	-3.5	0	-3	-0.6	-2.3	3
17	2.6	1.7	0.9	1.4	0	2.8	-0.2	2.9	-5.9	0.2	-0.8	-0.4	-0.5	0.4	0.3	0
18	2.4	2.2	0.2	-2	2.9	-0.2	-2.4	-0.2	0.8	-2.2	-4.9	0.7	-1.6	-0.5	-1.2	1.4
19	1.8	1	0.8	-5.5	-0.6	1.6	-4.6	-2.9	5.2	-2.2	-4.1	-0.2	-1.7	-0.4	0.3	0.7
20	-0.8	0.1	-0.9	0.8	-4.9	-2.1	-1.3	-1.1	-5.5	1.6	-1.4	3.5	-4.2	0.3	-1.5	-4.3
21	5	4.5	0.5	-2.8	1.1	0.5	-3.8	0.3	-1.2	-2.6	-3.3	2.8	0	-1.5	0.6	-0.5
22	1	1.2	-0.1	-2.5	1.9	-0.7	-3	6.6	-1.5	-1	-2.6	-7.4	1.7	-0.4	4.2	-0.7
23	0.4	0.1	0.4	-0.5	-4.9	0.7	-1.5	3.3	4.8	1	-0.9	-1	-1.2	-0.5	-4.2	-4.3
24	2.2	1.6	0.6	-2.7	-0.7	0.9	-2.4	-1.8	-0.8	-1.6	-2.3	3.2	-1.8	-0.9	1.5	-0.8

APPENDIX C (continued)

TABLE VII. (continued)

RAW DATA. DIFFERENCE BETWEEN ANGULATED SKULL VS IDEAL SKULL

POSITION (Δ)

Skull #	15															
	SNA	SNB	ANB	FMA	U1-SN	NA-APo	SGn-FH	Ar-Go-Me	L1-MP	MP-SN	N-Me	Go-Me	S-Go	S-N	ANS-PNS	U1-PP
1	4.8	3.8	0.9	1.6	4.1	1.1	1.8	1.7	-3.6	-3.3	-4	-3.3	2	-2	-2.2	-1.9
2	2.2	2	0.2	2	-4	-0.1	2.4	-1.3	-3.2	-2.6	-4.4	0.1	-1	-0.7	5.8	-5.1
3	2	2.2	-0.2	-3	-0.3	-0.9	-1	-0.3	-3.3	-4.5	-4.4	0.7	0.8	-1.1	-6.3	-0.2
4	-1.7	-1.1	-0.6	0.6	-0.3	-1.5	-1.8	0.7	1.3	1.1	-3.4	-1.9	-4	2.3	3.7	2.4
5	2.3	2.1	0.2	0.5	3.4	0	0.5	1.4	-0.4	-2.6	-2.7	0.2	0.7	0.1	-0.9	3.7
6	2.8	2.7	0.1	1	7.2	0	0.5	3.1	-2.8	-2	-3.2	-0.7	0.2	-0.8	1.8	6.5
7	0.6	0.1	0.6	-3.1	3	1.1	-3.1	3.8	-1.1	-0.6	-4.3	-5.4	-0.6	-0.6	0.9	4.3
8	1.2	1.1	0.2	-1.6	1.2	0.8	-1.4	4.5	2.3	-1.5	-2.2	-3.1	1	-0.5	-2	-0.4
9	1.4	0.3	1	2	1.2	1	1.8	6.2	8	-1.5	-3.7	-3.9	-0.1	0.9	-1.2	2.3
10	1.1	1.2	-0.2	0.7	-1.8	-0.1	-0.3	2.8	1.2	0.3	-2.3	-0.8	-1.5	-1.4	0.9	-2.3
11	1.7	1.4	0.3	2.8	1.6	-0.6	2.1	4.5	-0.9	-1.6	-7	-4.5	-2.3	-1.5	-1.5	0
12	1.3	0.4	0.9	-0.7	-0.5	1.8	-1.6	7.1	-3.5	0.2	-4	-7.7	0.5	-1.3	1.7	-1.2
13	2.2	1.8	0.5	-1.7	-0.2	-0.3	-1.8	1.9	-3.2	-2.7	-4.3	-4.3	0.9	0.3	0.2	-1.8
14	1.3	0.9	0.4	0.5	-1.3	0.5	-1.6	2.1	-5.5	0.7	-3.8	0.2	-4	0.1	-3.6	0.7
15	0.4	0.6	-0.2	-3.9	4.2	-0.6	-5.1	1.3	-1	-0.3	-2.9	1.8	-2.9	0.3	-2.5	5.5
16	-0.4	0.1	-0.5	-2.6	1.5	-1.2	-4.6	-0.9	0.5	0.4	-4.7	2.5	-5.2	0.8	-2.8	3.3
17	4.7	3	1.7	-2.7	4.3	3.3	-3.6	1.5	-0.4	-2.9	-3.8	-2.3	0.4	1.2	-0.4	3.3
18	3.5	3.9	-0.4	-5.3	9.4	-1.3	-6.4	-0.2	-0.6	-4.4	-7.9	0	-1.9	2.1	-0.2	8
19	1.4	1.2	0.2	-9.1	0.7	-0.3	-8	-4.6	5.1	-3.7	-6.6	0.1	-2.5	0.3	0	2.4
20	-0.6	0.1	-0.7	0.4	-1.6	-1.9	-0.1	-1	0.3	0.1	0.8	0.6	0.2	0.8	-0.6	-1.6
21	5.8	5.2	0.6	-5.3	2.4	1.2	-5.8	0.3	-1.5	-3.7	-6.3	1	-0.9	-2.5	1.3	0.2
22	1.6	1.6	0	-2.5	3.2	-0.2	-2.3	5.8	-2.6	-2.2	-4.3	-8	1.4	-0.6	-1.6	3.1
23	2.9	2.2	0.7	-3.9	-3.7	0.8	-4.1	2.2	3.6	-1.2	-1.8	1.3	-0.2	-2.1	-4.5	-5.9
24	1.6	1.1	0.5	-3.7	1.3	0.4	-4.5	-0.5	-1.2	-0.5	-2.3	4.4	-3.1	-0.3	1.9	0

APPENDIX C (continued)

TABLE VIII. T-TEST STATISTICS

T-Test/ One-Sample Statistics

	N	Mean	Std. Deviation	Std. Error Mean
S-N 15 mm	24	-0.2583	1.24897	0.25495
Go-Me 15 mm	24	-1.2917	3.06011	0.62464
ANS-PNS 15 mm	24	-0.5958	2.7106	0.5533
N-Me 15 mm (Anterior Facial Height)	24	-3.8958	1.84213	0.37602
S-Go 15 mm (Posterior Facial Height)	24	-0.9208	1.93053	0.39407
SNA 15 (°)	24	1.7958	1.64356	0.33549
SNB 15 (°)	24	1.5792	1.42858	0.29161
ANB 15 (°)	24	0.2583	0.56792	0.11593
FMA 15 (°)	24	-1.7750	2.86148	0.5841
U1-SN 15 (°)	24	1.3333	2.95144	0.60246
NA-APo 15 (°) Angle of Convexity	24	0.1250	1.16218	0.23723
SGn-FH 15 (°) Y-axis	24	-2.0000	2.84758	0.58126
Ar-Go-Me 15 (°) Gonial Angle	24	1.6708	2.74376	0.56007
L1-MP 15 (°)	24	-0.5208	3.08178	0.62907
SN-MP 15 (°) Mandibular Plane Angle	24	-1.6250	1.66505	0.33988
U1-PP 15 (°)	24	1.1375	3.30689	0.67502
S-N 12 mm	24	-0.2042	0.55127	0.11253
Go-Me 12 mm	24	-0.6917	2.29421	0.4683
ANS-PNS 12 mm	24	-0.3292	1.79237	0.36587
N-Me 12 mm (Anterior Facial Height)	24	-2.4917	1.25071	0.2553
S-Go 12 mm (Posterior Facial Height)	24	-0.7625	1.9726	0.40265
SNA 12 (°)	24	0.9833	0.87609	0.17883
SNB 12 (°)	24	0.8625	0.72521	0.14803
ANB 12 (°)	24	0.1250	0.5628	0.11488
FMA 12 (°)	24	-0.3708	2.60826	0.53241
U1-SN 12 (°)	24	-0.0250	2.20498	0.45009
NA-APo 12 (°) Angle of Convexity	24	0.1292	1.28045	0.26137
SGn-FH 12 (°) Y-axis	24	-0.7667	2.48817	0.5079
Ar-Go-Me 12 (°) Gonial Angle	24	1.4417	2.50198	0.51072
L1-MP 12 (°)	24	-0.1708	2.59187	0.52906
SN-MP 12 (°) Mandibular Plane Angle	24	-0.7042	1.34955	0.27548
U1-PP 12 (°)	24	0.1583	2.37137	0.48405
S-N 9 mm	24	-0.1250	0.56434	0.1152
Go-Me 9 mm	24	0.5208	1.81179	0.36983
ANS-PNS 9 mm	24	-0.4875	1.54309	0.31498

APPENDIX C (continued)

TABLE VIII. T-TEST STATISTICS (continued)

N-Me 9 mm (Anterior Facial Height)	24	-1.1542	0.95461	0.19486
S-Go 9 mm (Posterior Facial Height)	24	-1.1292	1.38045	0.28178
SNA 9 (°)	24	0.7125	0.90377	0.18448
SNB 9 (°)	24	0.6583	0.6507	0.13282
ANB 9 (°)	24	0.0542	0.62134	0.12683
FMA 9 (°)	24	0.0458	2.05807	0.4201
U1-SN 9 (°)	24	-0.0167	2.20112	0.4493
NA-APo 9 (°) Angle of Convexity	24	-0.0042	1.27227	0.2597
SGn-FH 9 (°) Y-axis	24	-0.3000	1.90833	0.38954
Ar-Go-Me 9 (°) Gonial Angle	24	0.7750	1.56573	0.3196
L1-MP 9 (°)	24	-0.2167	2.46094	0.50234
SN-MP 9 (°) Mandibular Plane Angle	24	0.0125	0.99796	0.20371
U1-PP 9 (°)	24	0.4667	1.65967	0.33878
S-N 6 mm	24	-0.0958	0.47866	0.09771
Go-Me 6 mm	24	-0.4958	1.94232	0.39647
ANS-PNS 6 mm	24	-0.2042	1.28316	0.26192
N-Me 6 mm (Anterior Facial Height)	24	-0.4042	0.963	0.19657
S-Go 6 mm (Posterior Facial Height)	24	-0.1583	1.39873	0.28551
SNA 6 (°)	24	0.3333	0.81862	0.1671
SNB 6 (°)	24	0.3042	0.6403	0.1307
ANB 6 (°)	24	0.0625	0.45855	0.0936
FMA 6 (°)	24	-0.0125	1.86205	0.38009
U1-SN 6 (°)	24	0.3167	1.74123	0.35543
NA-APo 6 (°) Angle of Convexity	24	0.0708	0.99235	0.20256
SGn-FH 6 (°) Y-axis	24	-0.1000	2.00326	0.40891
Ar-Go-Me 6 (°) Gonial Angle	24	0.6250	1.82977	0.3735
L1-MP 6 (°)	24	-0.1083	2.07551	0.42366
SN-MP 6 (°) Mandibular Plane Angle	24	0.0875	1.11016	0.22661
U1-PP 6 (°)	24	0.4667	1.65967	0.33878
S-N 3 mm	24	-0.0458	0.45776	0.09344
Go-Me 3 mm	24	0.1333	1.7502	0.35726
ANS-PNS 3 mm	24	-0.0167	1.15105	0.23496
N-Me 3 mm (Anterior Facial Height)	24	-0.0667	0.96173	0.19631
S-Go 3 mm (Posterior Facial Height)	24	0.1042	1.09484	0.22348
SNA 3 (°)	24	0.1292	0.6054	0.12358
SNB 3 (°)	24	0.2875	0.5535	0.11298

APPENDIX C (continued)

TABLE VIII. T-TEST STATISTICS (continued)

ANB 3 (°)	24	-0.1417	0.47632	0.09723
FMA 3 (°)	24	-0.1292	1.38265	0.28223
U1-SN 3 (°)	24	-0.3542	1.1489	0.23452
NA-APo 3 (°) Angle of Convexity	24	-0.3292	0.97868	0.19977
SGn-FH 3 (°) Y-axis	24	0.1083	1.35387	0.27636
Ar-Go-Me 3 (°) Gonial Angle	24	-0.1042	1.50751	0.30772
L1-MP 3 (°)	24	0.1500	1.71414	0.3499
SN-MP 3 (°) Mandibular Plane Angle	24	-0.1583	0.81823	0.16702
U1-PP 3 (°)	24	-0.3500	1.36031	0.27767

APPENDIX C (continued)

TABLE VIII. T-TEST STATISTICS (continued)

T-Test/ One-Sample Statistics

	N	Mean	Std. Deviation	Std. Error Mean
S-N -15 mm	24	0.3667	0.96173	0.19631
Go-Me -15 mm	24	-2.175	3.28279	0.6701
ANS-PNS -15 mm	24	-1.2208	1.7869	0.36475
N-Me -15 mm (Anterior Facial Height)	24	-4.8958	1.99553	0.40734
S-Go -15 mm (Posterior Facial Height)	24	-1.4708	2.19178	0.4474
SNA -15 (°)	24	0.275	1.4674	0.29953
SNB -15 (°)	24	0.1875	1.12687	0.23002
ANB -15 (°)	24	0.0792	0.66003	0.13473
FMA -15 (°)	24	-1.9958	2.63017	0.53688
U1-SN -15 (°)	24	0.225	2.36335	0.48242
NA-APo -15 (°) Angle of Convexity	24	-0.0042	1.47338	0.30075
SGn-FH -15 (°) Y-axis	24	-1.3375	2.83607	0.57891
Ar-Go-Me -15 (°) Gonial Angle	24	0.525	2.54272	0.51903
L1-MP -15 (°)	24	-0.1125	4.20355	0.85805
SN-MP -15 (°) Mandibular Plane Angle	24	-2.2583	1.7212	0.35134
U1-PP -15 (°)	24	0.125	2.46458	0.50308
S-N -12 mm	24	0.4917	0.51408	0.10494
Go-Me -12 mm	24	-1.55	1.87036	0.38179
ANS-PNS -12 mm	24	-0.6833	2.12023	0.43279
N-Me -12 mm (Anterior Facial Height)	24	-3.1042	1.10197	0.22494
S-Go -12 mm (Posterior Facial Height)	24	-0.8292	2.00748	0.40978
SNA -12 (°)	24	-0.1042	1.22172	0.24938
SNB -12 (°)	24	-0.1875	0.91286	0.18634
ANB -12 (°)	24	0.075	0.58551	0.11952
FMA -12 (°)	24	-1.9167	2.00752	0.40978
U1-SN -12 (°)	24	-0.5375	2.02029	0.41239

APPENDIX C (continued)

TABLE VIII. T-TEST STATISTICS (continued)

NA-APo -12 (°) Angle of Convexity	24	0.1042	1.198	0.24454
SGn-FH -12 (°) Y-axis	24	-1.375	2.1708	0.44311
Ar-Go-Me -12 (°) Gonial Angle	24	0.4333	2.19697	0.44845
L1-MP -12 (°)	24	-0.2375	2.69409	0.54993
SN-MP -12 (°) Mandibular Plane Angle	24	-1.3958	1.50607	0.30742
U1-PP -12 (°)	24	0.2667	2.347	0.47908
S-N -9 mm	24	0.3958	0.66364	0.13546
Go-Me -9 mm	24	-0.7208	2.62082	0.53497
ANS-PNS -9 mm	24	-0.3125	1.74089	0.35536
N-Me -9 mm (Anterior Facial Height)	24	-1.7125	1.15432	0.23562
S-Go -9 mm (Posterior Facial Height)	24	-0.9208	1.15381	0.23552
SNA -9 (°)	24	-0.4208	1.15833	0.23644
SNB -9 (°)	24	-0.4	0.78906	0.16107
ANB -9 (°)	24	-0.0167	0.66898	0.13656
FMA -9 (°)	24	-0.9583	2.18392	0.44579
U1-SN -9 (°)	24	-0.7833	1.75367	0.35797
NA-APo -9 (°) Angle of Convexity	24	-0.1708	1.42141	0.29014
SGn-FH -9 (°) Y-axis	24	-0.6958	1.8191	0.37132
Ar-Go-Me -9 (°) Gonial Angle	24	0.6375	1.75098	0.35742
L1-MP -9 (°)	24	-0.2875	2.95448	0.60308
SN-MP -9 (°) Mandibular Plane Angle	24	-0.35	1.13903	0.2325
U1-PP -9 (°)	24	-0.15	1.49376	0.30491
S-N -6 mm	24	0.2375	0.58741	0.11991
Go-Me -6 mm	24	-0.4708	2.27758	0.46491
ANS-PNS -6 mm	24	-0.3125	1.28919	0.26315
N-Me -6 mm (Anterior Facial Height)	24	-0.9542	1.08907	0.22231
S-Go -6 mm (Posterior Facial Height)	24	-0.4833	1.43335	0.29258

APPENDIX C (continued)

TABLE VIII. T-TEST STATISTICS (continued)

SNA -6 (°)	24	-0.15	0.97043	0.19809
SNB -6 (°)	24	-0.2417	0.53966	0.11016
ANB -6 (°)	24	0.1	0.70772	0.14446
FMA -6 (°)	24	-0.9333	2.12494	0.43375
U1-SN -6 (°)	24	-0.6875	1.57129	0.32074
NA-APo -6 (°) Angle of Convexity	24	0.1042	1.47986	0.30207
SGn-FH -6 (°) Y-axis	24	-0.7958	2.09564	0.42777
Ar-Go-Me -6 (°) Gonial Angle	24	0.3583	1.57891	0.32229
L1-MP -6 (°)	24	-0.8208	2.16152	0.44122
SN-MP -6 (°) Mandibular Plane Angle	24	-0.15	0.99957	0.20404
U1-PP -6 (°)	24	-0.5417	1.81848	0.3712
S-N -3 mm	24	0.1208	0.52002	0.10615
Go-Me -3 mm	24	-0.2	1.68342	0.34363
ANS-PNS -3 mm	24	-0.1292	1.40449	0.28669
N-Me -3 mm (Anterior Facial Height)	24	-0.1167	0.97252	0.19852
S-Go -3 mm (Posterior Facial Height)	24	-0.225	1.26706	0.25864
SNA -3 (°)	24	-0.2958	0.59453	0.12136
SNB -3 (°)	24	-0.2333	0.41668	0.08505
ANB -3 (°)	24	-0.0583	0.44907	0.09167
FMA -3 (°)	24	-0.85	2.31817	0.47319
U1-SN -3 (°)	24	-0.4292	1.32287	0.27003
NA-APo -3 (°) Angle of Convexity	24	-0.3	1.03083	0.21042
SGn-FH -3 (°) Y-axis	24	-0.2917	1.73904	0.35498
Ar-Go-Me -3 (°) Gonial Angle	24	0.5208	1.62828	0.33237
L1-MP -3 (°)	24	-0.6583	1.75299	0.35783
SN-MP -3 (°) Mandibular Plane Angle	24	0.225	0.85935	0.17541
U1-PP -3 (°)	24	0.1708	1.61796	0.33027

APPENDIX C (continued)

TABLE IX. T-TEST STATISTICS

One-Sample Test

Test Value = 0

	t	df	Sig. (2-tailed)	Mean Difference	95% Confidence Interval of the Difference	
					Lower	Upper
S-N 15 mm	-1.013	23	0.321	-0.25833	-0.7857	0.2691
Go-Me 15 mm	-2.068	23	0.05	-1.29167	-2.5838	0.0005
ANS-PNS 15 mm	-1.077	23	0.293	-0.59583	-1.7404	0.5488
N-Me 15 mm (Anterior Facial Height)	-10.361	23	0	-3.89583	-4.6737	-3.118
S-Go 15 mm (Posterior Facial Height)	-2.337	23	0.029	-0.92083	-1.736	-0.1056
SNA 15 (°)	5.353	23	0	1.79583	1.1018	2.4898
SNB 15 (°)	5.415	23	0	1.57917	0.9759	2.1824
ANB 15 (°)	2.228	23	0.036	0.25833	0.0185	0.4981
FMA 15 (°)	-3.039	23	0.006	-1.775	-2.9833	-0.5667
U1-SN 15 (°)	2.213	23	0.037	1.33333	0.087	2.5796
NA-APo 15 (°) Angle of Convexity	0.527	23	0.603	0.125	-0.3657	0.6157
SGn-FH 15 (°) Y-axis	-3.441	23	0.002	-2	-3.2024	-0.7976
Ar-Go-Me 15 (°) Gonial Angle	2.983	23	0.007	1.67083	0.5122	2.8294
L1-MP 15 (°)	-0.828	23	0.416	-0.52083	-1.8222	0.7805
SN-MP 15 (°) Mandibular Plane Angle	-4.781	23	0	-1.625	-2.3281	-0.9219
U1-PP 15 (°)	1.685	23	0.105	1.1375	-0.2589	2.5339
S-N 12 mm	-1.814	23	0.083	-0.20417	-0.4369	0.0286
Go-Me 12 mm	-1.477	23	0.153	-0.69167	-1.6604	0.2771
ANS-PNS 12 mm	-0.9	23	0.378	-0.32917	-1.086	0.4277
N-Me 12 mm (Anterior Facial Height)	-9.76	23	0	-2.49167	-3.0198	-1.9635
S-Go 12 mm (Posterior Facial Height)	-1.894	23	0.071	-0.7625	-1.5955	0.0705
SNA 12 (°)	5.499	23	0	0.98333	0.6134	1.3533
SNB 12 (°)	5.826	23	0	0.8625	0.5563	1.1687
ANB 12 (°)	1.088	23	0.288	0.125	-0.1126	0.3626
FMA 12 (°)	-0.697	23	0.493	-0.37083	-1.4722	0.7305
U1-SN 12 (°)	-0.056	23	0.956	-0.025	-0.9561	0.9061
NA-APo 12 (°) Angle of Convexity	0.494	23	0.626	0.12917	-0.4115	0.6699
SGn-FH 12 (°) Y-axis	-1.509	23	0.145	-0.76667	-1.8173	0.284
Ar-Go-Me 12 (°) Gonial Angle	2.823	23	0.01	1.44167	0.3852	2.4982
L1-MP 12 (°)	-0.323	23	0.75	-0.17083	-1.2653	0.9236

APPENDIX C (continued)

TABLE IX. T-TEST STATISTICS (continued)

SN-MP 12 (°) Mandibular Plane Angle	-2.556	23	0.018	-0.70417	-1.274	-0.1343
U1-PP 12 (°)	0.327	23	0.747	0.15833	-0.843	1.1597
S-N 9 mm	-1.085	23	0.289	-0.125	-0.3633	0.1133
Go-Me 9 mm	1.408	23	0.172	0.52083	-0.2442	1.2859
ANS-PNS 9 mm	-1.548	23	0.135	-0.4875	-1.1391	0.1641
N-Me 9 mm (Anterior Facial Height)	-5.923	23	0	-1.15417	-1.5573	-0.7511
S-Go 9 mm (Posterior Facial Height)	-4.007	23	0.001	-1.12917	-1.7121	-0.5463
SNA 9 (°)	3.862	23	0.001	0.7125	0.3309	1.0941
SNB 9 (°)	4.956	23	0	0.65833	0.3836	0.9331
ANB 9 (°)	0.427	23	0.673	0.05417	-0.2082	0.3165
FMA 9 (°)	0.109	23	0.914	0.04583	-0.8232	0.9149
U1-SN 9 (°)	-0.037	23	0.971	-0.01667	-0.9461	0.9128
NA-APo 9 (°) Angle of Convexity	-0.016	23	0.987	-0.00417	-0.5414	0.5331
SGn-FH 9 (°) Y-axis	-0.77	23	0.449	-0.3	-1.1058	0.5058
Ar-Go-Me 9 (°) Gonial Angle	2.425	23	0.024	0.775	0.1138	1.4362
L1-MP 9 (°)	-0.431	23	0.67	-0.21667	-1.2558	0.8225
SN-MP 9 (°) Mandibular Plane Angle	0.061	23	0.952	0.0125	-0.4089	0.4339
U1-PP 9 (°)	1.377	23	0.182	0.46667	-0.2341	1.1675
S-N 6 mm	-0.981	23	0.337	-0.09583	-0.298	0.1063
Go-Me 6 mm	-1.251	23	0.224	-0.49583	-1.316	0.3243
ANS-PNS 6 mm	-0.779	23	0.444	-0.20417	-0.746	0.3377
N-Me 6 mm (Anterior Facial Height)	-2.056	23	0.051	-0.40417	-0.8108	0.0025
S-Go 6 mm (Posterior Facial Height)	-0.555	23	0.585	-0.15833	-0.749	0.4323
SNA 6 (°)	1.995	23	0.058	0.33333	-0.0123	0.679
SNB 6 (°)	2.327	23	0.029	0.30417	0.0338	0.5745
ANB 6 (°)	0.668	23	0.511	0.0625	-0.1311	0.2561
FMA 6 (°)	-0.033	23	0.974	-0.0125	-0.7988	0.7738
U1-SN 6 (°)	0.891	23	0.382	0.31667	-0.4186	1.0519
NA-APo 6 (°) Angle of Convexity	0.35	23	0.73	0.07083	-0.3482	0.4899
SGn-FH 6 (°) Y-axis	-0.245	23	0.809	-0.1	-0.9459	0.7459
Ar-Go-Me 6 (°) Gonial Angle	1.673	23	0.108	0.625	-0.1476	1.3976
L1-MP 6 (°)	-0.256	23	0.8	-0.10833	-0.9847	0.7681
SN-MP 6 (°) Mandibular Plane Angle	0.386	23	0.703	0.0875	-0.3813	0.5563
U1-PP 6 (°)	1.377	23	0.182	0.46667	-0.2341	1.1675
S-N 3 mm	-0.491	23	0.628	-0.04583	-0.2391	0.1475
Go-Me 3 mm	0.373	23	0.712	0.13333	-0.6057	0.8724

APPENDIX C (continued)

TABLE IX. T-TEST STATISTICS (continued)

ANS-PNS 3 mm	-0.071	23	0.944	-0.01667	-0.5027	0.4694
N-Me 3 mm (Anterior Facial Height)	-0.34	23	0.737	-0.06667	-0.4728	0.3394
S-Go 3 mm (Posterior Facial Height)	0.466	23	0.646	0.10417	-0.3581	0.5665
SNA 3 (°)	1.045	23	0.307	0.12917	-0.1265	0.3848
SNB 3 (°)	2.545	23	0.018	0.2875	0.0538	0.5212
ANB 3 (°)	-1.457	23	0.159	-0.14167	-0.3428	0.0595
FMA 3 (°)	-0.458	23	0.651	-0.12917	-0.713	0.4547
U1-SN 3 (°)	-1.51	23	0.145	-0.35417	-0.8393	0.131
NA-APo 3 (°) Angle of Convexity	-1.648	23	0.113	-0.32917	-0.7424	0.0841
SGn-FH 3 (°) Y-axis	0.392	23	0.699	0.10833	-0.4634	0.68
Ar-Go-Me 3 (°) Gonial Angle	-0.339	23	0.738	-0.10417	-0.7407	0.5324
L1-MP 3 (°)	0.429	23	0.672	0.15	-0.5738	0.8738
SN-MP 3 (°) Mandibular Plane Angle	-0.948	23	0.353	-0.15833	-0.5038	0.1872
U1-PP 3 (°)	-1.26	23	0.22	-0.35	-0.9244	0.2244

APPENDIX C (continued)

TABLE IX. T-TEST STATISTICS (continued)

One-Sample Test

	Test Value = 0					
	t	df	Sig. (2-tailed)	Mean Difference	95% Confidence Interval of the Difference	
					Lower	Upper
S-N -15 mm	1.868	23	0.075	0.36667	-0.0394	0.7728
Go-Me -15 mm	-3.246	23	0.004	-2.175	-3.5612	-0.7888
ANS-PNS -15 mm	-3.347	23	0.003	-1.22083	-1.9754	-0.4663
N-Me -15 mm (Anterior Facial Height)	-12.019	23	0	-4.89583	-5.7385	-4.0532
S-Go -15 mm (Posterior Facial Height)	-3.288	23	0.003	-1.47083	-2.3963	-0.5453
SNA -15 (°)	0.918	23	0.368	0.275	-0.3446	0.8946
SNB -15 (°)	0.815	23	0.423	0.1875	-0.2883	0.6633
ANB -15 (°)	0.588	23	0.563	0.07917	-0.1995	0.3579
FMA -15 (°)	-3.717	23	0.001	-1.99583	-3.1065	-0.8852
U1-SN -15 (°)	0.466	23	0.645	0.225	-0.773	1.223
NA-APo -15 (°) Angle of Convexity	-0.014	23	0.989	-0.00417	-0.6263	0.618
SGn-FH -15 (°) Y-axis	-2.31	23	0.03	-1.3375	-2.5351	-0.1399
Ar-Go-Me -15 (°) Gonial Angle	1.012	23	0.322	0.525	-0.5487	1.5987
L1-MP -15 (°)	-0.131	23	0.897	-0.1125	-1.8875	1.6625
SN-MP -15 (°) Mandibular Plane Angle	-6.428	23	0	-2.25833	-2.9851	-1.5315
U1-PP -15 (°)	0.248	23	0.806	0.125	-0.9157	1.1657
S-N -12 mm	4.685	23	0	0.49167	0.2746	0.7087
Go-Me -12 mm	-4.06	23	0	-1.55	-2.3398	-0.7602
ANS-PNS -12 mm	-1.579	23	0.128	-0.68333	-1.5786	0.212
N-Me -12 mm (Anterior Facial Height)	-13.8	23	0	-3.10417	-3.5695	-2.6388
S-Go -12 mm (Posterior Facial Height)	-2.023	23	0.055	-0.82917	-1.6769	0.0185
SNA -12 (°)	-0.418	23	0.68	-0.10417	-0.6201	0.4117
SNB -12 (°)	-1.006	23	0.325	-0.1875	-0.573	0.198
ANB -12 (°)	0.628	23	0.536	0.075	-0.1722	0.3222
FMA -12 (°)	-4.677	23	0	-1.91667	-2.7644	-1.069
U1-SN -12 (°)	-1.303	23	0.205	-0.5375	-1.3906	0.3156
NA-APo -12 (°) Angle of Convexity	0.426	23	0.674	0.10417	-0.4017	0.61
SGn-FH -12 (°) Y-axis	-3.103	23	0.005	-1.375	-2.2917	-0.4583
Ar-Go-Me -12 (°) Gonial Angle	0.966	23	0.344	0.43333	-0.4944	1.361
L1-MP -12 (°)	-0.432	23	0.67	-0.2375	-1.3751	0.9001
SN-MP -12 (°) Mandibular Plane Angle	-4.54	23	0	-1.39583	-2.0318	-0.7599
U1-PP -12 (°)	0.557	23	0.583	0.26667	-0.7244	1.2577

APPENDIX C (continued)

TABLE IX. T-TEST STATISTICS (continued)

S-N -9 mm	2.922	23	0.008	0.39583	0.1156	0.6761
Go-Me -9 mm	-1.347	23	0.191	-0.72083	-1.8275	0.3858
ANS-PNS -9 mm	-0.879	23	0.388	-0.3125	-1.0476	0.4226
N-Me -9 mm (Anterior Facial Height)	-7.268	23	0	-1.7125	-2.1999	-1.2251
S-Go -9 mm (Posterior Facial Height)	-3.91	23	0.001	-0.92083	-1.408	-0.4336
SNA -9 (°)	-1.78	23	0.088	-0.42083	-0.91	0.0683
SNB -9 (°)	-2.483	23	0.021	-0.4	-0.7332	-0.0668
ANB -9 (°)	-0.122	23	0.904	-0.01667	-0.2992	0.2658
FMA -9 (°)	-2.15	23	0.042	-0.95833	-1.8805	-0.0361
U1-SN -9 (°)	-2.188	23	0.039	-0.78333	-1.5238	-0.0428
NA-APo -9 (°) Angle of Convexity	-0.589	23	0.562	-0.17083	-0.771	0.4294
SGn-FH -9 (°) Y-axis	-1.874	23	0.074	-0.69583	-1.464	0.0723
Ar-Go-Me -9 (°) Gonial Angle	1.784	23	0.088	0.6375	-0.1019	1.3769
L1-MP -9 (°)	-0.477	23	0.638	-0.2875	-1.5351	0.9601
SN-MP -9 (°) Mandibular Plane Angle	-1.505	23	0.146	-0.35	-0.831	0.131
U1-PP -9 (°)	-0.492	23	0.627	-0.15	-0.7808	0.4808
S-N -6 mm	1.981	23	0.06	0.2375	-0.0105	0.4855
Go-Me -6 mm	-1.013	23	0.322	-0.47083	-1.4326	0.4909
ANS-PNS -6 mm	-1.188	23	0.247	-0.3125	-0.8569	0.2319
N-Me -6 mm (Anterior Facial Height)	-4.292	23	0	-0.95417	-1.414	-0.4943
S-Go -6 mm (Posterior Facial Height)	-1.652	23	0.112	-0.48333	-1.0886	0.1219
SNA -6 (°)	-0.757	23	0.457	-0.15	-0.5598	0.2598
SNB -6 (°)	-2.194	23	0.039	-0.24167	-0.4695	-0.0138
ANB -6 (°)	0.692	23	0.496	0.1	-0.1988	0.3988
FMA -6 (°)	-2.152	23	0.042	-0.93333	-1.8306	-0.0361
U1-SN -6 (°)	-2.143	23	0.043	-0.6875	-1.351	-0.024
NA-APo -6 (°) Angle of Convexity	0.345	23	0.733	0.10417	-0.5207	0.7291
SGn-FH -6 (°) Y-axis	-1.86	23	0.076	-0.79583	-1.6807	0.0891
Ar-Go-Me -6 (°) Gonial Angle	1.112	23	0.278	0.35833	-0.3084	1.0251
L1-MP -6 (°)	-1.86	23	0.076	-0.82083	-1.7336	0.0919
SN-MP -6 (°) Mandibular Plane Angle	-0.735	23	0.47	-0.15	-0.5721	0.2721
U1-PP -6 (°)	-1.459	23	0.158	-0.54167	-1.3095	0.2262
S-N -3 mm	1.138	23	0.267	0.12083	-0.0988	0.3404
Go-Me -3 mm	-0.582	23	0.566	-0.2	-0.9108	0.5108
ANS-PNS -3 mm	-0.451	23	0.657	-0.12917	-0.7222	0.4639
N-Me -3 mm (Anterior Facial Height)	-0.588	23	0.562	-0.11667	-0.5273	0.294

APPENDIX C (continued)

TABLE IX. T-TEST STATISTICS (continued)

S-Go -3 mm (Posterior Facial Height)	-0.87	23	0.393	-0.225	-0.76	0.31
SNA -3 (°)	-2.438	23	0.023	-0.29583	-0.5469	-0.0448
SNB -3 (°)	-2.743	23	0.012	-0.23333	-0.4093	-0.0574
ANB -3 (°)	-0.636	23	0.531	-0.05833	-0.248	0.1313
FMA -3 (°)	-1.796	23	0.086	-0.85	-1.8289	0.1289
U1-SN -3 (°)	-1.589	23	0.126	-0.42917	-0.9878	0.1294
NA-APo -3 (°) Angle of Convexity	-1.426	23	0.167	-0.3	-0.7353	0.1353
SGn-FH -3 (°) Y-axis	-0.822	23	0.42	-0.29167	-1.026	0.4427
Ar-Go-Me -3 (°) Gonial Angle	1.567	23	0.131	0.52083	-0.1667	1.2084
L1-MP -3 (°)	-1.84	23	0.079	-0.65833	-1.3986	0.0819
SN-MP -3 (°) Mandibular Plane Angle	1.283	23	0.212	0.225	-0.1379	0.5879
U1-PP -3 (°)	0.517	23	0.61	0.17083	-0.5124	0.854

VITA

NAME: Kan Tsunoda

EDUCATION: B.S., Neuroscience, Brigham Young University, Provo, Utah, 2003

D.C., Chiropractic, Palmer College of Chiropractic, Davenport, Iowa, 2008

D.M.D., Midwestern University College of Dental Medicine-Illinois, Downers Grove, Illinois, 2016

M.S., Oral Sciences, University of Illinois at Chicago, Chicago, Illinois, 2019

Specialty Certificate, Orthodontics, University of Illinois at Chicago, Chicago, Illinois, 2019

HONORS: Pierre Fauchard Academy, International Certificate of Merit Honors

Award for Outstanding Academic Achievements and Contribution to Dental Literature, Midwestern University College of Dental Medicine-Illinois, Downers Grove, Illinois, 2016

Salutatorian, Summa Cum Laude, Palmer College of Chiropractic, Davenport, Iowa 2008

Phi Tau Delta International Honors, Palmer College of Chiropractic, Davenport, Iowa 2008

AWARDS: American Association of Oral Biologists (AAOB) – Oral Biology Award, Midwestern University College of Dental Medicine-Illinois, Downers Grove, Illinois, 2016

Hinman National Student Research – Award of Excellence in Research by University of Tennessee HSC, Memphis TN, 2014

Dr. Suarez Midwestern University Research Best Research Award, Midwestern University College of Dental Medicine-Illinois, Downers Grove, Illinois, 2014

Presidential Scholar Award, Palmer College of Chiropractic, Palmer College of Chiropractic, Davenport, Iowa 2008

TEACHING: Graduate Teaching Assistant, Midwestern University College of Dental Medicine-Illinois, Downers Grove, Illinois, 2016: Predoctoral Integrated Basic Sciences

PROFESSIONAL MEMBERSHIPS: American Association of Orthodontists
American Dental Association
Chicago Dental Society
Illinois Society of Orthodontists
Illinois State Dental Society

PUBLICATIONS: K.Tsunoda, O. Couture, N. Chandar. Regulation of Bone Specific Gene Expression by Menin. *J Dent Res* 94 (Spec Iss A):4615, 2015